

**CHARACTERIZATION OF POLYETHYLENE GLYCOL HYDROGELS FOR  
BIOMEDICAL APPLICATIONS**

A Thesis

Submitted to the Graduate Faculty of the  
Louisiana State University and  
Agricultural and Mechanical College  
in partial fulfillment of the  
requirements for the degree of  
Master of Science in Chemical Engineering

in

The Department of Chemical Engineering

by  
Anushree Datta  
B.E. University of Pune, India, 2005  
August 2007

# Acknowledgments

I would like to thank my research advisor, Dr. James Henry for his patience, guidance and support over the course of this research. He was a constant inspiration, and his assistance and suggestions were invaluable towards the completion of this work.

I would also like to thank the members of my exam committee, Dr. Todd Monroe and Dr. Karsten Thompson for their efforts in reviewing and evaluating my research. I would like to acknowledge and thank the Department of Chemical Engineering at Louisiana State University for the various opportunities that have helped to make this journey an educational as well as an enjoyable one. I would also like to thank Mia Dvora for her helpful insights and invaluable suggestions throughout the course of this research.

I would like to dedicate this research work to my family. To my parents, who have always encouraged me to pursue my goals, always succeed, and never admit defeat. From them I have learned to be the best that I can be. To my sister, who is my guide, my conscience and my best friend. Thank you for being a part of my life.

# Table of Contents

<b>Acknowledgments .....</b>	<b>ii</b>
<b>List of Tables .....</b>	<b>vi</b>
<b>List of Figures .....</b>	<b>vii</b>
<b>Abstract .....</b>	<b>ix</b>
<b>Chapter 1 : An Introduction to Hydrogels.....</b>	<b>1</b>
1.1 Introduction .....	1
1.2 Properties of Hydrogels .....	2
1.2.1 Mechanical Properties .....	3
1.2.2 Biocompatible Properties .....	3
1.3 Classification of Hydrogels .....	4
1.4 Preparation Methods of Hydrogels .....	4
1.4.1 Chemically Crosslinked Gels.....	5
1.4.2 Physically Crosslinked Gels .....	8
1.5 Monomers Used for Fabrication of Hydrogels .....	10
1.6 PEG (polyethylene glycol) as Suitable Material .....	11
1.7 Applications of Hydrogels .....	12
1.7.1 Drug Delivery .....	13
1.7.2 Hydrogels in Drug Delivery .....	14
1.7.3 Properties Useful in Drug Delivery.....	15
1.7.4 Applications of Hydrogels in Drug Delivery.....	16
1.8 References .....	21
<b>Chapter 2 : Network Structure .....</b>	<b>25</b>
2.1 Introduction .....	25
2.2 Cross Linked Structure .....	26
2.2.1 Real Networks and Network Defects .....	26
2.3 Swelling Parameters and Their Significance .....	27
2.4 Significance of Mesh Size.....	30
2.5 Swelling Theories .....	32
2.5.1 Equilibrium Swelling Theory .....	32
2.5.2 Rubber Elasticity Theory.....	35
2.5.3 Calculation of Mesh Size.....	36
2.6 References .....	37
<b>Chapter 3 :Analysis of Drug Transport Mechanism .....</b>	<b>39</b>
3.1 Introduction .....	39
3.2 Diffusion Controlled System.....	40
3.2.1 Reservoir System .....	41
3.2.2 Matrix System.....	42

3.3 Chemically Controlled System.....	43
3.4 Swelling Controlled Systems .....	46
3.4.1 Empirical Models .....	48
3.4.2 Release from Swellable Devices.....	49
3.4.3 Coupling of Diffusion and Relaxation for Anomalous Diffusion .....	50
3.4.4 Mechanistic Models .....	52
3.4.5 Fundamentals of Diffusion .....	53
3.4.6 Analysis of Drug Release for Non-Swellable and Swellable Polymers.....	55
3.5 References .....	59
<b>Chapter 4 : Preparation of PEGDA Hydrogels and Study of Release Kinetics.....</b>	<b>62</b>
4.1 Overview .....	62
4.2 Introduction .....	63
4.3 Materials and Methods.....	64
4.3.1 Materials .....	64
4.3.2 Preparation of PEGDA .....	65
4.3.3 Preparation of Hydrogel for Swelling Studies .....	65
4.3.4 Mesh Size Calculation.....	66
4.3.5 Swelling Studies.....	68
4.3.6 Preparation of Gels for Diffusion Studies with Dye .....	70
4.3.7 Dye Release Experiments.....	70
4.4 Mathematical Analysis of Drug Transport Mechanism.....	71
4.5 Mathematical Analysis of the Drug Release Kinetics .....	72
4.6 Results and Discussions .....	73
4.6.1 Acrylation Chemistry .....	73
4.6.2 Swelling Parameters.....	73
4.6.3 Swelling Studies and Analysis.....	76
4.6.4 Dye Diffusion Studies .....	79
4.7 Conclusions .....	81
4.8 References .....	82
<b>Chapter 5 : Study of Mixtures of PEGDA Hydrogels .....</b>	<b>84</b>
5.1 Introduction .....	84
5.2 Materials and Methods.....	85
5.2.1 Materials .....	85
5.2.2 Preparation of Mixed PEGDA Hydrogels.....	85
5.2.3 Sample Mixture Preparation .....	86
5.2.4 Calculation of Mesh Size.....	86
5.2.5 Study of Swelling Characteristic of PEG 200/14000 Mixture .....	88
5.3 Results and Discussion .....	90
5.3.1 Mesh Sizes for Different Mixture Combination .....	91
5.3.2 Variation of Mass fractions in Mixture .....	94
5.3.3 Swelling Properties of Mixture.....	97
5.4 Conclusions .....	101
5.5 References .....	102
<b>Chapter 6 : Summary and Future Work .....</b>	<b>103</b>

6.1 Summary .....	103
6.2 Future Work .....	105
<b>Vita .....</b>	<b>107</b>

# List of Tables

<b>Table 1.1</b> Monomers used in synthesis of hydrogels for pharmaceutical applications. From Table 1 in ref [1.16] .....	11
<b>Table 3.1</b> Diffusional exponent and mechanism of diffusional release from various swellable controlled systems. From Table 1 in [3.15].....	49
<b>Table 3.2</b> Summary of drug diffusion coefficient equations. From Table 2 in ref [3.12].....	55
<b>Table 4.1</b> Calculated values of $M_c$ and mesh size .....	75
<b>Table 4.2</b> $n$ and $k$ values obtained from power law fit .....	77
<b>Table 4.3</b> Variation of diffusion coefficient with molecular weight.....	78
<b>Table 4.4</b> $n$ and $k$ values obtained from power law fit .....	79
<b>Table 4.5</b> Peppas equation parametes.....	80
<b>Table 4.6</b> Variation of Diffusion coefficients with molecular weight .....	80
<b>Table 5.1</b> Mixtures of PEGDA with its constituent molecular weights .....	85
<b>Table 5.2</b> Various concentration combination of PEGDA mixture 200/14K.....	89
<b>Table 5.3</b> Mesh sizes and molecular weight between crosslinks for all mixture combinations ..	92
<b>Table 5.4</b> Table of calculated and experimental values of $M_c$ for each mixture combination. The increasing mass fractions are those of PEG 200.....	95
<b>Table 5.5</b> Values of $n$ and $k$ obtained from fitting swelling data to power law expression. The values are shown along with the variance and 95% confidence limits of the fit.....	99
<b>Table 5.6</b> Diffusion coefficients for mixtures whose $n$ value is close to 0.45.....	100

# List of Figures

Figure 1.1 Tissue locations applicable for hydrogel based drug delivery systems. From Figure 2 in ref [1.16].....	17
Figure 2.1 Ideal Gaussian network $M_c$ is the molecular weight between crosslinks. From Fig 3 in ref[2.12].....	27
Figure 2.2 Network Defects (A) Loops (B) Entanglements (C) Unreacted Functionality. From Fig 4 in ref[2.12].....	28
Figure 2.3 Schematic of mesh size in hydrogels at (A) deswollen state (B) swollen state. $\xi$ is mesh size. Adapted from Fig 1 in Ref [2.5]. ....	30
Figure 2.4 Schematic of solute mass transfer in gel (1) solute traversing through network (2)crosslinked network (3) solvent surrounding gel. From Fig 1 in ref [2.13] .....	31
Figure 3.1 Schematic illustration of cross section of drug loaded spheres (a) reservoir system (b) dissolved drug system (c) dispersed drug system. (Adapted from Fig 1 in ref[3.1]) .....	41
Figure 3.2 Schematic diagram showing concentration profile in sphere of dispersed drug system in perfect sink system. From Fig 2 in Ref[3.1].....	44
Figure 3.3 Schematic of one dimensional swelling process due to solvent diffusion and polymer dissolution as proposed by Lee. From Fig 5 in ref[3.1].....	48
Figure 3.4 Variation of the Fickian diffusional exponent $m$ with aspect ratio $2a/l$ . From Fig 3 in Ref[3.16] .....	51
Figure 4.1 FTIR Spectra of PEG 200. Red -PEG, Blue-PEGDA.....	74
Figure 4.2 FTIR spectra of PEG 10000. Red-PEGDA, Blue-PEG .....	74
Figure 4.3 Effect of average molecular weight on the molecular weight between crosslinks ( $M_c$ ). The dotted line represents the linear trendline fit .....	75
Figure 4.4 Variation of mesh size with average molecular weight. The dotted line represents the linear trendline fit.....	76
Figure 4.5 Power law fits for different PEG 200 and PEG 400. The dotted line represents equation fit.....	78
Figure 5.1 Comparison of theoretical and calculated mesh sizes for all mixtures. The theoretical mesh size is the weighted average of individual PEG mesh sizes.....	92

Figure 5.2 Comparison of theoretical and experimental Molecular weight between crosslinks for mixtures. The theoretical values are weighted averages of the individual PEG  $M_c$  values .....94

Figure 5.3 Comparison of theoretical and experimental  $M_c$  (mixture) with variation of mass fractions of constituent PEGs. The increasing mass fractions represented are those of PEG 200. ....95

Figure 5.4 Effect of changes in mass fraction ratios on the mesh size of the mixtures. The trend line shows a linear fit. ....96

Figure 5.5 Swelling of mixtures with time. The mixtures represented here are for PEG 200 mass fractions from 0.1 to 0.5 .....97

Figure 5.6 Swelling of mixtures with time. The mixtures shown are gels with PEG 200 mass fractions ranging from 0.5 to 0.8 .....98

Figure 5.7 Curve fitting of mixtures to power law expression. The mass fractions represented here are that of PEG 200. The dotted line represents the fitted data, while the markers represent experimental data..... 100

# Abstract

Polyethylene glycol is one of the most widely used synthetic materials for biomedical applications. Its biocompatibility, flexibility, and ‘stealth’ properties make it ideal for use in drug delivery applications. The main objective of this paper is to characterize the structural and mass transfer properties of polyethylene glycol hydrogels for applications in drug delivery and biological immobilization. Swelling behavior of the gels was studied to determine the mesh size, and other significant structural parameters of the gel. For accurate design of drug delivery device, along with network design, mathematical modeling of release profiles was performed.

The study of PEG hydrogels was done in two distinct phases. The first stage consisted of analyzing diffusion properties of homogenous PEG hydrogels with varying molecular weights (MW 200, 400, 8000, 10000, 14000, 20000). The release of fluorescein dye from each gel was analyzed, and it was observed that diffusive properties of PEG gels vary drastically with molecular weight. The lower molecular weight PEGs had lower diffusion coefficients, but their Fickian release profile was easy to analyze and predict. The higher molecular weight PEGs, on the other hand had large diffusion coefficients, but with anomalous release profiles that were difficult to analyze analytically. This led to the investigation of combination gels, or binary mixtures of two different molecular weight PEGs. These gels were found to have intermediate properties, in accordance with the mass fractions of its constitutive PEGs. This linear relationship allowed for development of a hybrid gel with required diffusive properties, and a predictable mechanism of analyte release.

# Chapter 1 : An Introduction to Hydrogels

## 1.1 Introduction

Man has always been plagued with ailments and diseases of both the body and the mind. However dedicated research from scientists all over the world has made it possible to treat, prevent and eradicate many of these diseases that plague man. The field of pharmaceutical science has been developing steadily over the years, and has today become invaluable in helping to keep us healthy and prevent disease. An avenue of research that has progressed a great deal in the past few decades is the treatment of diseases via biomolecules such as drugs, proteins etc. Initially these could only be administered in limited manner, due to limitations of drug delivery through harmful environments in the body. Thus limited mobility reduced the effectiveness of administered drugs [1.16]. Progress came with the development of biomaterial carriers which could be encapsulated, or immobilized with drugs, allowing the drug to safely reach the required site without harm. These carriers allowed for the release of drug in sites which were previously inaccessible. The nature of these carriers progressed over the years from ceramics, to natural, to synthetic materials [1.23]. Factors such as integrity, biocompatibility and flexibility were considered, and lead to the use of hydrophilic three dimensional matrices as carrier materials. These are a class of materials known as *Hydrogels*. These three dimensional polymer matrices are capable of imbibing large amounts of water, and biological fluids. This property of hydrogels is the reason behind its varied applications ranging from food additives to pharmaceuticals and clinical applications. Synthetic hydrogels prepared from a varied range of monomers have found many applications especially in tissue-engineering scaffolds, as carriers for implantable devices, and drug delivery devices. Out of all these applications, at the forefront

of this research are hydrogel- based drug delivery devices. Synthetic hydrogels provide an effective and controlled way in which to administer protein and peptide based drugs for treatment of a number of diseases. A successful drug delivery device relies not only on competent network design, but also on accurate mathematical modeling of drug release profiles. Hydrogels have ordered polymer networks, with well-defined chemistries yielding well-defined physicochemical properties and easily reproducible drug release profiles [1.16]. In order to accurately understand and model drug release profiles from a material, it becomes essential to have a quantitative mathematical understanding of material properties, interaction parameters, kinetics, and transport phenomena within the material in question. The network structure also plays a key role in diffusional behavior, mesh size and stability of incorporated drug. It is this well-defined order that enables accurate network design by identifying key parameters and mechanisms that govern the rate and extent of drug release. Hydrogels have thus become a premier material used for drug delivery formulations and biomedical implants, due to its biocompatibility, network structure, and molecular stability of the incorporated bioactive agent.

## **1.2 Properties of Hydrogels**

Hydrogels are water swollen polymer matrices, with a tendency to imbibe water when placed in aqueous environment. This ability to swell, under biological conditions, makes it an ideal material for use in drug delivery and immobilization of proteins, peptides, and other biological compounds. Due to their high water content, these gels resemble natural living tissue more than any other type of synthetic biomaterial [1.15]. These networks, have a three dimensional structure, crosslinked together either physically (entanglements, crystallites), or chemically (tie-points, junctions). This insoluble crosslinked structure allows immobilization of active agents, biomolecules effectively, and allows for its release in well-defined specific

manner. Thus the hydrogels' biocompatibility and crosslinked structure are responsible for its varied applications.

### **1.2.1 Mechanical Properties**

For non biodegradable applications, it is essential that the carrier gel matrix maintain physical and mechanical integrity. Mechanical stability of the gel is, therefore, an important consideration when designing a therapeutic system. For example, drugs and other biomolecules must be protected from the harmful environments in the body such as, extreme pH environment before it is released at the required site. To this end, the carrier gel must be able to maintain its physical integrity and mechanical strength in order to prove an effective biomaterial. The strength of the material can be increased by incorporating crosslinking agents, comonomers, and increasing degree of crosslinking. There is however an optimum degree of crosslinking, as a higher degree of crosslinking also leads to brittleness and less elasticity. Elasticity of the gel is important to give flexibility to the crosslinked chains, to facilitate movement of incorporated bioactive agent. Thus a compromise between mechanical strength and flexibility is necessary for appropriate use of these materials.

### **1.2.2 Biocompatible Properties**

It is important for synthetic materials, such as hydrogels, to be biocompatible and non-toxic in order for it to be a useful biomedical polymer. Most polymers used for biomedical application must pass a cytotoxicity and in-vivo toxicity tests. Most toxicity problems associated with hydrogels arise due to unreacted monomers, oligomers and initiators that leach out during application. Thus an assessment of the potential toxicity of all materials used for fabrication of gel is an integral part of determining suitability of the gel for biological applications. To lower chances of toxic effects, the use of initiators is being eliminated, with the advent of gamma irradiation as polymerization technique. Steps are also taken to eliminate contaminants from

hydrogels, by repeated washing and treatment. Also, kinetics of polymerization has been studied, so as to achieve higher conversion rates, and avoid unreacted monomers and side products.

### **1.3 Classification of Hydrogels**

Hydrogels can be classified as neutral or ionic, based on the nature of side groups. In neutral hydrogels, the driving force for swelling is due to the water-polymer thermodynamic mixing contribution to the overall free energy, along with elastic polymer contribution [1.16]. The swelling of ionic hydrogels is also affected by the ionic interactions between charged polymers and free ions [1.31]. Ionic hydrogels containing ionic groups, such as carboxylic acid, imbibe larger amount of water, because of its increased hydrophilicity. Examples of such gels are poly(acrylic acid), and polyamines. Hydrogels are also classified as homopolymers or copolymers, based on the method of preparation. Hydrogels can be classified based on the physical structure of the network as amorphous, semicrystalline, hydrogen bonded structures, supermolecular structures and hydrocolloidal aggregates [1.16]. An important class of hydrogels are the stimuli responsive gels [1.21]. These gels show swelling behavior dependent on their physical environment. These gels can swell, or deswell in response to changes in pH, temperature, ionic strength, and electromagnetic radiation [1.27]. These properties allow for usage in a number of applications, such as separation membranes, biosensors, artificial muscles, and drug delivery devices [1.15].

### **1.4 Preparation Methods of Hydrogels**

Hydrogels are polymeric networks. This implies that crosslinks have to be present in order to avoid dissolution of the hydrophilic polymer chain in aqueous solution. Hydrogels are most frequently used for controlled release of bioactive agents and for encapsulation of cells and

biomolecules. In many of these cases the three dimensional structure of the hydrogels have to disintegrate into harmless non toxic products to ensure biocompatibility of the gel. The nature of the degradation products can be tailored by a proper selection of the hydrogel building blocks. Keeping this consideration in mind, various chemical and physical crosslinking methods are used today for the design of biocompatible hydrogels. Chemically crosslinked gels have ionic or covalent bonds between polymer chains. Even though this leads to more mechanical stability, some of the crosslinking agents used can be toxic, and give unwanted reactions, thus rendering the hydrogel unsuitable for biological use. These adverse effects can be removed with the use of physically crosslinked gels. In physically crosslinked gels, dissolution is prevented by physical interactions between different polymer chains. Both of these methods are used today for preparation of synthetic hydrogels and are discussed in detail. In this paper, the hydrogels were crosslinked via free radical polymerization on exposure to UV radiation, without the use of a crosslinking agent.

#### **1.4.1 Chemically Crosslinked Gels**

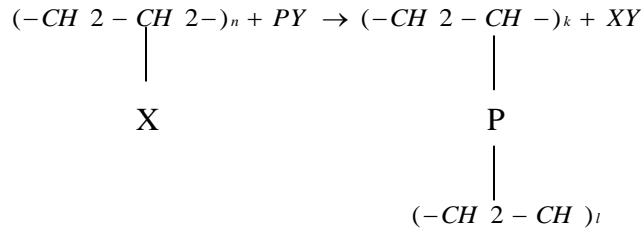
As stated earlier, chemically crosslinked gels are mechanically quite stable due to the ionic and covalent bond which comprises these gels. However the addition of crosslinking agent leads to adverse effects if the compound is toxic, which on liberation in the body becomes quite harmful. The various methods for chemical crosslinking are as follows:

- Crosslinking of Polymers

In this method chemically crosslinked gels are formed by radical polymerization of low molecular weight monomers, or branched homopolymers, or copolymers in the presence of crosslinking agent. This reaction is mostly carried out in solution for biomedical applications. Most hydrophilic polymers have pendant hydroxyl group, thus agents such as aldehydes, maleic and oxalic acid, dimethylurea, diisocyanates etc that condense when organic hydroxyl groups

are used as crosslinking agents. The solvent used for these reactions is usually water, but methanol, ethanol and benzyl alcohol have also been used. These solvents can be used only if after formation of network structure, the solvent can be exchanged with water.

A typical reaction scheme for this type of crosslinking is shown [1.37]:



**Equation 1.1 Typical reaction scheme for Flory type crosslinked structure.**

End-linking and crosslinking reactions may also occur in the absence of cross-linking agents if a free radical initiator can be used which forms free radicals in the backbone chain.

• Copolymerization/Crosslinking Reactions

Copolymerization reactions are used to produce polymer gels, Many hydrogels are produced in this fashion, for example poly (hydroxyalkyl methylacrylates). Initiators used in these reactions are radical and anionic initiators. Various initiators are used, such as Azobisisobutyronitrile (AIBN), benzoyl peroxide etc. Solvents can be added during the reaction to decrease the viscosity of the solution.

○ Kinetic Mechanism

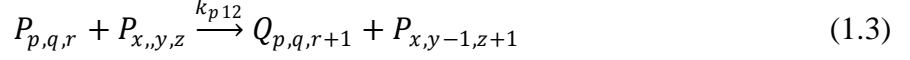
The whole crosslinking mechanism consists of four steps: initiation, propagation, crosslinking, and termination. Termination can occur by combination, disproportionation, and chain transfer to monomer. An example of a representative reaction scheme follows [1.37]:

*Initiation*

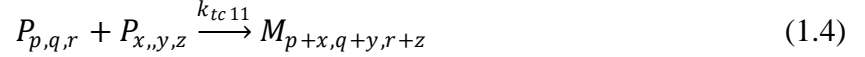




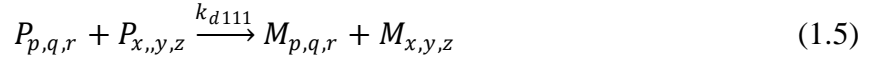
*Propagation and cross-linking*



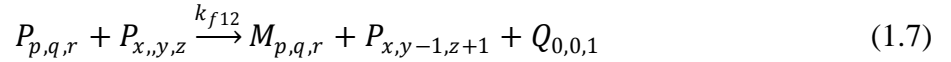
*Termination by combination*



*Termination by disproportionation*



*Chain Transfer to monomer*



HEMA as the monomethacryl monomer and EGDMA as the dimethylacryl monomer, I is the initiator, and A is a molecule with initiated radical. Here  $P_{p,q,r}$  and  $Q_{p,q,r}$  represent living polymer chains with monomethacryl and dimethylacryl monomer terminal groups, respectively and  $M_{p,q,r}$  us dead polymer chain. The subscripts p, q, r are used to describe primary chain; they refer to monomethacryl units, pendant methacryl groups, and cross-links per chain respectively.

- Crosslinking by High Energy Radiation

High energy radiation, such as gamma [1.38] and electron beam radiation can be used to polymerize unsaturated compounds. Water soluble polymers derivatized with vinyl groups can be converted into hydrogels using high energy radiation. For example, PEG derivatized to PEGDA can form hydrogels once irradiated with UV radiations. Polymers without additional vinyl groups can also be crosslinked via radiation. On exposure to gamma or electron beam

radiation, aqueous solutions of polymers form radicals on the polymer chains (e.g by the hemolytic scission of C-H bonds). Also the radiolysis of water molecules generates the formation of hydroxyl groups which can attack polymer chains also resulting in the formation of microradicals. Recombination of these microradicals on different chains results in the formation of covalent bonds and finally in a crosslinked structure. The swelling and permeability characteristics of the gel depend on the extent of polymerization, a function of polymer and radiation dose (in general crosslinking density increases with increasing radiation dose). The advantage of using this process for gel formation is that it can be done in water under mild conditions without the use of a crosslinking agent. However there are some drawbacks to using this method, the bioactive material has to be loaded after gel formation, as irradiation might damage the agent. Also in some gels like PEG and PVA, the crosslinks consist of C-C bonds, which are not biodegradable.

- Crosslinking Using Enzymes

Recently a new method was published [1.5] using an enzyme to synthesize PEG-based hydrogels. A tetrahydroxy PEG was functionalized with addition of glutaminy groups and networks were formed by addition of transglutaminase into solution of PEG and poly (lysine-co-phenylalanine). This enzyme catalyzed reaction between  $\gamma$ -carboxamide group of PEG and the  $\epsilon$ - amine group of lysine to obtain an amide linkage between polymers. The gel properties can be tailored by changing ratios of PEG and lysine.

#### **1.4.2 Physically Crosslinked Gels**

Chemically crosslinked gels imply use of a crosslinking agent, which is often toxic. This requires that the crosslinking agent be removed from gel, which can affect the gel integrity. For these reasons, physically crosslinked gels are now coming into prominence. Several methods

have been investigated exploring preparation of physically crosslinked gels. Below are mentioned some of the most widely used methods and their areas of application.

- Crosslinking by Ionic Interactions

An example of crosslinking via ionic interactions is crosslinking of Alginate. Alginate consists of glucuronic acid residues and mannuronic residues and can be crosslinked by calcium ions. Crosslinking can be carried out at normal temperature and pH. These gels are used as matrix for encapsulation of cells and for release of proteins. Also Chitosan based hydrogels, as well as dextran based hydrogels, crosslinked with potassium ions are also other gels synthesized with ionic interactions. In addition to anionic polymers being crosslinked with metallic ions, hydrogels can also be obtained by complexation of polyanions and polycations.

- Crosslinking by Crystallization

An aqueous solution of PVA that undergoes a freeze-thaw process yields a strong highly elastic gel. Gel formation is attributed to the formation of PVA crystallites which act as physical crosslinking sites in the network. The gel properties could be modified by varying polymer concentration, temperature, and freezing and thawing cycle times. These gels have been shown to be useful for drug release [1.9].

- Crosslinking by Hydrogen Bonds

Poly(acrylic acid) and poly(methacrylic acid) form complexes with poly(ethylene glycol) by hydrogen bonding between the oxygen of the poly(ethylene glycol) and the carboxylic acid group of poly((meth)acrylic acid) [1.3]. Also hydrogen bonding has been observed in poly (methacrylic acid-g-ethylene glycol). The hydrogen bonds are only formed when the carboxylic acid groups are protonated. This also implies that the swelling of gels is pH dependent. Recently a hydrogel system was developed using the principle of DNA hybridization via hydrogen bonding [1.11]. In this approach, oligodeoxyribonucleotides were coupled to a

water soluble polymer. Hydrogels were prepared by addition of a complementary oligonucleotide (ODN) either conjugated to the same water soluble polymer or, in its free form, to an aqueous solution of the ODN derivatized water soluble copolymer.

- By Protein Interaction

Genetic Engineering has also been used for the preparation of hydrogels. The major advantage is that the sequence of peptides and, therefore its physical and chemical properties can be precisely controlled by the proper design of the genetic code in synthetic DNA sequences [1.12]. Cappello and colleagues prepared sequential block copolymers containing a repetition of silk-like and elastine –like blocks, in which the insoluble silk like segments are associated in the form of aligned hydrogen bonded beta strands or sheets. These hydrogels can also be used for drug delivery with drug release influenced by concentration, polymer composition, and temperature. Crosslinking by antigen-antibody interaction was also performed [1.13], in which an antigen (rabbit IgG) was grafted to chemically crosslinked polyarylaide in the presence of an additional crosslinker. Additionally hydrogels have been prepared by immobilizing both the antigen and the antibody in the form of an interpenetrating network polymer network. This approach might permit drug delivery in response to specific antigen.

## **1.5 Monomers Used for Fabrication of Hydrogels**

The monomers used for fabrication of these biocompatible hydrogels have expanded from a handful of choices, to several novel materials with tailor-made properties suited to particular applications. The first synthesis of hydrogel was that of Wichterle and Lin [1.17] using PHEMA (poly (hydroxyethyl methacrylate)) as the monomer. Depending upon the application, hydrogel monomers are chosen according to their properties, ease of delivery or encapsulations, as well as cost and availability. One of the most traditional monomers used for drug delivery of proteins is biodegradable PLGA (polymers of lactic and glycolic acid).

However these hydrophobic materials have a tendency to denature protein as well as cause inflammation due to degradation. These problems were overcome when researchers turned towards hydrophilic monomers. Monomers such as acrylic acid, polyethylene glycol, and methacrylic acid are all materials used in therapeutic applications. Researchers are today trying to custom-make materials to suit specific applications. PNIPAAm (poly (N-isopropylacrylamide), PVA (polyvinyl alcohol) are all synthesized by new preparation techniques, for distinct applications. Table 1.1 provides a list of popular monomers used for biomaterial synthesis.

**Table 1.1 Monomers used in synthesis of hydrogels for pharmaceutical applications. From Table 1 in ref [1.16]**

Monomer abbreviation	Monomer
HEMA	Hydroxyethyl methacrylate
HEEMA	Hydroxyethoxyethyl methacrylate
HDEEMA	Hydroxydiethoxyethyl methacrylate
MEMA	Methoxyethyl methacrylate
MEEMA	Methoxyethoxyethyl methacrylate
MDEEMA	Methoxydiethoxyethyl methacrylate
EGDMA	Ethylene glycol dimethacrylate
NVP	<i>N</i> -vinyl-2-pyrrolidone
NIPAAm	<i>N</i> -isopropyl AAm
VAc	Vinyl acetate
AA	Acrylic acid
MAA	MAA
HPMA	<i>N</i> -(2-hydroxypropyl) methacrylamide
EG	Ethylene glycol
PEGA	PEG acrylate
PEGMA	PEG methacrylate
PEGDA	PEG diacrylate
PEGDMA	PEG dimethacrylate

## 1.6 PEG (polyethylene glycol) as Suitable Material

It is known that hydrophilic monomers provide a distinct advantage in both fabrication and application of hydrogels. The premier material used today for both drug delivery, cell

encapsulation and as adhesion promoters is Poly (ethylene glycol) hydrogels. PEG has many unique properties which make it an ideal choice. PEG and its “stealth “ properties , that is once its attached to certain formulations, it allows slow release of the formulation, thus enabling controlled release, as well as reduce uptake of harmful immunoglobins. This allows longer dosage and reduces immunogenicity of substances such as adenosine deaminase (ADA) and asparaginase [1.22]. PEG is non toxic, thus ideal for biological applications, and can be injected into the body without adverse effects. It is also an FDA approved materials for use in humans. PEGylation is an important technique being developed for drug delivery, involves attachment of PEG to proteins and drugs, and has great potential for improving pharmokinetic and pharmodynamic properties of delivered drugs. Thus PEG has varied uses in the medical field, including drug delivery (e.g.; treatment of hepatitis C), laxatives, cell immobilization, (as adhesion promoters), biosensor materials, and encapsulation of islets of langerhans for treatment of diabetes. It is also used as carrier material for encapsulated cells for tissue engineering purposes. Thus PEG, with its biocompatibility, flexibility and stealth properties is an ideal material for use in pharmaceutical applications.

## **1.7 Applications of Hydrogels**

Water- swollen crosslinked hydrogels have varied applications in fields such as food additives [1.10], pharmaceutical [1.16] as well as biomedicine [1.14]. The pioneering work on crosslinked HEMA hydrogels was done by Wichterle and Lim in 1954[1.17]. From their research, and discovery of the hydrophilic and biocompatible properties of hydrogels, there emerged a new class of hydrogel technologies based on biomaterial application. Lim and Sun [1.18] in 1980 demonstrated the successful use of calcium alginate microcapsules for cell encapsulation. Later natural polymers such as collagen, and shark cartilage were incorporated into hydrogels as wound dressings. Natural and synthetic polymers are used for encapsulation of

cells, as well as encapsulation of islets in a semipermeable membrane [1.19]. Hydrogels have been used to prevent adhesions and prevent thrombosis after surgery [1.21], and as cell adhesion resistant surfaces [1.13]. Microfabricated hydrogel arrays are also used for biosensing[1.25]. Hydrogels now play an important role in tissue engineering scaffolds, biosensor and BioMEMS devices and drug carriers.

Among these applications, hydrogel-based drug delivery devices have become a major area of study, and several commercially available products are already in the market [1.36]. Proteins, peptides, DNA based drugs can all be delivered via hydrogel carrier devices. The various properties of hydrogels such as biocompatibility, hydrophilicity, flexibility all make it ideal for use as drug delivery matrix.

Hydrogels show good compatibility with blood and other body fluids, thus are used as materials for contact lenses, burn wound dressings, membranes, and as coating applied to living surfaces. Natural and synthetic polymers have applications as wound dressings [1.32], encapsulation of cells [1.26], and recently are being used in the new field of tissue engineering as matrices for repairing and regenerating a wide variety of tissues and organs [1.23]. When parts, or whole tissues, organs fail, treatments include repair, replacement with a natural or synthetic substitute, or regeneration. Implants have been reasonably successful; however tissue engineering holds great promise for regeneration. Hydrogels are now being considered as ideal matrices for tissue engineering [1.23].

### **1.7.1 Drug Delivery**

Treatment of diseases has always been a major issue for researchers for as long as mankind has existed. As technology has advanced, proteins, peptides, and other materials have been identified as “drugs” which can be used to treat physiological life processes, pain, and discomfort. Drugs can vary in their characteristics to the extent that drugs used to treat the same

symptoms might differ in characteristics such as hydrophilicity, chemical composition, size and effectiveness. An increasing understanding of cellular biology at the molecular level and breakthroughs in proteomics have led to the concept of gene delivery. Drugs have to reach the site of action following administration (oral intravenous, transdermal etc) in a specific manner and in specific quantity. This is the basis of the drug delivery field. Drug delivery aims at delivering the right drug at the right place, at right concentration for the right period of time. Sometimes direct delivery of such drugs is difficult, due to the treacherous route of delivery or discomfort caused to the patient. For such cases, strategies have been developed for delivering drug with a carrier. The drug carrier, whether it be an implantable device, or long chain polymer must be biocompatible with the drug and the body. Drug delivery systems alter the biodistribution and pharmacokinetics of the drug. Therefore one must take into account obstacles such as drug solubility, enzyme degradation, toxicity, inability to cross biological barriers as well as adverse environmental conditions. In order to make the delivery of the drug effective without causing an immune response in the body, proper design and engineering of the drug delivery system is essential.

### **1.7.2 Hydrogels in Drug Delivery**

Localized drug delivery can be achieved by introducing the drug directly at the target site. The major class of biomaterials considered as implantable drug delivery systems are hydrogels. These hydrophilic networks are capable of absorbing great amounts of water while maintaining structural integrity [1.37]. Their structural similarity to the extracellular matrix makes it biocompatible. These synthetic polymers have generated wide interests and are now at the forefront of drug delivery research.

In order to incorporate a preformed gel into the body, an opening must be created, with at least the same dimension as that of the gel. This leads to potential risk and discomfort to the

patient. Thus focus has shifted to developing injectable materials with ability to form three dimensional matrices under physiological matrices. This in situ formation can be achieved through specific chemical crosslinking reactions. Gel structuring is triggered by environmental stimuli (pH, temperature, solvent exchange etc). Synthetic hydrogels, with their ability to imbibe water, flexibility, and biocompatibility, are ideal carriers for the development for novel pharmaceutical formulations and for the delivery of drugs, proteins, and as targeting agents for drug delivery. The network structure and the nature of components play a key role in the diffusional behavior, molecular mesh size changes, and stability of the incorporated bioactive agent. The use of hydrogels allows not only delivery of drugs, but also controlled release, in the manner required by the pharmaceutical scientists. For example, drugs can be delivered only when needed, may be directed to specific site, and can be delivered at specific rates required by the body. In the last 20 years, advanced drug delivery formulations have been examined in great detail. Reviews related to the various applications of hydrogels in drug delivery and various sites available in the body for such are readily available [1.7, 1.2,1.1].

### **1.7.3 Properties Useful in Drug Delivery**

Hydrogels possess several properties that make them an ideal material for drug delivery. First, hydrogels can be tailored to respond to a number of stimuli [1.15]. This enables sustained drug delivery corresponding to external stimuli such as pH or temperature. These pH sensitive gels are useful in oral drug delivery as they can protect proteins in the digestive track. pH responsiveness is also useful for lysosomal escape during gene delivery. Second, Hydrogels can also be synthesized to exhibit bioadhesiveness to facilitate drug targeting, especially through mucus membranes, for non-invasive drug administration [1.30]. Finally, Hydrogels also have a “stealth” characteristic in vivo circulation time of delivery device by evading the host immune response and decreasing phagocytic activity [1.20].

#### **1.7.4 Applications of Hydrogels in Drug Delivery**

Advances in recombinant protein technology have identified several protein and peptide therapeutics for disease treatment. However, the problem which plagued researchers was how to effectively deliver these biomolecules. Due to their large molecular weight, and three dimensional structure, the most commonly used route for drug administration is by intravenous or subcutaneous injection. Unfortunately proteins and peptides are prone to proteolytic degradation, thus they experience short plasma circulation times and rapid renal clearance, leading to multiple daily injections or increased dosage in order to maintain the required drug therapeutic levels . Multiple injections are difficult for the patient, while high doses might be toxic, and induce serious immune response. Hydrophobic polymeric controlled release formulations, such as PLGA, offer a sustained release mechanism in which drug release rates can manipulated by changing polymer molecular weight and composition. These polymers however induce adverse effects to the encapsulated proteins or peptides during network preparation and delivery [1.16], as well as trigger the immune response. Hydrophilic hydrogels, on the other hand, provide relatively mild network fabrication technique and drug encapsulation conditions, making them the ideal material for use in drug delivery. Thus hydrogels are primarily used for encapsulation of bioactive materials and their subsequent controlled release. If designed properly, hydrogels can be used in a variety of applications such as sustained, targeted, or stealth biomolecule delivery. Hydrogel based delivery devices can be used for oral, ocular, epidermal and subcutaneous application. The Fig 1.1 below indicates various sites that are available for the application of hydrogels for drug delivery. These applications are discussed in detail below.

- Drug Delivery in the GI Tract

The ease of administration of drugs, and the large surface area for absorption makes the GI tract most popular route for drug delivery. It is however, also a very complex route, so that versatile approaches are needed to deliver drugs for effective therapy. Hydrogel-based devices can be designed to deliver drugs locally to specific sites in the GI tract.

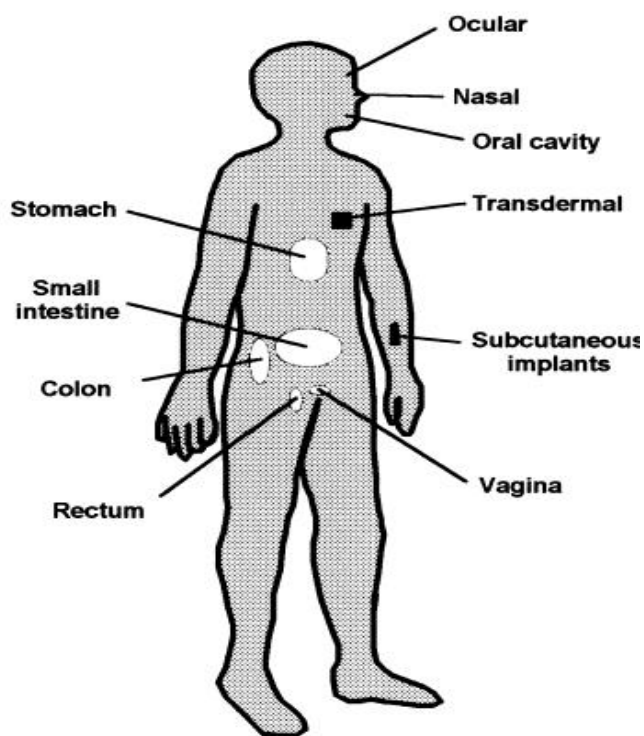


**Figure 1.1 Tissue locations applicable for hydrogel based drug delivery systems. From Figure 2 in ref [1.16]**

For example, Patel and Amiji [1.35] proposed stomach –specific antibiotic drug delivery systems for the treatment of *Helicobacter pylori* infection in peptic ulcer disease. They developed cationic hydrogels with pH sensitive swelling and drug release properties for antibiotic delivery in the acidic environment of the stomach. There are still many drawbacks for peroral delivery of peptides and proteins to GI tract, like protein inactivation by digestive enzymes in the GI tract and poor epithelial permeability of the drugs. However certain

hydrogels may overcome some of these problems by appropriate molecular design or formulation. For example Akiyama [1.26] reported novel peroral dosage forms of hydrogel formulations with protease inhibitory activities.

Recently oral insulin delivery using pH responsive complexation hydrogels was reported [1.37]. The hydrogels used were crosslinked copolymers of PMMA with graft chains of polyethylene glycol. These hydrogels protect the insulin in the harsh, acidic environment of the stomach before releasing the drug in the small intestine.

The colonic region has also been considered as a possible absorption site for orally administered proteins and peptides, mostly due to a lower proteolytic activity in comparison to that in the small intestine. Several hydrogels are currently being investigated as potential devices for colon-specific drug delivery. These include chemically or physically crosslinked polysaccharides such as dextran [1.8], guar gum [1.28] and insulin [1.18]. They are designed to be highly swollen or degraded in the presence of colonic enzymes or microflora, providing colon-specificity in drug delivery.

- Rectal Delivery

This route has been used to deliver many types of drugs for treatment of diseases associated with the rectum, such as hemorrhoids. This route is an ideal way to administer drugs suffering heavy first-pass metabolism. There are however, some drawbacks associated with rectal delivery. For example, due to discomfort arising from given dosage forms, there is substantial variability in patient's acceptance of treatment. Also, if drugs diffusing out of the suppositories are delivered in an uncontrolled manner, they are unable to be retained at a specific position in the rectum, and tend to migrate upwards to the colon. This leads to variation of availability of drugs, especially those that undergo extensive first-pass elimination.

Hydrogels offer a way in which to overcome these limitations, provided that the hydrogels show bioadhesive properties. It was reported [1.19] that increased bioavailability of propanol subject to extensive first-pass metabolism was observed by adding certain mucoadhesive polymeric compounds to poloxamer –based thermally gelling suppositories. The polymeric compounds tested were polycarbophil and sodium alginate. Miyazaki et al. [1.34] investigated the potential application of xyloglucan gels with a thermal gelling property as matrices for drug delivery. Another important issue in rectal drug delivery is to avoid rectal irritation. The products discussed above, indicated no such mucosal irritation after drug administration.

- Ocular Delivery

Drug delivery to the eye is difficult due to its protective mechanisms, such as effective tear drainage, blinking, and low permeability of the cornea. Thus, eye drops containing drug solution tends to be eliminated rapidly from the eye and the drugs show limited absorption, leading to poor ophthalmic bioavailability. Due to the short retention time, a frequent dosing regimen is necessary for required therapeutic efficacy. These challenges have motivated researchers to develop drug delivery systems that provide prolonged residence time.

The earlier dosage forms, such as suspension and ointments could be retained in the eye, but sometimes gave patients an unpleasant feeling because of the nature of solids and semi-solids. Hydrogels, because of their elastic properties can represent an ocular drainage-resistant device. In-situ forming hydrogels are attractive as an ocular drug delivery system because of their facility in dosing as a liquid, and long term retention property as a gel after dosing.

Cohen et al [1.26] developed an in-situ gelling system of alginate with high gluronic acid contents for the ophthalmic delivery of pilocarpine. This system extended the duration of the pilocarpine to 10 hr, compared to 3 hr when pilocarpine nitrate was dosed as a solution. Chetoni

et al.[1.34] reported silicone rubber hydrogel composite ophthalmic inserts. An in-vivo study using rabbits showed a prolonged release of oxytetracycline from the inserts for several days.

- Transdermal Delivery

Drug delivery to the skin has been generally used to treat skin diseases or for disinfection of the skin. In recent years, however a transdermal route for the delivery of drugs has been investigated. Swollen hydrogels can be delivered for long duration and can be easily removed. These hydrogels can also bypass hepatic first-class metabolism, and are more comfortable for the patient. Hydrogel based delivery devices have been proposed by Sun et al. [1.4], such as composite membranes of crosslinked PHEMA with a woven polyester support. Also hydrogels have been reported [1.11] which have been obtained by the copolymerization of bovine serum albumin (BSA) and PEG. These hydrogels can be used as controlled release devices in the field of wound dressing. Hubbell [1.12] has also carried out extensive research on in-situ photopolymerization made from terminally diacrylated ABA block copolymers of lactic acid oligomers (A) and PEG (B) for barriers and local drug delivery in the control of wound healing.

Current research in this field is now focused on electrically-assisted delivery using iontophoresis and electroporation [1.35]. Hydrogel-based formulations are being looked at for transdermal iontophoresis to obtain enhanced permeation of products in question such as, hormones [1.35] and nicotine.

- Subcutaneous Delivery

Among the varied possible pharmaceutical applications of hydrogels, the most substantial application is probably in implantable therapeutics. Implantable devices that are subcutaneously inserted tend to illicit immune response of the body, leading to inflammation, carcinogenicity and immunogenicity. Thus biocompatibility becomes a major issue, and all

implantable materials must be compatible with the body. Hydrogels are an ideal candidate for implantable materials. They have high water content, environment similar to biological tissue, making them relatively biocompatible. They also have other properties which make them a viable choice [1.1]; (1) minimal mechanical irritation upon in-vivo implantation due to their soft, elastic properties (2) prevention of protein absorption and cell adhesion arising from the low interfacial tension between water and hydrogels (3) broad acceptability for individual drugs with different hydrophilicities and molecular sizes, and (4) can manipulate crosslinking density and swelling for release of incorporated drug in specific manner. Thus hydrogels are an ideal material to be used for delivery of proteins and peptides.

Hydrogel formulations for subcutaneous delivery of anticancer drugs have been proposed. For example, crosslinked PHEMA was applied to cyratabine (Ara-C) [1.6]. Current studies on implantable hydrogels are leading towards the development of biodegradable systems, which don't require surgical removal once the drug has been administered. Biodegradable PEG hydrogels are now at the forefront of this research, and several novel systems have been developed. One type is synthesized via a polycondensation reaction between functional PEG acids and branched PEG polyols. Another type is PEG based hydrogels having functional groups in which the protein drugs can be covalently attached to the gel network via ester linkages. In this case, the release of the immobilized proteins would be controlled by the hydrolysis of ester linkage between the gel and protein, followed by diffusion of protein, and degradation of gel.

## 1.8 References

- 1.1. Park, H. and K. Park, *Biocompatibility Issues of Implantable Drug Delivery Systems*. Pharmaceutical Research, 1996. **13**(12): p. 1770-1776.
- 1.2. Nagai, T. and Y. Machida, *Buccal delivery systems using hydrogels*. Advanced Drug Delivery Reviews, 1993. **11**(1-2): p. 179-191.

- 1.3. Eagland, D., N.J. Crowther, and C.J. Butler, *Complexation between polyoxyethylene and polymethacrylic acid--the importance of the molar mass of polyoxyethylene*. European Polymer Journal, 1994. **30**(7): p. 767-773.
- 1.4. Sun, Y.-M., et al., *Composite poly(2-hydroxyethyl methacrylate) membranes as rate-controlling barriers for transdermal applications*. Biomaterials, 1997. **18**(7): p. 527-533.
- 1.5. Sperinde, J.J. and L.G. Griffith, *Control and Prediction of Gelation Kinetics in Enzymatically Cross-Linked Poly(ethylene glycol) Hydrogels*. 2000. p. 5476-5480.
- 1.6. Teijon, J.M., et al., *Cytarabine trapping in poly(2-hydroxyethyl methacrylate) hydrogels: drug delivery studies*. Biomaterials, 1997. **18**(5): p. 383-388.
- 1.7. Serra, L., J. Domenech, and N.A. Peppas, *Design of poly(ethylene glycol)-tethered copolymers as novel mucoadhesive drug delivery systems*. European Journal of Pharmaceutics and Biopharmaceutics, 2006. **63**(1): p. 11-18.
- 1.8. Simonsen, L., et al., *Dextran hydrogels for colon-specific drug delivery. V. Degradation in human intestinal incubation models*. European Journal of Pharmaceutical Sciences, 1995. **3**(6): p. 329-337.
- 1.9. Takamura, A., F. Ishii, and H. Hidaka, *Drug release from poly(vinyl alcohol) gel prepared by freeze-thaw procedure*. Journal of Controlled Release, 1992. **20**(1): p. 21-27.
- 1.10. Chen, X., et al., *Enzymatic and chemoenzymatic approaches to synthesis of sugar-based polymer and hydrogels*. Carbohydrate Polymers, 1995. **28**(1): p. 15-21.
- 1.11. Gayet, J.C. and G. Fortier, *High water content BSA-PEG hydrogel for controlled release device: Evaluation of the drug release properties*. Journal of Controlled Release, 1996. **38**(2-3): p. 177-184.
- 1.12. Hubbell, J.A., *Hydrogel systems for barriers and local drug delivery in the control of wound healing*. Journal of Controlled Release, 1996. **39**(2-3): p. 305-313.
- 1.13. Peppas, N.A. and J.J. Sahlin, *Hydrogels as mucoadhesive and bioadhesive materials: a review*. Biomaterials, 1996. **17**(16): p. 1553-1561.
- 1.14. Hoffman, A.S., *Hydrogels for biomedical applications*. Advanced Drug Delivery Reviews, 2002. **54**(1): p. 3-12.
- 1.15. Lin, C.-C. and A.T. Metters, *Hydrogels in controlled release formulations: Network design and mathematical modeling*. Advanced Drug Delivery Reviews, 2006. **58**(12-13): p. 1379-1408.
- 1.16. Peppas, N.A., et al., *Hydrogels in pharmaceutical formulations*. European Journal of Pharmaceutics and Biopharmaceutics, 2000. **50**(1): p. 27-46.

- 1.17. Wichterle, O. and D. Lim, *Hydrophilic Gels for Biological Use*. Nature, 1960. **185**(4706): p. 117-118.
- 1.18. Kim, B. and N.A. Peppas, *In vitro release behavior and stability of insulin in complexation hydrogels as oral drug delivery carriers*. International Journal of Pharmaceutics, 2003. **266**(1-2): p. 29-37.
- 1.19. Ryu, J.-M., et al., *Increased bioavailability of propranolol in rats by retaining thermally gelling liquid suppositories in the rectum*. Journal of Controlled Release, 1999. **59**(2): p. 163-172.
- 1.20. Veronese, F.M., et al., *Influence of PEGylation on the Release of Low and High Molecular-Weight Proteins from PVA Matrices*. 1999. p. 315-330.
- 1.21. Ji, H., et al., *Kinetics of thermally induced swelling of hydrogels*. International Journal of Solids and Structures, 2006. **43**(7-8): p. 1878-1907.
- 1.22. Russell, R.J., et al., *Mass transfer in rapidly photopolymerized poly(ethylene glycol) hydrogels used for chemical sensing*. Polymer, 2001. **42**(11): p. 4893-4901.
- 1.23. Lee, S.-H. and H. Shin, *Matrices and scaffolds for delivery of bioactive molecules in bone and cartilage tissue engineering*. Advanced Drug Delivery Reviews. **In Press, Corrected Proof**.
- 1.24. De Laporte, L. and L.D. Shea, *Matrices and scaffolds for DNA delivery in tissue engineering*. Advanced Drug Delivery Reviews. **In Press, Corrected Proof**.
- 1.25. Yadavalli, V.K., et al., *Microfabricated protein-containing poly(ethylene glycol) hydrogel arrays for biosensing*. Sensors and Actuators B: Chemical, 2004. **97**(2-3): p. 290-297.
- 1.26. Cohen, S., et al., *A novel in situ-forming ophthalmic drug delivery system from alginates undergoing gelation in the eye*. Journal of Controlled Release, 1997. **44**(2-3): p. 201-208.
- 1.27. Dolbow, J., E. Fried, and H. Ji, *A numerical strategy for investigating the kinetic response of stimulus-responsive hydrogels*. Computer Methods in Applied Mechanics and Engineering, 2005. **194**(42-44): p. 4447-4480.
- 1.28. George, M. and T.E. Abraham, *pH sensitive alginate-guar gum hydrogel for the controlled delivery of protein drugs*. International Journal of Pharmaceutics, 2007. **335**(1-2): p. 123-129.
- 1.29. Patel, V.R. and M.M. Amiji, *Preparation and Characterization of Freeze-dried Chitosan-Poly(Ethylene Oxide) Hydrogels for Site-Specific Antibiotic Delivery in the Stomach*. Pharmaceutical Research, 1996. **13**(4): p. 588-593.

- 1.30. Achar, L. and N.A. Peppas, *Preparation, characterization and mucoadhesive interactions of poly (methacrylic acid) copolymers with rat mucosa*. Journal of Controlled Release, 1994. **31**(3): p. 271-276.
- 1.31. Peppas, N.A. and A.R. Khare, *Preparation, structure and diffusional behavior of hydrogels in controlled release*. Advanced Drug Delivery Reviews, 1993. **11**(1-2): p. 1-35.
- 1.32. Aji, Z., I. Othman, and J.M. Rosiak, *Production of hydrogel wound dressings using gamma radiation*. Nuclear Instruments and Methods in Physics Research Section B: Beam Interactions with Materials and Atoms, 2005. **229**(3-4): p. 375-380.
- 1.33. Ritger, P.L. and N.A. Peppas, *A simple equation for description of solute release I. Fickian and non-fickian release from non-swellable devices in the form of slabs, spheres, cylinders or discs*. Journal of Controlled Release, 1987. **5**(1): p. 23-36.
- 1.34. Miyazaki, S., et al., *Thermally reversible xyloglucan gels as vehicles for rectal drug delivery*. Journal of Controlled Release, 1998. **56**(1-3): p. 75-83.
- 1.35. Fang, J.-Y., et al., *Transdermal iontophoresis of sodium nonivamide acetate: V. Combined effect of physical enhancement methods*. International Journal of Pharmaceutics, 2002. **235**(1-2): p. 95-105.
- 1.36. Panza, J.L., et al., *Treatment of rat pancreatic islets with reactive PEG*. Biomaterials, 2000. **21**(11): p. 1155-1164.
- 1.37. N.A. Peppas: *Hydrogels in Medicine and Pharmacy, Vol. 1. Fundamentals*, CRC Press, Boca Raton, FL, 1986, 180 pages.
- 1.38. Malcolm B. Huglin, M.B.Z., *Swelling properties of copolymeric hydrogels prepared by gamma irradiation*. 1986. p. 457-475

# Chapter 2 : Network Structure

## 2.1 Introduction

The properties of the hydrogel which make it favorable for use in various pharmaceutical as well as medicinal purposes arise mostly from its crosslinked structure. The crosslinked structure of the gel is determined by the nature of monomers, method of preparation, and nature of crosslinking agent. To understand the crosslinked structure of the gel, the most common approach used is the study of gel swelling. The swelling of the gel is studied and certain parameters of swelling are calculated. Knowledge of the swelling characteristics of the gel is the first step in understanding the network structure of the gel and its capacity to function as a drug delivery carrier. Several theories have been proposed to explain the network structure of the gel, as well as the mechanism of swelling of gel. Some theories take into account the real network structure with defects, while others consider ideal network structure, due to its simplicity in analysis. In each of these cases, the hydrogel is exposed to a penetrant solvent and allowed to swell until equilibrium is reached. Once the hydrogel is exposed to solvent, the gel swells, and the thermodynamically driven swelling force is counterbalanced by the retractive force of the crosslinked structure, leading to an equilibrium state. This swollen state allows widening of the gap between the crosslinks and mesh size, thus facilitating the transfer of different solutes through the gel. The transfer of the solute is controlled by the swelling of the gel. Once this information is known, the gel can be manipulated by varying mesh size, and property of drug to enable diffusion of required drug in specific manner.

## 2.2 Cross Linked Structure

Hydrogels are actually cross linked three dimensional matrices, which can be formed by covalent, ionic, and, in some cases, by Van der waals and hydrogen bonds [2.12]. The network structure of the hydrogel depends on its constituent monomers, the method of preparation and method of crosslinking. Most hydrogels used for biomedical applications are noncrystalline. These networks contain localized ordered structures or nonhomogenous structures, unlike the common Flory [2.3] picture of a randomly crosslinked mass of molecular chains. Characterization of the hydrogel network structure is quite complicated because of the many types of possible networks, including regular, irregular, loosely crosslinked, highly crosslinked and imperfect networks. For the purposes of characterizing the network structure for medical applications, an ideal network of chains is usually assumed. An ideal network that is, a Gaussian network is usually assumed, with a collection of Gaussian chains between multifunctional junction points (crosslinks). This Gaussian model has two significant assumptions [2.12].

- crosslinked polymer chains are represented by a Gaussian distribution . This implies that the end to end distance is much smaller than the contour length of the chain.
- Crosslinks, on an average are tetra functional.

### 2.2.1 Real Networks and Network Defects

Real polymer networks always deviate from the ideal Gaussian model. Imperfections can arise for a number of reasons. There might be deviations from the original conditions of crosslinking, crosslinking of already crosslinked networks and end-linking.

Imperfections which occur are generally of the following form [2.12]:

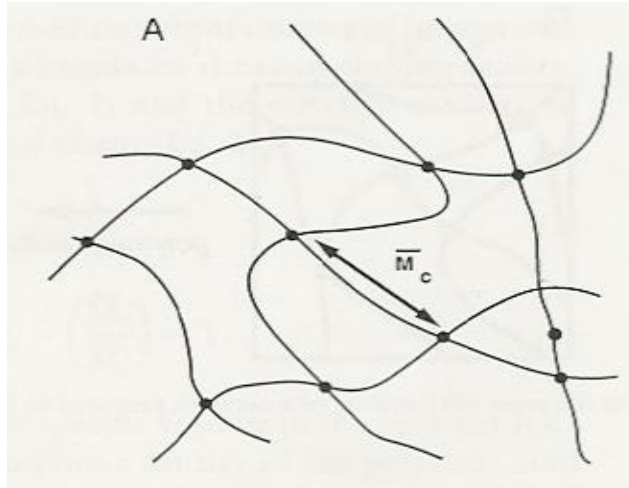


**Figure 2.1 Ideal Gaussian network  $\overline{M}_c$  is the molecular weight between crosslinks. From Fig 3 in ref[2.12]**

- Pre-Existing Order

These types of imperfections include crystallites showing three dimensional structure, non-randomly oriented segment sequences, artificially oriented chains, and micellar and globular structures. These are probably caused due to the association of dissimilar parts of the chain.

- Network Defects

These include closed loops, unreacted functionalities, and chain entanglements [Fig 2]

- Inhomogeneities
- Phase Separation Structures

Phase separation occurs when the critical value of crosslinking density is exceeded, because the amount of solvent in the gel has exceeded maximum swelling capacity.

### **2.3 Swelling Parameters and Their Significance**

As mentioned earlier, for biomedical purposes, the hydrogel network is considered to be ideal. In order to study the network structure of the hydrogels, it is essential that certain parameters of

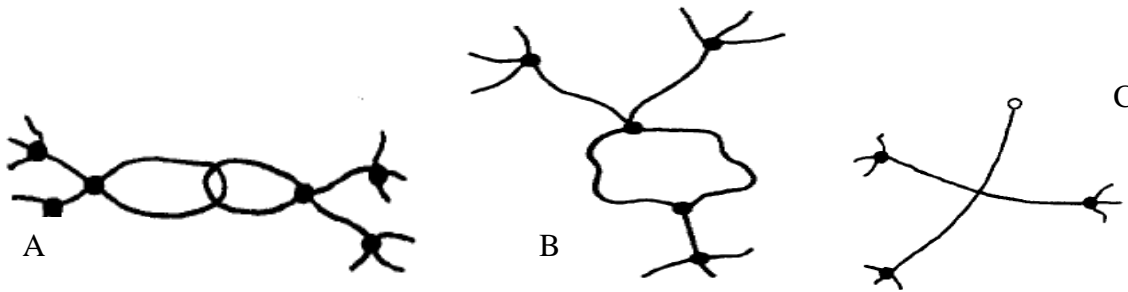


**Figure 2.2 Network Defects (A) Loops (B) Entanglements (C) Unreacted Functionality. From Fig 4 in ref[2.12]**

the gel network are determined. The most important parameters used to characterize network structure are the polymer volume fraction in the swollen state ( $v_{2,s}$ ), molecular weight of the polymer chain between two neighboring cross links ( $M_c$ ), and the corresponding mesh size ( $\xi$ ) [2.8]. Due to the random nature of the polymerization process, only average values of  $M_c$  can be calculated. The polymer volume fraction in the swollen state is a measure of the amount of fluid absorbed and retained by the gel.  $M_c$  is a measure of the degree of crosslinking of the polymer, regardless of the nature (physical or chemical) crosslinking. The mesh size, or the correlation distance between two adjacent crosslinks, provides a measure of the space available between the macromolecular chains available for diffusion and movement of particles. This is also an average value. These three parameters can be determined using the equilibrium swelling theory [2.3]. The three parameters are critical in describing the nanostructure of the crosslinked hydrogels.

- Polymer Volume Fraction

The polymer volume fraction is described as the ratio of the polymer volume ( $V_p$ ) to the swollen gel volume ( $V_g$ ). It is also a reciprocal of the volumetric swollen ratio ( $Q$ ), which can be related

to the densities of the solvent ( $\rho_1$ ) and polymer ( $\rho_2$ ) and the mass swollen ratio ( $Q_m$ ) as given by [2.5]:

$$v_{2,s} = \frac{V_p}{V_g} = Q^{-1} = \frac{\frac{1}{\rho_2}}{\frac{Q_m + 1}{\rho_1 \rho_2}} \quad (2.1)$$

- Molecular Weight Between Crosslinks

The average molecular weight between crosslinks  $\bar{M}_c$ , in gels crosslinked during polymerization is given by a modified version of the Flory-Rehner expression [2.8].

$$\frac{1}{\bar{M}_c} = \frac{2}{\bar{M}_n} - \frac{\left(\frac{v}{V_1}\right) [\ln(1-v_{2,s}) + v_{2,s} + \chi_1 v_{2,s}^2]}{v_{2,s}^{\frac{1}{3}} \frac{v_{2,s}}{2}} \quad (2.2)$$

Here  $\bar{M}_n$  is the average molecular weight of the linear polymer chains,  $v$  is the specific volume of polymer,  $V_1$  is the molar volume of water, and  $\chi_1$  is the polymer-water interaction parameter.

- Mesh Size

Mesh size can be described using the following equation [2.8]:

$$\xi = v_{2,s}^{-\frac{1}{3}} (\bar{r}_0^2)^{\frac{1}{2}} = Q^{\frac{1}{3}} (\bar{r}_0^2)^{\frac{1}{2}} \quad (2.3)$$

$(\bar{r}_0^2)^{1/2}$  is the root mean squared end to end distance of network chains between two adjacent crosslinks in the unperturbed state.

Once the nanostructure of the gel is known, a clear idea is obtained about its suitability for use in drug delivery. The amount of liquid retained, the distance between polymer chains, and flexibility of those chains together determine the mobility of the encapsulated molecule and their rates of diffusion within the matrix.

## 2.4 Significance of Mesh Size

For drug delivery formulations with matrix carrier, it is essential to understand the mechanism by which solute mass transfer takes place from the gel matrix to the specific site [2.2]. For non-biodegradable gels, diffusion is the main mechanism of transport of the solute, and in the case of hydrogels, this mass transfer is achieved by the swelling of the gel. To understand the mass transfer in the gel, one must study its water-sorption characteristics, thus obtaining a clear view of the morphological structure of the gel. Once the crosslinked gel is exposed to solvent, it absorbs the solvent and swells until it reaches its equilibrium swelling state. As the gel swells, the cross linked chains widen, thus increasing the mesh size and allowing solute transfer to take place from the gel. This degree of swelling is directly related to the amount of solute transfer, as shown below [2.5]:

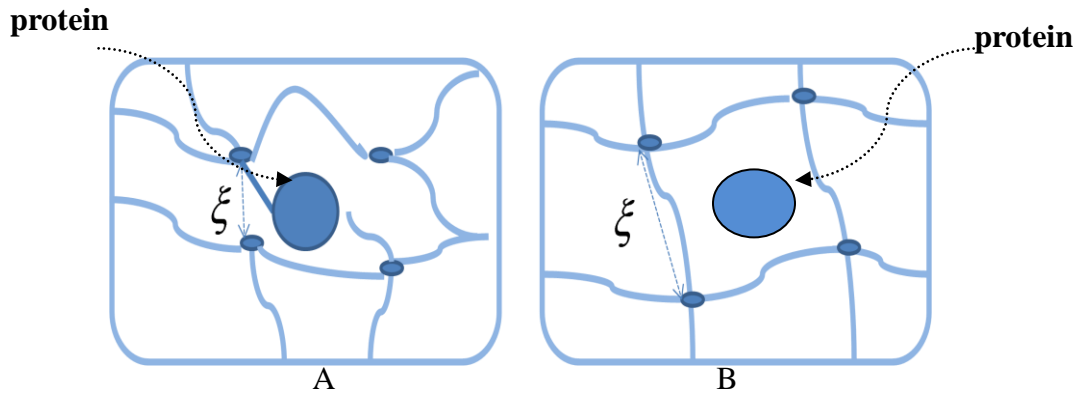


**Figure 2.3 Schematic of mesh size in hydrogels at (A) deswollen state (B) swollen state.  $\xi$  is mesh size. Adapted from Fig 1 in Ref [2.5].**

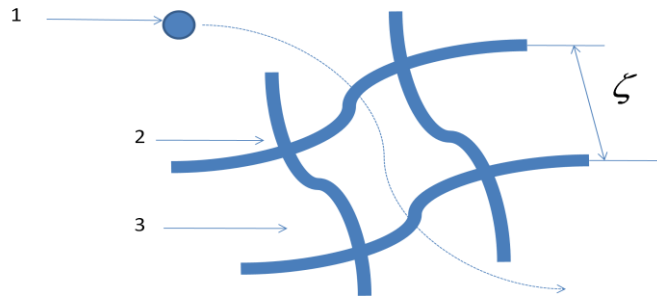


**Figure 2.4 Schematic of solute mass transfer in gel (1) solute traversing through network (2)crosslinked network (3) solvent surrounding gel. From Fig 1 in ref [2.13]**

Once the gel has imbibed liquid, the mesh size widens, allowing free passage of the solute in question. From the swelling experiments, mesh size of the gel can be determined. Once the mesh size has been calculated, it can be compared to the hydrodynamic diameter of solute molecules to determine whether diffusion of solute is possible. Theoretically no solute diffusion is possible within the matrix when the mesh size is close to the size of the solute [2.5].

Mesh size is affected by many factors [2.5]:

- Degree of crosslinking of the gel
- Stimuli such as temperature, pH and ionic strength
- Chemical structure of the constituting monomers

Mesh size is an important factor for determining mechanical strength, degradability, and diffusivity of the releasing molecule [2.9, 2.10, 2.1]. Most hydrogels used in biomedical applications have mesh sizes ranging from 5 to 100nm [2.7], in their swollen state. These size scales are much larger than most small molecular weight drugs used in pharmaceutical formulations, and, therefore, diffusion of these drugs in swollen matrices is not hindered. However large macromolecules, such as large molecular weight proteins, peptides, and oligonucleotides may be retarded in the swollen gel due to their large hydrodynamic radii in

comparison to the gel mesh size. If designed effectively, the structure and mesh size of the gel can be manipulated in order to obtain desired rates of macromolecule diffusion.

## 2.5 Swelling Theories

As mentioned earlier, there are different theoretical models used to determine the crosslinking density of a hydrogel. The two most commonly used theories to this end are the equilibrium swelling theory and the rubber elasticity theory [2.8].

### 2.5.1 Equilibrium Swelling Theory

This is the most well known model used to calculate the number average molecular weight between crosslinks. It is also known as the Gaussian model (Flory-Rehner). The model is based on two assumptions:

- The crosslinked polymer chains can be represented by a Gaussian distribution.
- The crosslinks on the average are tetrafunctional

If an uncrossed polymer is soluble in a certain solvent, then that same polymer, when crosslinked will swell on exposure to that solvent [2.7]. As the matrix is swollen by the liquid, the chains between the cross-links become elongated so that a force opposite to the elastic retractive force of the chain develops. On further swelling of the polymer matrix, the force increases whereas the thermodynamic force of dilution decreases. This theory states that these forces come to equilibrium that is the thermodynamic force of mixing and the retractive force of the polymer chain.

$$\Delta G_{total} = \Delta G_{elastic} + \Delta G_{mixing} \quad (2.4)$$

Here,  $\Delta G_{elastic}$  is the contribution due to the elastic forces developed inside the gel, and  $\Delta G_{mixing}$  is the result of spontaneous mixing of fluid molecules in the polymer chains, and is a measure of how compatible the polymer is with the molecules of the surrounding fluid.

$$\Delta G_{mixing} = kT [n_1 \ln v_1 + n_2 \ln v_2 + \chi n_1 v_2] \quad (2.5)$$

Where,

$n_1$  - moles of swelling agent

$n_2$  - moles of polymer

$v_1$  - volume fraction of swelling agent

$v_2$  - volume fraction of polymer

k- Boltzmann constant

$\chi$  - Flory polymer-solvent interaction parameter

For a cross-linked system without uncrosslinked polymer chains ( $n_2 = 0$ )

$$\Delta G_{mix} = kT [n_1 \ln v_1 + \chi n_1 v_2] \quad (2.6)$$

The deformation process must occur without appreciable change in the internal energy, thus the internal energy and, therefore, the elastic free energy is defined by

$$\Delta G_{el} = -T \Delta S_{el} \quad (2.7)$$

Where  $\Delta S_{el}$  is the change in entropy from deformation process. For isotropic swelling, elastic free energy is,

$$\Delta G_{el} = \left( \frac{kT v_e}{2} \right) (3\alpha_s^2 - 3 - \ln \alpha_s^3) \quad (2.8)$$

$v_e$  - effective number of chains in the network

$\alpha_s$  - Expansion factor expressing the linear deformation of a network structure due to isotropic swelling

The chemical potential of a solvent in a swollen gel is,

$$\mu_1 - \mu_{1,0} = N \left( \frac{\partial \Delta G_{mix}}{\partial n_1} \right)_{T,P} + N \left( \frac{\partial \Delta G_{el}}{\partial \alpha_s} \right)_{T,P} \left( \frac{\partial \alpha_s}{\partial n_1} \right)_{T,P} \quad (2.9)$$

N-Avogadro's number

Also,

$$\alpha_s^3 = \frac{1}{v_2} = \frac{(V_0 + \frac{n_1 V_1}{N})}{V_0} \quad (2.10)$$

$V_0$  = molecular weight of the network before swelling

$V_1$  = molar volume of the swelling agent

Considering the derivative of  $\alpha_s$  with respect to  $n_1$  gives the following,

$$\left( \frac{\partial \alpha_s}{\partial n_1} \right)_{T,P} = \frac{V_1}{3\alpha_s^2 V_0 N} \quad (2.11)$$

Using this relationship between Eq (2.11) and Eq (2.10) and also evaluating the two remaining derivatives, the following relation is obtained:

$$\mu_1 - \mu_{1,0} = RT \left[ \ln(1 - v_{2,s}) + v_{2,s} + \chi v_{2,s}^2 + V_1 \left( \frac{v_e}{V_0} \right) \left( v_{2,s}^{1/3} - \frac{v_{2,s}}{2} \right) \right] \quad (1)$$

$v_{2,s}$  is defined as the concentration at which activity of the swelling agent one.

Then at equilibrium state,

$$\left[ \ln(1 - v_{2,s}) + v_{2,s} + \chi v_{2,s}^2 \right] = V_1 (v_e/V_0) (v_{2,s}^{1/3} - v_{2,s}/2) \quad (2)$$

Now writing above equation (2.13) in terms of the following two equations Eq (2.14) and (2.15):

$$v_e = v \left( 1 - 2 \frac{\overline{M}_c}{\overline{M}_n} \right) \quad (2.14)$$

And,

$$v = \overline{V} / \overline{v} \overline{M}_c \quad (2.15)$$

And upon rearrangement, one obtains the Flory-Rehner model:

$$\frac{1}{\bar{M}_c} = \frac{2}{\bar{M}_n} - \frac{\left(\frac{v}{v_1}\right)[\ln(1-v_{2,s})+v_{2,s}+\chi_1 v_{2,s}^2]}{v_{2,s}^{\frac{1}{3}} - \frac{v_{2,s}}{2}} \quad (2.16)$$

$\bar{M}_c$  - number average molecular weight between crosslinks

$\bar{M}_n$  - number average molecular weight of polymer before crosslinking

Peppas and Merrill modified the above original Flory-Rehner model for hydrogels prepared in the presence of water. The presence of water modifies the change of chemical potential due to elastic forces. There must now be a term which accounts for the volume fraction density of the chains during crosslinking. The equation below predicts the molecular weight between crosslinks in a neutral hydrogel prepared in the presence of penetrant [2.8].

$$\frac{1}{\bar{M}_c} = \frac{2}{\bar{M}_n} - \frac{\left(\frac{v}{v_1}\right)[\ln(1-v_{2,s})+v_{2,s}+\chi_1 v_{2,s}^2]}{v_{2,r} \left[ \left(\frac{v_{2,s}}{v_{2,r}}\right)^{\frac{1}{3}} - \left(\frac{v_{2,s}}{2v_{2,r}}\right) \right]} \quad (2.17)$$

$v_{2,r}$  - polymer volume fraction in the relaxed state( after crosslinking, before swelling)

### 2.5.2 Rubber Elasticity Theory

The other theory used to determine crosslinked structure of a gel is the rubber elasticity theory. Hydrogels resemble natural rubbers in their property to elastically respond to applied stress. Thus when a crosslinked network is stretched, it reaches an equilibrium strain while the stress remains constant. A hydrogel subjected to small deformation, less than 20% [2.5] will fully recover to its original dimension rapidly. The rubber elasticity theory [2.7] is used to explain this behavior, thermodynamically. This theory was first developed by Treolar [2.11] and

Flory [2.7] for vulcanized rubbers and modified to polymers. Later expressions were developed which apply to hydrogels prepared in presence of solvent [2.6].

According to the modified theory for hydrogels prepared in presence of solvent, we have [2.8],

$$\tau = \frac{\rho RT}{\bar{M}_c} \left(1 - \frac{2\bar{M}_c}{\bar{M}_n}\right) \left(\alpha - \frac{1}{\alpha^2}\right) \left(\frac{v_{2,s}}{v_{2,r}}\right)^{\frac{1}{3}} \quad (2.18)$$

Here  $\tau$  is the stress applied to the polymer sample,  $\rho$  is the density of the polymer, R is the universal gas constant, T is the absolute experimental temperature, and  $\bar{M}_c$  the average molecular weight between crosslinks.

To be able to analyze the structure of the hydrogel using this theory, experiments need to be performed using a tensile system. This theory can be used to analyze chemically, physically crosslinked as well as hydrogels exhibiting temporary crosslinks due to hydrogen bonding.

### 2.5.3 Calculation of Mesh Size

The mesh size defines the space between macromolecular chains in a crosslinked network, and is characterized by the correlation length,  $\xi$  between two adjacent crosslinks. The calculations for the mesh size can be conducted as follows using the following equations [2.8]:

$$\xi = \alpha (\bar{r}_0^2)^{\frac{1}{2}} \quad (2.19)$$

Here  $\alpha$  is the elongation ratio of the polymer chains in any direction, and  $(\bar{r}_0^2)^{1/2}$  is the root mean square, unperturbed end to end distance of the polymer chains between two neighboring crosslinks [2.8].

For isotropically swollen hydrogels,  $\alpha$  is related to the polymer volume fraction  $v_{2,s}$  as follows:

$$\alpha = (v_{2,s})^{-\frac{1}{3}} \quad (2.20)$$

$(\bar{r}_0^2)^{1/2}$  can be calculated using the following equation[2.4]:

$$(\bar{r}_0^2)^{1/2} = l(C_n N)^{1/2} \quad (2.21)$$

Where  $C_n$  the Flory characteristic ratio is  $l$  is the length of the bond along the polymer backbone, and  $N$  is the number of links that is calculated using [2.8]:

$$N = \frac{2\bar{M}_c}{M_r} \quad (2.22)$$

$M_r$  is the molecular weight of the repeating units from which the polymer chain is composed. When one combines the above equations Eq (2.20), (2.21), (2.22) and rearranges them, we obtain the equation for calculation of the mesh size in a swollen hydrogel:

$$\xi = (v_{2,s})^{-\frac{1}{3}} (\bar{r}_0^2)^{1/2} \quad (2.23)$$

Thus calculation of the mesh size and other swelling parameters allow for proper design and characterization of diffusion of model drugs and proteins into the complex structure of gels.

## 2.6 References

- 2.1. Amsden, B., *Solute diffusion in hydrogels. An examination of the retardation effect.* Polymer Gels and Networks, 1998. **6**(1): p. 13-43.
- 2.2. Favre, E., et al., *Diffusion of polyethyleneglycols in calcium alginate hydrogels.* Colloids and Surfaces A: Physicochemical and Engineering Aspects, 2001. **194**(1-3): p. 197-206.
- 2.3. Flory, P.J., *Molecular theory of rubber elasticity.* Polymer, 1979. **20**(11): p. 1317-1320.
- 2.4. Hickey, A.S. and N.A. Peppas, *Mesh size and diffusive characteristics of semicrystalline poly(vinyl alcohol) membranes prepared by freezing/thawing techniques.* Journal of Membrane Science, 1995. **107**(3): p. 229-237.
- 2.5. Lin, C.-C. and A.T. Metters, *Hydrogels in controlled release formulations: Network design and mathematical modeling.* Advanced Drug Delivery Reviews, 2006. **58**(12-13): p. 1379-1408.

- 2.6. Nikolaos A. Peppas, E.W.M., *Crosslinked poly(vinyl alcohol) hydrogels as swollen elastic networks*. 1977. p. 1763-1770.
- 2.7. Paul J. Flory, N.R.M.C.S., *Dependence of elastic properties of vulcanized rubber on the degree of cross linking*. 1949. p. 225-245.
- 2.8. Peppas, N.A., et al., *Hydrogels in pharmaceutical formulations*. European Journal of Pharmaceutics and Biopharmaceutics, 2000. **50**(1): p. 27-46.
- 2.9. Peppas, N.A., et al., *Poly(ethylene glycol)-containing hydrogels in drug delivery*. Journal of Controlled Release, 1999. **62**(1-2): p. 81-87.
- 2.10. Tiziana Canal, N.A.P., *Correlation between mesh size and equilibrium degree of swelling of polymeric networks*. 1989. p. 1183-1193.
- 2.11. Turner, A., Jr., *The physics of rubber elasticity*. L. R. G. Treloar, Oxford Univ. Press, New York, 1949, 262 pp. 1950. p. 387.
- 2.12. N.A. Peppas: *Hydrogels in Medicine and Pharmacy, Vol. 1. Fundamentals*, CRC Press, Boca Raton, FL, 1986, 180 pages.
- 2.13. Hoffman, A.S., *Hydrogels for biomedical applications*. Advanced Drug Delivery Reviews, 2002. **54**(1): p. 3-12.

# Chapter 3 :Analysis of Drug Transport Mechanism

## 3.1 Introduction

For a successful drug delivery system, it is imperative that one can predict the mechanism of release of the active agent. This is also one of the most challenging fields in drug delivery, and over the years researchers have predicted the release of active drugs as a function of time, using both simple and sophisticated mathematical models. Mathematical models give us an insight into mass transport, as well as the effect of design parameters, such as device geometry and drug loading, on the release mechanism of the active agent in question. These models are important in both the design stage as well as in the experimental verification of the release mechanism [3.21]. Thus accurate data, along with models accurately representing the data, together provide a valuable insight into the actual release mechanism. Most of the theoretical models found in literature are based on diffusion equations. Diffusion is a phenomenon largely dependent on the structure of the gel matrix through which it occurs; thus the morphology of the polymeric materials must be taken into account for an accurate model to be selected [3.12]. Controlled release systems can be categorized based on the rate limiting step and can be classified as follows [3.12]:

- Diffusion-Controlled (drug diffusion from the non-degraded polymer)
- Swelling-Controlled (enhanced drug diffusion due to polymer swelling)
- Chemically Controlled (drug release due to polymer degradation and erosion)

Ordinary diffusion takes place to a certain degree, in each of these mechanisms, thus an understanding of the fundamentals of diffusion, and related mathematical relations are an

integral part of understanding the release mechanism of any agent through these gel matrices. For a non biodegradable matrix, drug release occurs due to the concentration gradient either via diffusion or matrix swelling. For biodegradable matrices, release is controlled by the hydrolytic cleavage of polymer chains that lead to matrix erosion [3.12]. Thus each system has different models which are developed according to the type of release. Simple equations have been developed for describing drug release of various polymers of different shapes using the principles of diffusion. The diffusion coefficient is defined in several different ways according to the nature of pores in the system. It is observed that diffusion can be Fickian, anomalous, or Case-II type diffusion. Fickian diffusion and its diffusion coefficient can be easily described using equations derived from Fick's law and its solutions. Short time approximations of these solutions have been shown to be effective only for the first 60% of drug release, when the aspect ratios are consistent with those of either a flat disk, or a long cylinder. Three dimensional analysis of cylindrical polymers is challenging, thus one dimensional approximate solutions are used to understand the diffusion of drug from long cylinders. Though most of the equations elucidated in this paper were developed for non-swellable polymers, most also hold true for moderately swellable polymers. The mathematics of the diffusion equation does not change, only the interpretation of the diffusion coefficient is altered.

### **3.2 Diffusion Controlled System**

Diffusion controlled is the most widely used for describing controlled release of drugs. Fick's law of diffusion with either constant or variable diffusion coefficients is used in modeling this controlled release. For diffusion-controlled microspheres, the drug release profile is obtained by solving Fick's second law of diffusion with appropriate boundary conditions. Fick's second law [3.3] is solved to obtain various analytical solutions to different boundary conditions. The

boundary conditions are determined by mass transfer process at the surface and the volume of the surrounding system.

Given below is a schematic illustration of the cross sections of drug loaded spheres [3.1].

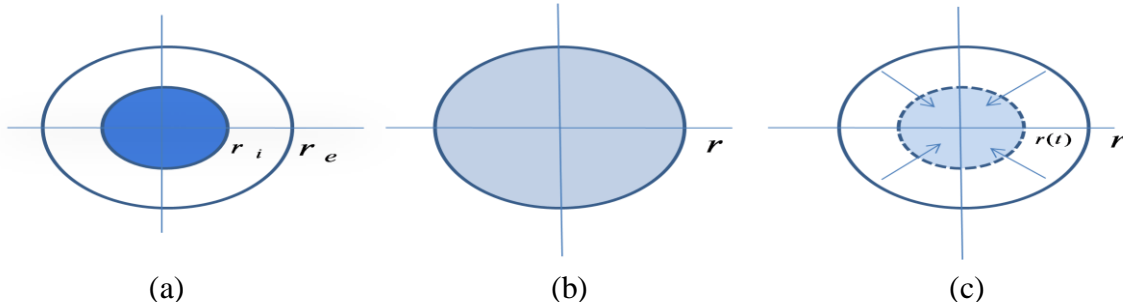


**Figure 3.1 Schematic illustration of cross section of drug loaded spheres (a) reservoir system (b) dissolved drug system (c) dispersed drug system. (Adapted from Fig 1 in ref[3.1])**

Based on the matrix region where most of the drug diffusion takes place, the diffusion controlled system can be further divided into reservoir and matrix systems [3.1]. The reservoir system consists of a drug reservoir surrounded by the polymer matrix shell. In the matrix system, the drug is incorporated in the matrix, either in dissolved or dispersed condition.

### 3.2.1 Reservoir System

The reservoir model consists of a bioactive agent containing a core that is separated from the external environment by a polymer membrane [3.1]. It assumes that the drug is restrained by a spherical shell of outer radius  $r_e$  and inner radius  $r_i$ , thus the drug diffuses through a layer of thickness  $(r_e - r_i)$ .

On solving Fick's second law of diffusion, the drug distribution within the shell boundary, along with appropriate boundary conditions, gives the rate of release of the drug, and the total amount of drug released for systems of spherical geometry [3.12].

$$\frac{dM_t}{dt} = \frac{4\pi D_{ip} K}{(r_e - r_i)/(r_e r_i)} (c_{i2} - c_{i1}) \quad (3.1)$$

$$M_t = \frac{4\pi D_{ip} K (c_{i2} - c_{i1})}{(r_e - r_i)/(r_e r_i)} \quad (3.2)$$

Here,

$D_{ip}$  - Concentration independent diffusion coefficient

$M_t$  - Amount of drug released at time t

K- Drug partition coefficient

$c_{i2}$  - Drug concentrations outside

$c_{i1}$  - Drug concentration inside

On developing analogous equations for different geometries such as, planar and cylindrical it was concluded that drug release can be controlled by the geometry of the system. The drug released can also be influenced by different factors such as thickness of the membrane, the concentration gradients across the membrane, and structure of the polymer.

### 3.2.2 Matrix System

This model assumes that the drug is uniformly distributed inside the polymer matrix. This model is valid for non biodegradable polymers. In this type of model, there are two sub-classifications [3.1]:

- Initial drug loading is lower than the solubility of the drug inside the polymer matrix (dissolved drug system)
- Initial drug loading is higher than the solubility of drug in polymer matrix (dispersed drug system)

- Dissolved Drug System

When the surface resistance to mass transfer at the surface is negligible, then fractional amount of drug released is expressed as [3.24]:

$$\frac{M_t}{M_\infty} = 1 - \frac{6}{\pi^2} \sum_{n=1}^{\infty} \frac{1}{n^2} \exp\left(\frac{-Dn^2\pi^2t}{R^2}\right) \quad (3.3)$$

$M_\infty$  is the cumulative drug released at infinite time

On the other hand, if convective mass transfer is dominant, then the fractional amount of drug released can be expressed as [3.5]:

$$\frac{M_t}{M_\infty} = 1 - \sum_{n=1}^{\infty} \frac{6Sh^2}{\beta_n^2(\beta_n^2 + Sh^2 - Sh)} \exp\left(-\frac{\beta_n^2}{R^2}Dt\right) \quad (3.4)$$

Sh is the Sherwood number, defined as  $Sh = hR/D$ , and the  $\beta_n$ s are the roots of the equation  $\beta_n \cot \beta_n = 1 - Sh$ . Thus the finite mass transfer solution depends on Sh.

- Dispersed Drug System

In this model, the polymer matrix can be divided into two regions [3.1]:

- Core in which undissolved solute exists at concentration  $C_0$  (non diffusing region)
- Dissolved (diffusing) region, where all solute is dissolved and diffusion occurs.

This model is not applicable if  $C_0/C_s$  is not very large. This separation between the two regions is valid when  $C_0 > C_s$ . The core region in this model shrinks as drug diffuses out, thus allowing for a moving boundary system. This system is however difficult to solve analytically. A schematic illustration of concentration profiles for this type of system is as shown [3.1]

### 3.3 Chemically Controlled System

Based on the mechanisms that control drug release, chemically controlled systems can be divided into two systems [3.12]:

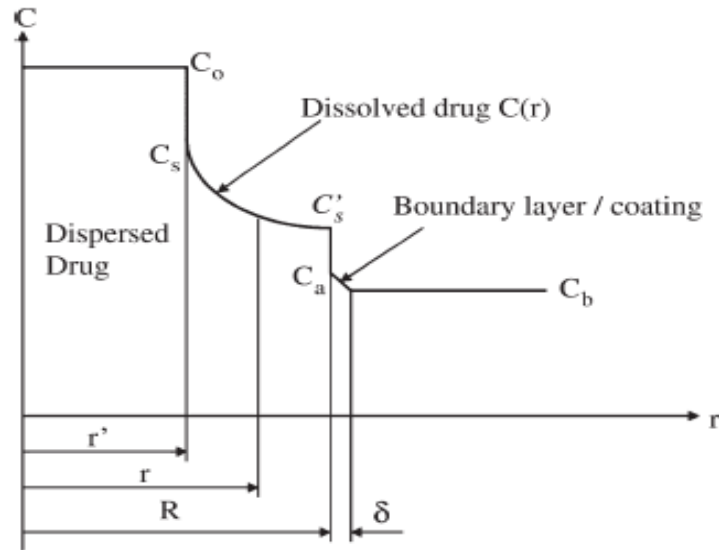


**Figure 3.2 Schematic diagram showing concentration profile in sphere of dispersed drug system in perfect sink system. From Fig 2 in Ref[3.1]**

- Erodible system- drug release rate is controlled by degradation or dissolution of the polymer.
- Pendant chain system- drug is attached to the polymer via a hydrolytically or enzymatically labile bond, and drug release is controlled by rate of degradation of bond. Bioerodible polymers have now found uses in biomedical applications especially for drug delivery systems due to a variety of reasons [3.12]:
- Chemistry and surfaces can be manipulated to stabilize bioactive agents, and enhance tissue for site-targeting
- Erosion kinetics can be customized by careful selection of polymer and different techniques of encapsulation of drug, to control drug release.

The polymer erosion is mainly described by the terms degradation and erosion. Degradation refers to the polymer chain/bond cleavage/scission reaction, whereas erosion designates the loss of polymer material in monomers or oligomers. Thus erosion may consist of

several physical and chemical steps, including degradation. Erosion controlled systems are quite complex, so the physiochemical characteristics of drug devices are an important factor that must be known in order to understand the mechanism of drug release. It is necessary to identify the dominant mechanism of release, and to this end, transient conditions are imposed on the system to obtain a more accurate model. Several techniques have been used to study the release properties of polymeric devices [3.11]. Gel permeation chromatography is used to monitor molecular weight changes in the polymer during drug release and erosion. The cumulative monomer release can be related to cumulative drug release profiles to indicate the relative contributions of erosion and degradation on drug release. Differential scanning calorimetry can measure the degree of crystallinity and glass temperature ( $T_g$ ) changes.  $T_g$  is important since in polymers, systems above the  $T_g$  are characterized by a rubbery state and high mobility of polymer chains, leading to a free volume for diffusion of drug to occur. If the system is below the  $T_g$ , then the polymer is in glassy state and diffusion is difficult. Scanning electron Microscopy (SEM) is used to understand the microstructure of the polymer matrix.

The two possible mechanisms of erosion, heterogeneous and homogenous, can be predicted from polymer hydrophobicity and morphology. Hydrophilic polymers absorb water, so erosion takes place throughout the polymer matrix (homogenous erosion). Hydrophobic polymers will erode only at surface, or (heterogeneously), since water is excluded from the bulk of the matrix. In the pharmaceutical field however, hydrophobic polymer matrices are more useful as they exhibit near zero-order release kinetics.

Several mathematical models have been developed to explain controlled release in erosion controlled systems. Erosion mechanism involves drug dissolution, polymer degradation, porosity creation, micro environmental pH change due to degradation, diffusion of drug in matrix, and autocatalytic effect during polymer degradation. Due to this complex set of

mechanisms, it is difficult to develop an accurate model that is able to predict all the mechanism contributions on drug release kinetics from an erosion controlled polymer. The models developed so far have been divided into empirical and mechanistic models. Empirical models are commonly developed for surface eroding systems that exhibit zero order releases, and do not take into account complex physiochemical phenomena. The mechanistic models on the other hand take into account physiochemical phenomena that involves diffusional mass transfer and chemical reaction processes. Empirical models consider the erosion process as a transport process of combined diffusion and chemical reaction processes, whereas mechanistic models consider erosion process as a random event.

### **3.4 Swelling Controlled Systems**

Hydrophilic matrices incorporated with drug in which drug release is controlled by the inward flux of solvent molecules and subsequent swelling of the polymer matrix is considered swelling controlled systems. The impetus behind the swelling polymer is to provide more control over the release of drug when diffusivity in the matrix is low. In some polymers, the diffusivity is low and it is difficult for drugs to diffuse out. To this end, swellable polymers are used which, imbibe water and cause polymer disentanglement. Once the water is imbibed in the matrix, it decreases the polymer concentration and changes the level of polymer disentanglement. Once the chain disentanglement decreases, it also leads to matrix swelling that results in a “rubbery” region in which there is enhanced diffusion allowing easier movement of drug out of the matrix. In this system the release of the drug can be described by Fick’s Law. However the deviation from the Fickian model is observed when drug release is controlled not only by the diffusion of the drug in the matrix, but also by polymer matrix entanglement and dissolution process.

The extent of swelling of the hydrophilic polymer depends on the composition of the polymer as well as the geometry of the gel. There are several mathematical models derived for swelling controlled systems, mostly for cylindrical geometry, while other geometry models can be derived from these by transformation of coordinates [3.21, 3.9]. HPMC, PEG, PVA are examples of hydrophilic polymers. Peppas and Lee [3.7] developed a model that describes matrix swelling by account for swelling moving fronts. When the polymer network comes in contact with aqueous solutions, swelling occurs to achieve thermodynamic equilibrium due to the water concentration gradient. As water is imbibed in the gel, the glass transition temperature of the polymer decreases, and the polymer transforms from a glassy to a rubbery state, in which drug diffusivity is high. So during the whole swelling process, two different states, the “glassy core” and gel layer (rubbery), exist. Thus there also exist two moving fronts, the glass-rubbery front(R) and the rubbery solvent front(S). During initial swelling, front R moves inward and front S outward. As soon as the polymer at interface S reaches its thermodynamic equilibrium with the surrounding medium, interface S starts dissolving, and front S moves inward. Both the fronts move inward, until the front R diminishes as the glassy core disappears. Eventually only R region is present and dissolution at interface S controls the shrinking process. On contact with water, the drug dissolves due to a concentration gradient between the interfaces of two states.

If water penetration is negligible, polymer relaxation is negligible, and drug release is controlled by Fickian diffusion [3.1]. When the extent of swelling is large, polymer relaxation is dominant [3.22], and Case II transport characterizes drug release [3.22]. Drug release is generally zero order since it is controlled by the polymer dissolution process. In many polymers however, anomalous transport is observed, which has intermediate characteristics to these two extreme cases. Anomalous transport is actually a combination of Fickian diffusion and polymer

relaxation, occurring together, thus making it impossible to distinguish between them. There are several models found in the literature describing each of the above mentioned scenarios [3.15].

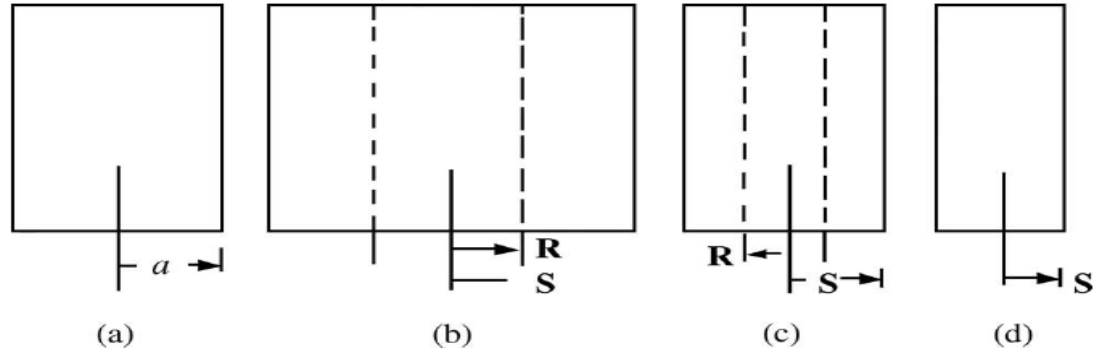


**Figure 3.3 Schematic of one dimensional swelling process due to solvent diffusion and polymer dissolution as proposed by Lee. From Fig 5 in ref[3.1]**

Both empirical and mechanistic models have been developed to characterize drug release from hydrophilic polymers, or hydrogels.

### 3.4.1 Empirical Models

A simple empirical equation based on a power law expression, relating fractional release of drug to the release time is one of the most widely used to interpret release data for non swellable devices (swelling controlled systems). The equation is as follows [3.1]:

$$\frac{M_t}{M_\infty} = kt^n \tag{3.5}$$

Here n is the diffusional exponent. The value of n is an indication of the nature of transport occurring in the system. The power law equation is thought to be a superposition of two processes, Fickian and Case II diffusion. As the transport varies from Fickian (n=0.5) to Case II diffusion (n=1), the value of n varies as well. In between these two processes, anomalous diffusion is characterized by intermediate values of n (0.5<n<1) [3.15]. These values of n also

depend largely on the geometry of the polymer system in question. The table below shows different values of  $n$ , for different geometries in different transport regimes [3.15].

**Table 3.1 Diffusional exponent and mechanism of diffusional release from various swellable controlled systems. From Table 1 in [3.15]**

Diffusion Exponent(m)			Mechanism
Film	Cylinder	Sphere	
0.5	0.45	0.43	Fickian diffusion
$0.5 < m < 1.00$	$0.45 < m < 0.89$	$0.43 < m < 0.85$	Anomalous Transport
1	0.89	0.85	Case-II Transport

The Eq (3.5) has however been shown to be valid only for the first 60% of the total amount of drug released regardless of the geometry of the polymer [3.16]. Peppas [3.16] incorporated the aspect ratio in describing the controlled release system. The diffusional exponent  $n$  can be defined for Fickian diffusion as a function of the aspect ratio. According to this analysis, cylinders with an aspect ratio smaller than 0.2, have  $n$  equal to 0.45. An aspect ratio of 0.2 defines the maximum aspect ratio ( $2a/l$ ) for which one dimensional diffusion in a cylinder is valid. Also to be noted is that particle size distribution also influences the value of  $n$ , and therefore the release behavior of the polymeric system [3.16].

### 3.4.2 Release from Swellable Devices

The power law Eq (3.5) is used to describe release behavior of solutes in non-swellable devices. In most swellable polymer devices, however the rate at which the solvent enters the polymer might have a significant effect on the drug release. Thus in most swellable polymers, a combination of diffusion and macromolecular relaxation takes place and the drug diffuses with behavior indicated by the relative ratios of Fickian and relaxation. The modeling of these

devices, however are modeled via moving boundary problems. Crank [3.24] and Stefan-Neumann [3.10, 3.14] have elucidated the difficulty of actually being able to obtain exact analytical solutions to the complicated equations for swellable devices. Thus one resorts to using numerical solutions. However the power law expression [3.17] can still be used to describe release data in these systems, as long as they swell only moderately in the presence of the penetrant. Mostly the polymer should not swell more than 25% of its original volume. As is the case with non swellable polymers, the diffusional exponent is greatly influenced by the geometry of the polymer, the value of  $n$ , and its limits for Fickian diffusion and Case-II transport for swellable systems (as shown in table (Table 3.1)). Similarly the particle size distribution changes the observed kinetics of the system, thus altering release behavior.

### 3.4.3 Coupling of Diffusion and Relaxation for Anomalous Diffusion

Fickian diffusion occurs by molecular diffusion of drug due to chemical potential gradient, whereas Case II relaxation release is due to the stresses and state –transition in hydrogels. Table [3.1] gives the various values of the exponent  $n$  for these two limiting states. Regardless of the geometry of the polymer, it can be seen that value of the exponent for Case-II diffusion is always twice that of pure Fickian diffusion. This observation was the basis for the development of the heuristic approach described below [3.22].

Alfred et al. [3.22] considered for the case of solvent transport in a polymer that two phenomena of Fickian diffusion and polymer relaxation can be considered to be additive, and can be written as:

$$\frac{M_t}{M_\infty} = k_1 t^m + k_2 t^{2m} \quad (3.6)$$

The first term on the left hand side of eq (3.7) is the Case-II relaxation contribution, where as the second term is the Fickian diffusion term. The coefficient  $m$  is the purely diffusion exponent

for a device of any geometrical shape. From literature [3.17], the coefficient  $m$  was shown to be constant for any geometry in two regions. For aspect ratios  $2a/l$ , varying from 0.1 to 100,  $m$  can be defined as in Eq (3.7) [3.15],

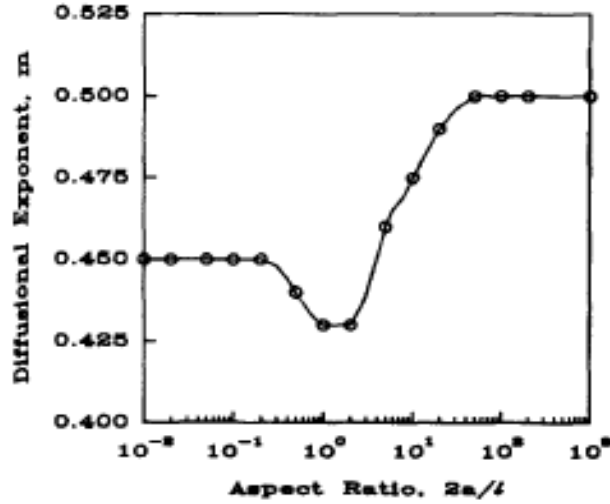


**Figure 3.4 Variation of the Fickian diffusional exponent  $m$  with aspect ratio  $2a/l$ . From Fig 3 in Ref[3.16]**

$$m = \begin{cases} 0.45 & \text{for } \frac{2a}{l} < 0.1 \\ 0.5 & \text{for } \frac{2a}{l} > 100 \end{cases} \quad (3.7)$$

The Eq (3.7) above can then be written as [3.16],

$$\frac{M_t}{M_\infty} = k_1 t^m \left[ 1 + \frac{k_2}{k_1} t^m \right] \quad (3.8)$$

The percentage of drug release due to Fickian mechanism  $F$  can then be written as [3.16],

$$F = \frac{1}{1 + \frac{t^m k_2}{k_1}} \quad (3.9)$$

which leads to the ratio of relaxation over Fickian contribution [3.16]:

$$\frac{R}{F} = \frac{k_2}{k_1} t^m \quad (3.10)$$

The above Eq (3.10) can also be modified with  $m=0.45$ , for aspect ratios  $2a/l < 0.1$

$$\frac{R}{F} = \frac{k_2}{k_1} t^{0.45} \quad (3.11)$$

This equation can approximate the controlled release of active agent of disks with the given aspect ratios, under the condition of swelling controlled systems. Using the estimated parameters,  $k_1$  and  $k_2$  obtained from fitting data to above Eq (3.11), the ratio of relaxation and Fickian contributions can be calculated, and an idea of the dominant mechanism of transport can be deduced. Thus from the above equations, one can estimate the approximate contributions of the diffusional and relaxation mechanisms in an anomalous solute release process by fitting the data to the above models.

#### 3.4.4 Mechanistic Models

Most of these empirical models are unable to describe how swelling affects the whole diffusional release behavior. Thus mechanistic models have been developed to describe the swelling behavior and its relation to controlled release. These models are based on moving fronts of the glassy and rubbery regions. The first model of swelling moving front was developed by Lee et al [3.7] for one dimensional swellable polymer systems without any drug loading (two component systems). Here the drug release is based on rational thermodynamics, including a complete viscoelastic description of the polymer matrix and concentration dependent diffusion coefficient of the drug [3.12]. Colombo et al [3.3] suggested that the gel layer consists of two regions of dissolved and undissolved drug gel layer thickness, where the distance of dissolved gel layer thickness is the important parameter that influences drug release. Harland et al [3.23] modified Lee's moving front model, by incorporating a third component,

the drug. Thus the three components are water (1), polymer (2) and drug (3). In this model, transport of drug and water is assumed to be Fickian. Narasimhan and Peppas [3.2] also used Lee's model with their own modifications. In this model, there are three components as well, with water and drug species formulated in volume fraction form based on Fick's second law. This model accounts for the superposition of Fickian diffusion and dissolution. Siepmann et al. [3.18] developed a model for drug release from HPMC tablets by combining diffusion, swelling, and dissolution mechanisms into Fujita-type exponential concentration dependent diffusivities. Drug and water diffusivities are exponentially dependent on the concentration of the swelling polymers due to their viscosity-inducing capabilities. Also, transport analysis is two dimensional in this model and integrated with the polymer swelling and dissolution. Siepmann et al. [3.19-3.20] further developed their previous model by utilizing Fick's second law in cylindrical coordinates and Fujita type exponential dependence of diffusion coefficients into a sequential layer model. The "sequential layer" model is performed in a computational grid and the modified structure of the grid is required for numerical analysis. Swelling is considered to take place layer by layer, in which the outermost layer swells first followed by inner layers. The model is able to account for substantial changes in the volume of the system in the outer layer. This is a marked improvement in the model, as being able to predict volume changes gives an accurate idea of the changes in concentration of all species, and the mobility of the species. Further work is being done to develop an additional feature to this model, a glassy core region that will enable the observation of two moving fronts during the drug release process.

### **3.4.5 Fundamentals of Diffusion**

In order for the release of drug to take place, the drug must move through the bulk of the polymer. This movement of the drug through the polymer matrix is known as diffusion. Diffusion is controlled by the mass transfer limitations at the boundary between the polymer and

its surroundings. On a macroscopic level, the diffusion of drug can be described by Fick's law of diffusion, stated as follows, for one dimensional transport [3.12].

$$j_i = -D_{ip} \frac{dc_i}{dx} \quad (3.12)$$

$$\frac{\partial c_i}{\partial t} = D_{ip} \frac{\partial^2 c_i}{\partial x^2} \quad (3.13)$$

The above equations are valid for a thin planar geometry, and the diffusion coefficient is independent of concentration. Similar equations have been developed for other geometries, such as thick slabs, cylinders, and spheres [3.24]. The initial and boundary conditions are indicative of the experimental conditions imposed upon the drug release device. Several solutions for varying initial and boundary conditions have been published in literature [3.24].

To better predict the release of the drug using Fickian diffusion theory, a concentration dependent diffusion coefficient is used in the above equations. They are rewritten as follows:

$$\frac{\partial c_i}{\partial t} = \frac{\partial}{\partial z} \left( D_{ip}(c_i) \frac{\partial c_i}{\partial x} \right) \quad (3.14)$$

The concentration dependent diffusion coefficient is affected by the structural characteristics of the polymer. Summary of various forms of diffusion coefficient is shown in Table 3.2 [3.12].

Several theories have been proposed in order to estimate the diffusion coefficient through a polymer carrier. One of the earliest approaches is the Eyring theory [3.4]. This theory represents the diffusion of solute through a medium as a series of jumps. . Fujita [3.5] used the idea of free volume in polymers to estimate a drug diffusion coefficient and found an exponential dependence on free volume. Yasuda and Lamaze [3.6] further modified Fujita's theory and proposed a molecular based theory. In this theory the normalized diffusion

coefficient is related to a degree of hydration, and free volume occupied by the swelling medium

**Table 3.2 Summary of drug diffusion coefficient equations. From Table 2 in ref [3.12]**

Type of carrier	Equation	Form of $D_p$	Reference
Porous	Eq. (21)	$D_p = \frac{\lambda^2 v}{6}$ (21)	[4]
Porous	Eq. (22)	$D_{eff} = D_w K_p K_r \frac{\epsilon}{\tau}$ (22)	[6]
Micro-porous	Eq. (23)	$\frac{D_p}{D_b} = (1 - \lambda)^2 (1 + \alpha\lambda + \beta\lambda^3 + \gamma\lambda^5)$ (23)	[7]
Non-porous	Eq. (24)	$D_p = D_o \exp\left\{-\frac{k}{v_r}\right\}$ (24)	[7]
Non-porous	Eq. (25)	$\frac{D_{2,13}}{D_{2,1}} = \varphi(q_s) \exp\left[-B\left(\frac{q_s}{V_{r,1}}\right)\left(\frac{1}{H} - 1\right)\right]$ (25)	[8]
Non-porous (highly swollen)	Eq. (26)	$\frac{D_{2,13}}{D_{2,1}} = k_1 \left(\frac{M_c - M_c^*}{M_n - M_c^*}\right) \exp\left(-\frac{k_2 r_g^2}{Q - 1}\right)$ (26)	[9]

. Peppas and Reinhart [3.10] also developed a theoretical model based on the free volume of the polymer matrix. This theory applies to drug transport in highly swollen non porous hydrogels. Another prediction of diffusion coefficient is using chemical engineering principles. The diffusion of a drug through a macro-or micro porous polymer is compared to the transport phenomena in porous rocks, ion exchange resins, and catalysts Thus several different theories have been developed to predict effective diffusion coefficients.

### 3.4.6 Analysis of Drug Release for Non- Swellable and Swellable Polymers

As noted above diffusion is the main mechanism of transport of the drug. There are several models to describe the kinetics of release of the drug, and models which estimate the

diffusion coefficients associated with controlled release. For non swellable polymers, Peppas developed simple equations to describe solute release. In this paper, we have dealt only with cylindrical hydrogels, thus will only elaborate on the equations describing release from cylindrically shaped polymer gels.

• Release from Cylinders

Consider one dimensional radial release from a cylinder of radius  $a$  and length  $l$ , under perfect sink initial and boundary conditions, and a constant drug coefficient  $D$ . Fick's law under these conditions, is:

$$\frac{\partial C}{\partial t} = D \left[ \frac{\partial^2 C}{\partial r^2} + \frac{1}{r} \frac{\partial C}{\partial r} \right] \quad (3.15)$$

Where,

$$t=0 \quad 0 < r < a \quad C = C_1 \quad ;$$

$$t=0 \quad r=a \quad C = C_0$$

On solving Eq (3.15), under these boundary conditions, we get the following equation [3.24]:

$$\frac{M_t}{M_\infty} = 1 - \sum_{n=1}^{\infty} \frac{4}{a^2 \alpha_n^2} \exp[-D \alpha_n^2 t] \quad (3.16)$$

$\alpha_n$  are the positive roots of  $J_0(a\alpha_n) = 0$ ,  $J_0$  is Bessel function of the first kind of zero order, and  $a\alpha_n$  are the zeros of that function. An alternative solution [3.15], for short time behavior is also as shown:

$$\frac{M_t}{M_\infty} = 4 \left[ \frac{Dt}{\pi a^2} \right]^{1/2} - \pi \left[ \frac{Dt}{\pi a^2} \right] - \frac{\pi}{3} \left[ \frac{Dt}{\pi a^2} \right]^{3/2} + \dots \quad (3.17)$$

The above approximations are true only for a cylinder with one dimensional radial flow. For analysis of three dimensional release from a cylinder, a new approach was taken. Fu et al [3.5]

was the first to develop a model for three dimensional release, and it is elucidated below. Fick's law was applied to cylindrical coordinates with diffusion occurring in both the radial direction,  $r$  and the axial direction,  $z$ . This model is applicable to systems ranging from a flat disk to that of a cylindrical rod.

• Three Dimensional Model

Consider release from a disk of diameter  $2a$  and thickness or length  $l$ . The system can be defined in terms of an aspect ratio  $2a/l$ . Initially the system is maintained at a constant uniform drug concentration,  $C_1$ , and the surfaces are at a constant drug concentration,  $C_0$ . The drug diffusion coefficient  $D$  is assumed to be constant with diffusion in both the  $r$  and  $z$  directions and initial and boundary conditions are as shown [3.15]:

$$\frac{\partial C}{\partial t} = D \left[ \frac{\partial^2 C}{\partial r^2} + \frac{1}{r} \frac{\partial C}{\partial r} + \frac{\partial^2 C}{\partial z^2} \right] \quad (3.18)$$

Where,

$$t=0 \quad -\frac{l}{2} < z < \frac{l}{2} \quad C=C_1$$

$$0 < r < a$$

$$t>0 \quad z=\pm l/2 \quad C=C_0$$

$$r=a$$

From drug concentration profile defined by the above diffusion equation, Fu et al [3.5], calculated the total drug transferred across the lateral surface and the two end surfaces of the disk. The equation defined in terms of normalized drug concentration was as follows:

$$\frac{M_t}{M_\infty} = 1 - \sum_{n=1}^{\infty} \frac{4}{a^2 \alpha_n^2} \exp[-D \alpha_n^2 t] \times \sum_{m=0}^{\infty} \frac{8}{\beta_m^2 l^2} \exp[-D \beta_m^2 t] \quad (3.19)$$

Where,  $\beta_m$  are defined as,

$$\beta_m = \frac{(2m+1)\pi}{l} \text{ and}$$

$\alpha_n$  are the positive roots of  $J_0(a\alpha_n) = 0$ ,  $J_0$  is the zero order Bessel Function of the first kind and  $a\alpha_n$  are the zeros of that function.

The above general equation reduces to the one dimensional diffusion release equations from a slab for  $a \rightarrow \infty$ , and from a long cylinder  $l \rightarrow \infty$ . Thus the above equation for three dimensional release with approximations can be reduced to the one dimensional release equations.

The short time approximation for one dimensional release from a flat disk can be obtained from Eq (3.19), and can be written as:

$$\sum_{m=0}^{\infty} \frac{8}{\beta_m^2 l^2} \exp[-D\beta_m^2 t] = 1 - 4 \left[ \frac{Dt}{\pi l^2} \right]^{1/2} \quad (3.20)$$

#### • Short Time Approximations

For short times, an analytical solution can be derived for describing one dimensional release from cylinders. Equating above the two equations, (3.16) and (3.17), we find that,

$$\sum_{n=1}^{\infty} \frac{4}{a^2 \alpha_n^2} \exp[-D\alpha_n^2 t] = 1 - 4 \left[ \frac{Dt}{\pi a^2} \right]^{1/2} + \pi \left[ \frac{Dt}{\pi a^2} \right] + \frac{\pi}{3} \left[ \frac{Dt}{\pi a^2} \right]^{3/2} \quad (3.21)$$

On substituting above Eq (3.20), (3.21) into Eq (3.19), we get

$$\frac{M_t}{M_{\infty}} = 4 \left[ \frac{Dt}{\pi a^2} \right]^{1/2} - \pi \left[ \frac{Dt}{\pi a^2} \right] - \frac{\pi}{3} \left[ \frac{Dt}{\pi a^2} \right]^{3/2} + 4 \left[ \frac{Dt}{\pi l^2} \right]^{1/2} - \frac{2a}{l} \left[ 8 \left( \frac{Dt}{\pi a^2} \right) - 2\pi \left( \frac{Dt}{\pi a^2} \right)^{3/2} - \frac{2\pi}{3} \left( \frac{Dt}{\pi a^2} \right)^2 \right] \quad (3.22)$$

This solution is actually a combination of the solutions of short time solutions for one dimensional diffusional release from the cylinder and the thin slab with an additional ‘‘coupling term’’ scaled according to the aspect ratio  $2a/l$ . Thus this equation can be applied to all disk shaped polymers with any aspect ratio. Peppas [3.15] compared the short time solutions given

by Eq (3.21) and the exact solution Eq(3.20). He found that for the aspect ratios  $2a/l \gg 1$  and  $2a/l \ll 1$  the short approximations is valid for the first approximations is valid for the first 65% to 70% of the total release of drug from the polymer carrier. Thus the short time approximation is valid for one dimensional diffusional release from cylinder ( $2a/l \ll 1$ )

### 3.5 References

- 3.1. Arifin, D.Y., L.Y. Lee, and C.-H. Wang, *Mathematical modeling and simulation of drug release from microspheres: Implications to drug delivery systems*. Advanced Drug Delivery Reviews, 2006. **58**(12-13): p. 1274-1325.
- 3.2. Balaji Narasimhan, N.A.P., *Molecular analysis of drug delivery systems controlled by dissolution of the polymer carrier*. 1997. p. 297-304.
- 3.3. Colombo, P., et al., *Analysis of the swelling and release mechanisms from drug delivery systems with emphasis on drug solubility and water transport*. Journal of Controlled Release, 1996. **39**(2-3): p. 231-237.
- 3.4. Eyring, H., *Theory of rate processes*. Journal of chemical Physics, 1936. **4**(4): p. 283-289.
- 3.5. J. C. Fu, C.H.D.L.M.E.W.N., *A unified mathematical model for diffusion from drug-polymer composite tablets*. 1976. p. 743-758.
- 3.6. Kenneth F. Zieminski, N.A.P., *Diluent diffusion in polymer-diluent systems near Migration of phthalic esters from PVC to water*. 1983. p. 1751-1765.
- 3.7. Lee, P.I. and N.A. Peppas, *Prediction of polymer dissolution in swellable controlled-release systems*. Journal of Controlled Release, 1987. **6**(1): p. 207-215.
- 3.8. Lisa Brannon and Nikolaos A. Peppas, M., *Solute diffusion in swollen membranes : Part VIII. Characterization of and diffusion in asymmetric membranes*. Journal of Membrane Science, 1987. **32**(2-3): p. 125-138.
- 3.9. Narasimhan, B., *Mathematical models describing polymer dissolution: consequences for drug delivery*. Advanced Drug Delivery Reviews, 2001. **48**(2-3): p. 195-210.
- 3.10. P.I, L., *Diffusional release of a solute from a polymeric matrix -- approximate analytical solutions*. Journal of Membrane Science, 1980. **7**(3): p. 255-275.
- 3.11. p.P, H.A.G.D., *Characterization of biodegradable poly(d,l-lactide-co-glycolide) polymers and microspheres* Journal of Pharmaceutical and Biomedical Analysis, 1995. **13**(6): p. 747-760.

- 3.12. Peppas, N.A., et al., *Hydrogels in pharmaceutical formulations*. European Journal of Pharmaceutics and Biopharmaceutics, 2000. **50**(1): p. 27-46.
- 3.13. Peppas, N.A. and J.J. Sahlin, *A simple equation for the description of solute release. III. Coupling of diffusion and relaxation*. International Journal of Pharmaceutics, 1989. **57**(2): p. 169-172.
- 3.14. N.A. Peppas: "Release of Bioactive Agents from Swellable Polymers: Theory and Experiments," in "Recent Advances in Drug Delivery Systems," J.M. Anderson and S.W. Kim, editors, pp. 279-290, Plenum Press, New York, N.Y., 1984
- 3.15. Ritger, P.L. and N.A. Peppas, *A simple equation for description of solute release I. Fickian and non-fickian release from non-swellable devices in the form of slabs, spheres, cylinders or discs*. Journal of Controlled Release, 1987. **5**(1): p. 23-36.
- 3.16. Ritger, P.L. and N.A. Peppas, *A simple equation for description of solute release I. Fickian and non-fickian release from non-swellable devices in the form of slabs, spheres, cylinders or discs*. Journal of Controlled Release, 1987. **5**(1): p. 23-36.
- 3.17. Ritger, P.L. and N.A. Peppas, *A simple equation for description of solute release I. Fickian and non-fickian release from non-swellable devices in the form of slabs, spheres, cylinders or discs*. Journal of Controlled Release, 1987. **5**(1): p. 26-48.
- 3.18. Siepmann, J., et al., *HPMC-Matrices for Controlled Drug Delivery: A New Model Combining Diffusion, Swelling, and Dissolution Mechanisms and Predicting the Release Kinetics*. Pharmaceutical Research, 1999. **16**(11): p. 1748-1756.
- 3.19. Siepmann, J., et al., *Calculation of the required size and shape of hydroxypropyl methylcellulose matrices to achieve desired drug release profiles*. International Journal of Pharmaceutics, 2000. **201**(2): p. 151-164.
- 3.20. Siepmann, J. and N.A. Peppas, *Hydrophilic Matrices for Controlled Drug Delivery: An Improved Mathematical Model to Predict the Resulting Drug Release Kinetics (the "sequential Layer" Model)*. Pharmaceutical Research, 2000. **17**(10): p. 1290-1298.
- 3.21. Siepmann, J. and N.A. Peppas, *Modeling of drug release from delivery systems based on hydroxypropyl methylcellulose (HPMC)*. Advanced Drug Delivery Reviews, 2001. **48**(2-3): p. 139-157.
- 3.22. T. K. Kwei, H.M.Z., *Diffusion in glassy polymers. I*. 1969. p. 867-877.
- 3.23. Harland, R.S., et al., *Drug/Polymer Matrix Swelling and Dissolution*. Pharmaceutical Research, 1988. **5**(8): p. 488-494.
- 3.24. The Mathematics of Diffusion (2nd Edition ed.),, Oxford University Press, Oxford (1979), p. 35. 11



# Chapter 4 : Preparation of PEGDA Hydrogels and Study of Release Kinetics

## 4.1 Overview

PEGDA hydrogels were prepared in order to study its suitability for biomedical applications. Swelling studies give an average mesh size, as well as a reasonable idea of the morphological structure of the gel. Diffusion studies with dyes can mimic controlled drug release studies. Thus swelling and diffusion studies together were an ideal combination to study the potential of these PEG hydrogels as drug delivery matrices, and as matrices for protein immobilization. Polyethylene glycol, with its hydroxyl moieties can be acrylated to form PEGDA (polyethylene diacrylate). Acrylate monomers are esters containing vinyl groups, that is two carbon atoms double bonded to each other, directly attached to the carbonyl atom. FTIR scans were used to determine the extent of acrylation, and C=C double bond conversion. The peaks in the absorbance spectra are an indication of the extent of conversion, the larger the magnitude of the peak, larger the extent of acrylation. As the molecular weight of the PEGs increases, the magnitude of the peak absorbance value at  $1714\text{cm}^{-1}$  also increases. On exposure to UV radiation, the photoinitiator, photofragments to yield radicals. These radicals initiate polymerization, by attacking the C=C double bonds present in the acrylate groups. In linear chain formation, branched as well as crosslinked structures are also formed, thus forming an insoluble three dimensional polymer network. This polymer network is the hydrogel, which can be used as a matrix for drug delivery, and as a matrix for encapsulation of biological material. Cylindrical hydrogels were prepared since they were relatively easy to manufacture as well as analyze. These cylindrical gels were allowed to swell in an aqueous environment, and morphological parameters, such as molecular weight between crosslinks and mesh size, were

determined. Release studies of dye were then performed, by placing gels in an aqueous solution, and allowing the dye to diffuse out of the gel. The release data obtained were fit to various mathematical models, and diffusion coefficients of the dye were subsequently determined.

## **4.2 Introduction**

Polyethylene glycol hydrogels are highly swollen biocompatible matrices. PEG is an FDA approved material which has found varied uses in the pharmaceutical and medical fields. Its biocompatibility, tendency to absorb water and flexibility make it one of the most widely used synthetic hydrogels. These PEG hydrogels have been used as drug delivery devices [4.17], as membranes for biosensors [4.13], as contact lenses [4.18] and for the encapsulation of islets for treatment of diabetes [4.19]. Many researchers have prepared PEG hydrogel networks fabricated from dilute solutions that were crosslinked using low energy light illumination with a photoinitiator [4.2], electron beam [4.6], or gamma irradiation [4.16]. Several PEG hydrogel applications such as for electrochemical [4.20] and optical biosensing [4.21] , drug delivery [4.5], and substrate materials for directed cell growth [4.22] use PEG formed by extremely rapid photopolymerization from highly concentrated solutions of PEG acrylates. However these gels may contain a large number of physical entanglements and microgels that can influence mass transfer within the gel.

In this paper, the PEG hydrogels were formed from PEG acrylate solutions which were polymerized along with photoinitiator, upon exposure to UV radiation. A variety of photoinitiators have been used by various researchers for this purpose. For our purposes, we chose a liquid photoinitiator in order to ensure ease of mixing of precursor solutions. Also, care was taken so that the magnitude of UV radiation from the UV lamp exceeded the threshold value required to activate the photoinitiator. To mimic drug delivery of small proteins, fluorescein dye is used to study controlled release from hydrogel. Fluorescein dye was chosen,

because its excitation and emission spectrums are well defined and has been used in various similar studies [4.12]. The excitation and emission spectrum of the dye also did not interfere with the wavelengths of UV radiation required for polymerization.

Various researchers have studied swelling and diffusion of solutes in different synthetic hydrogels such as PEG, poly (acrylic acid-g-ethylene glycol) [4.14], HPMC [4.15], PMMA [4.10]. Each synthetic material has different release characteristics depending on method of preparation, constituents, mode of polymerization, conditions of swelling and solute release, as well as mode of solute release. To better understand the release data obtained from experiments, the data were fit to various empirical and semi empirical mathematical models. Most models developed are based in some form on solutions of the Fickian diffusion equation [4.23]. The Higuchi model [4.24] is the most often used model to describe the release rate of solutes from gels. Also the power law model (Ritger-Peppas) [4.11], the Peppas and Sahlin model [4.9], and the Roseman and Higuchi model [4.25] are all semi-empirical models that have been used to describe release data from hydrogels. In our research the power law is the fundamental model used to determine the transport regime of the dye, and the Fickian diffusion equation is used to approximate a diffusion coefficient. The release data analysis is the first step in order to be able to predict the controlled release characteristics of these hydrogels. Once the kinetics of release, and, the mesh size are obtained, it becomes plausible to design a system, according to the mesh size required for the transport of specific sizes of protein, and uniform site specific release of drug.

## **4.3 Materials and Methods**

### **4.3.1 Materials**

Poly (ethylene glycol) diacrylate with molecular weights 200, 400 were obtained from Polysciences (Warrington, PA). 0.1 molar phosphate buffered saline (PBS, pH 7.4) was

prepared from potassium phosphate monobasic, sodium phosphate, potassium chloride, and 18megaohm deionized water via standard preparation method. Poly (ethylene glycol) (8000, 10000, 14000, and 20000 molecular weight), fluorescein, acryloyl chloride, trimethylamine and diphenyl (2, 4, 6 trimethyl benzoyl phosphine oxide/2-hydroxy-2-methyl propiophenone 50/50) were all obtained from Sigma Aldrich Co. (St. Louis, MO). 0.2 micron Teflon membrane filters as well as glass membrane filters were obtained from Molecular probes (Eugene, OR). All other reagents and chemicals, unless specifically mentioned, were supplied by Sigma-Aldrich (St. Louis, MO).

#### **4.3.2 Preparation of PEGDA**

Poly (ethylene glycol) diacrylate (PEGDA) of molecular weights 8000, 10000, 14000 and 20000 were prepared by acrylating the hydroxyl functionalities of dihydroxy PEG using a published protocol [4.7]. PEG (20g) was dissolved in 200 ml of dry benzene under nitrogen and heated at 40°C until fully dissolved. The solution was then allowed to cool to room temperature. The solution was placed in an ice bath, followed by addition of four fold molar excess (PEG hydroxyl groups) of acryloyl chloride and triethylamine. This mixture was then heated to reflux under nitrogen for 2 h, followed by stirring overnight under nitrogen at room temperature. Care was taken so that no moisture was allowed to disrupt the reaction in the reflux condenser. The solution was filtered, to remove the amine salts formed during the reaction. The polymer was precipitated in 2 L of hexane. The resulting precipitate was recovered via filtration, and then dried at room temperature to obtain the final product. The final product was then tested using a FTIR spectrometer (Nicolet 380) to determine degree of acrylation.

#### **4.3.3 Preparation of Hydrogel for Swelling Studies**

PEGDA (1 g), diphenyl (2,4,6 trimethyl benzoyl)-phosphine oxide/ 2-hydroxy-2-methyl propiophenone 50/50 (1 ml) (photoinitiator), and 0.1 M phosphate buffer solution (1 ml), were

vortexed at high speeds in a centrifuge tube to form a solution. The PEG and the PBS were vortexed first to form a solution with photoinitiator added later to facilitate easier mixing. The lower molecular weights were vortexed vigorously as they were waxy in nature, and had a tendency to form a biphasic system with the PBS and photoinitiator. The solution was heated if necessary, in order to obtain a well mixed solution. The solutions were then poured into acrylic tubes ( $D = 1/4\text{in}$ ,  $L = 2\text{in}$ ), covered with parafilm at one end, and exposed to UV radiation (INTELLI-RAY 600, 600 Watt UVA, 115/230V) for a period of 40 seconds. The dimensions of the cylindrical hydrogels formed were measured to ensure at most an aspect ratio of 0.2 [4.11]. This aspect ratio ( $2a/L$ ) ratio is the maximum aspect ratio for which the assumption of one dimensional diffusion in a cylinder is valid [11].

#### 4.3.4 Mesh Size Calculation

In order to characterize the hydrogel structure, the molecular weight between adjacent crosslinks ( $M_c$ ), the mesh size( $\xi$ ) and polymer volume fraction in swollen gel ( $v_{2,s}$ ) were all determined experimentally. All the experiments were performed with cylindrical hydrogels, with aspect ratios  $\leq 0.2$ .

The cylindrical hydrogels were initially weighed after crosslinking. The cylinders were then immersed in 10 ml of PBS solution and allowed to swell for one week. It is known that swelling degree increases up to a certain time and then becomes constant. This value of swelling degree is known as the equilibrium degree of swelling. The one week swell time allowed the gels to reach the equilibrium swell conditions, which was essential for the calculation of mesh size. After a week, the gel was removed from the PBS solution, weighed, and allowed to dry at room temperature for three days. The hydrogel desorbed all the phosphate buffer solution, leaving only the crosslinked polymer. The final gels were then weighed. The following

measurements were taken for each hydrogel, and for each individual molecular weight gel [4.18].

$W_{a,r}$  = sample weight after crosslinking

$W_{a,s}$  = sample weight after swelling

$W_{a,d}$  = sample weight after drying

These measurements were used to determine the volume of the hydrogel sample after crosslinking (but before swelling),  $V_{g,r}$ , and after equilibrium swelling,  $V_{g,s}$ . The following are the equations used to calculate these volumes.

$$V_{g,r} = \frac{W_{a,r}}{\rho_{a,r}} \quad (4.1)$$

$$V_{g,s} = \frac{W_{a,s}}{\rho_{a,s}} \quad (4.2)$$

$$V_p = \frac{W_{a,d}}{\rho_{a,d}} \quad (4.3)$$

Where,

$V_p$  = weight of dry polymer

$$\rho_{a,r} = \rho_{peg} x_{peg} + \rho_{photoinitiator (pi)} x_{pi} + \rho_{pbs} x_{pbs}$$

$$\rho_{a,s} = \rho_{peg} x_{peg} + \rho_{photoinitiator (pi)} x_{pi} + \rho_{pbs} x_{pbs}$$

$$\rho_{a,d} = \rho_{peg} x_{peg} + \rho_{photoinitiator (pi)} x_{pi}$$

Here,

$\rho_{peg}$  = density of PEG

$\rho_{photoinitiator (pi)}$  = density of photoinitiator

$\rho_{pbs}$  = density of phosphate buffer solution

$x_{pi}$ ,  $x_{pbs}$ ,  $x_{peg}$  are mole fractions of photoinitiator, PBS, PEG

The above calculated values are then input into the equation for calculation of  $M_c$  following a previously published procedure [4.18]:

$$\frac{1}{M_c} = \frac{2}{M_n} - \frac{\left(\frac{v}{v_1}\right) [\ln(1-v_{2,s}) + v_{2,s} + \chi_1 v_{2,s}^2]}{v_{2,r} \left[ \left(\frac{v_{2,s}}{v_{2,r}}\right)^{1/3} - \left(\frac{v_{2,s}}{2v_{2,r}}\right) \right]} \quad (4.4)$$

Here  $\chi$  (polymer solvent interaction parameter) = 0.55 and  $M_n$  is the average molecular weight of PEG before polymerization. The average mesh size of the polymer network  $\xi$ , was calculated as described by Peppas and Merrill [4.18]. The root mean squared end-to end distance of a randomly coiled polymer bonds with a length  $l$  and characteristic ratio  $C_n$  was calculated as:

$$(r^2)^{1/2} = C_n^{1/2} n^{1/2} l \chi \quad (4.5)$$

where,  $C_n = 4.0$  and  $l = 1.54 \text{ \AA}$  (for vinyl bonds),  $n = \frac{2M_c}{M_r}$

The average mesh size of the network was then calculated as,

$$\xi = v_{2,s}^{-1/3} (r^2)^{1/2} \quad (4.6)$$

### 4.3.5 Swelling Studies

The cylindrical hydrogels, were placed in a known amount of PBS (10ml), and allowed to swell. The initial weight of the gel was compared to the swollen weight. This allows for a transient analysis of the swelling of hydrogel. Weight of the gel was taken every ten minutes. The PBS was absorbed in the gel thus increasing the weight of the gel with time until equilibrium swelling weight is reached. While weighing the gels, care was taken to remove the PBS on the surface, so that only the weight of the PBS incorporated into the hydrogel was considered.

The following equation was used to determine the kinetics of the swelling process of these hydrogels [4.26]:

$$F = \left( \frac{W_s - W_p}{W_p} \right) = kt^n \quad (4.7)$$

Where,

F= g PBS/g polymer

$W_s$  = weight of swollen polymer at time t

$W_p$  = weight of the dry polymer at time t=0

Here k and n are the swelling constant and swelling exponent, respectively. The above equation is however applied only to the first 60% of swelling. The swelling data obtained were fit to the above equation using POLYMATH (version 5.0) and values of n and k were calculated.

Now for Fickian diffusion of PBS from the gels, we can approximate the diffusion coefficient for swelling of these cylindrical gels, allowing us to better control the mechanism of transport in these gels. The diffusion coefficients were calculated by using the following equation [4.26]:

$$F = 4(Dt/\pi r^2)^{1/2} \quad (4.8)$$

Here,

D= coefficient of diffusion

r= radius of the cylindrical gel

In the above equation, radial diffusion is assumed as the sole form of diffusion, and all end effects are neglected. Also it is assumed that the diffusion mechanism is Fickian diffusion.

Using POLYMATH (version 5.0) approximate values of D (coefficient of diffusion) were obtained and are compared.

#### **4.3.6 Preparation of Gels for Diffusion Studies with Dye**

For diffusion studies with the cylindrical hydrogels, a small molecular weight dye, fluorescein was used in order to mimic the release of a drug. Fluorescein stock solution of concentration 120 $\mu$ M was prepared with PBS as the solvent. PEGDA (1ml or 1g), stock solution (1ml) and Photoinitiator (1ml) were mixed vigorously. This solution was then poured into acrylic tubes (D = 1/4in L = 2in), and polymerized via exposure to UV radiation for a period of 40 seconds. The same procedure was followed for all the different molecular weight PEGs. The gels were cut, and measured lengthwise to assure that the aspect ratio remained below the requisite value of 0.2. The stock dye solution was poured in a cuvette, and the fluorescence spectra were obtained. The spectrofluorimeter (OLIS DM 45 Spectrofluorimeter) was used and dye solution was excited at 492nm while the emission was scanned from 500 to 540nm. The fluorescence intensity at 514 was recorded. This reading was used as the initial fluorescence of the gel before dye release.

#### **4.3.7 Dye Release Experiments**

Dye release kinetics was studied for the range of PEG molecular weights. The cylindrical gel was placed in a cuvette containing 2ml of PBS solution. The cylindrical gel was placed in the cuvette in such a way so that the path of light through the bottom half of the cuvette would not be obstructed. The top portion of the cuvette was covered with parafilm. The cuvettes were then placed on a magnetic stirrer, in order to agitate the solution in the cuvette and facilitate the diffusion of dye from the gel into the solution. Thus, as the solution inside the cuvettes was stirred, the gel absorbed the PBS, and in turn released the dye trapped inside the gel. At intervals of 10 minutes, the cuvette was removed from the stirrer and a fluorescence

reading was taken. The excitation wavelength was 492nm and the emission was scanned from 500 to 540 nm. The fluorescence intensity was recorded at 514nm. Thus the fluorescence intensity of the solution to which dye diffuses is taken over a period of time. These transient fluorescence intensity readings provide an insight into the diffusion mechanism of the dye. These reading are taken over a period of three hours, to ensure sufficient diffusion of the dye, and enough data points for further analysis. Care was taken to ensure that the gel did not obstruct the path of light during fluorescence readings. Also the stir plate speed was kept constant for all molecular weight PEGs.

#### 4.4 Mathematical Analysis of Drug Transport Mechanism

In order to study the dye transport mechanism from the cylindrical PEGDA hydrogels, two different diffusion models were considered to fit the experimental data. Model 1 is described by the Ritger-Peppas equation [4.11] given here.

$$\frac{M_t}{M_\infty} = kt^n \quad (4.9)$$

Where  $\frac{M_t}{M_\infty}$  is the fractional release of the dye release, k is a constant, t is the release time, and n is the diffusional exponent that can be related to the drug transport mechanism. For a cylindrical hydrogel, when n=0.45, the dye release mechanism is Fickian diffusion. When n = 0.89, Case II transport occurs, leading to zero order release. When the value of n is between 0.45 and 0.89, anomalous transport is observed [4.9].

Model 2 is described by the Peppas-Sahlin equation (4.10), which accounts for the coupled effects of Fickian diffusion and Case II transport [4.9]

$$\frac{M_t}{M_\infty} = k_1t^{1/2} + k_2t \quad (4.10)$$

using the estimated parameters  $k_1$  and  $k_2$  obtained from the experimental data fit from the above equation (Eq 4.10), the ratio of relaxation (R) and Fickian (F) contributions were calculated using (Eq 4.11)

$$\frac{R}{F} = \frac{k_2}{k_1} t^{1/2} \quad (4.11)$$

Thus experimental release data was fit to both these models, Eq (4.10) and Eq (4.11), and the contributions of both relaxation and Fickian diffusion was calculated. Using these values, the dominant mechanism of transport was determined. Experimental data was analyzed, and fit to Eq (4.10) and (4.11) using POLYMATH (version 5.0). Data are represented as the mean plus or minus the standard deviation of n independent measurements, where n = 3.

#### 4.5 Mathematical Analysis of the Drug Release Kinetics

For one-dimensional radial release from a cylinder of radius a, under perfect sink initial and boundary condition; with a constant dye diffusion coefficient D, Fick's second law is written as [23];

$$\frac{\partial C}{\partial t} = \left[ D \left[ \frac{\partial^2 C}{\partial r^2} \right] + \frac{1}{r} \frac{\partial C}{\partial r} \right] \quad (4.12)$$

Where

$$t=0 \quad 0 < r < a \quad C = C_1$$

$$t=0 \quad r = a \quad C = C_0$$

The solution to Fick's law under the above specified conditions for a long cylinder with end effects neglected, and an aspect ratio  $2a/l < 0.2$  [4.11]

$$\frac{M_t}{M_\infty} = 1 - \sum_{n=1}^{\infty} \frac{4}{a^2 \alpha_n^2} \exp[-D \alpha_n^2 t] \quad (4.13)$$

Where the terms  $\alpha_n$  are the positive roots of  $J_0(a\alpha_n)$

$J_0$  is the Bessel function of the first kind of zero order and  $a\alpha_n$  are the zeros of that function. On using a short time approximation for one dimensional release from a cylinder, the fractional release can be written as [4.11] after truncating higher order terms

$$\frac{M_t}{M_\infty} = 4 \left[ \frac{Dt}{\pi a^2} \right] - \pi \left[ \frac{Dt}{\pi a^2} \right] - \frac{\pi}{3} \left[ \frac{Dt}{\pi a^2} \right]^{3/2} \quad (4.14)$$

The experimental data is fit to this Eq (4.14) using POLYMATH 5.0 and the diffusion coefficient D is the parameter determined from fitting.

## 4.6 Results and Discussions

### 4.6.1 Acrylation Chemistry

Polyethylene glycol needs to be acrylated in order to make crosslinking possible. The vinyl polymer group, once attached to the PEG, will form crosslinks on exposure to UV light. To determine whether this reaction was successful, FTIR scans were performed on the material to determine whether double bond conversion had taken place. The figures (4.1), (4.2) below show the results. PEG 200 shows a significant peak at  $1721 \text{ cm}^{-1}$ . This is representative of double bond conversion. The intensity of this peak is 0.261 absorbance units. PEG 10000 also shows a significant peak at 1711.69, again indicative of double bond conversion. The peak intensity is almost 0.068.

### 4.6.2 Swelling Parameters

Swelling parameters such as mesh size ( $\xi$ ) and molecular weight between crosslinks ( $M_c$ ) are determined from swelling experiments of PEG hydrogels. PEGs of different molecular weights were all studied, and their parameters calculated. The results for the above experiments as shown in Table (4.1)

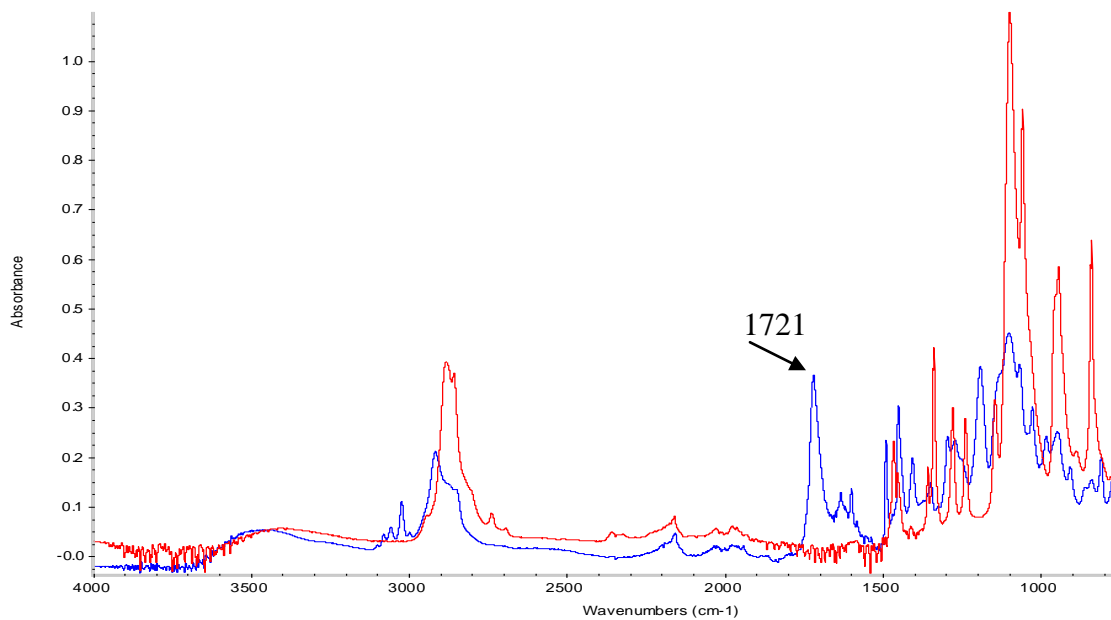


**Figure 4.1 FTIR Spectra of PEG 200. Red -PEG, Blue-PEGDA**

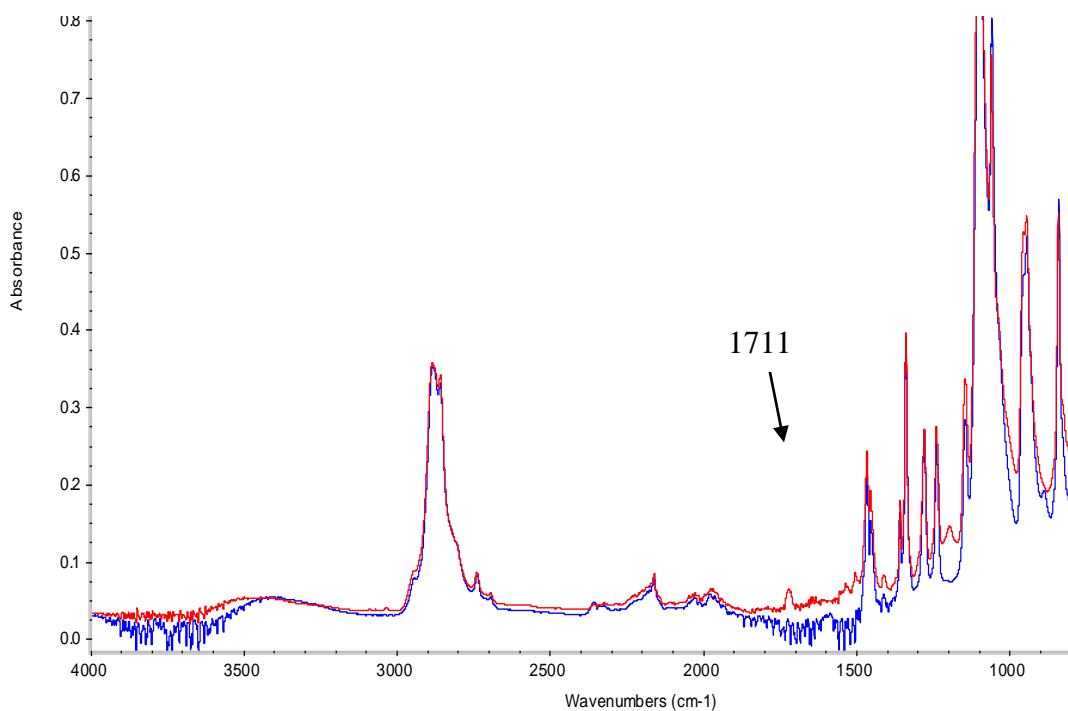


**Figure 4.2 FTIR spectra of PEG 10000. Red-PEGDA, Blue-PEG**

**Table 4.1 Calculated values of  $M_c$  and mesh size**

$M_n$ g/mole	$M_c$ (g/mole)	$\xi$ ( $\text{\AA}$ )
200	97.2	5.67
400	197.6	8.53
8000	3973	50.06
10000	4998.75	72.44
14000	6984.7	79.1
20000	9994.2	97.05

As can be seen, both the molecular weight between crosslinks and mesh size increase with increasing molecular weight of the PEG. This is expected, as increasing molecular weight, implies longer molecule, allowing more solvent to enter. This leads to widening of the mesh size. Figure (4.3) elucidates the relation between  $M_n$  and  $M_c$  in these gels.

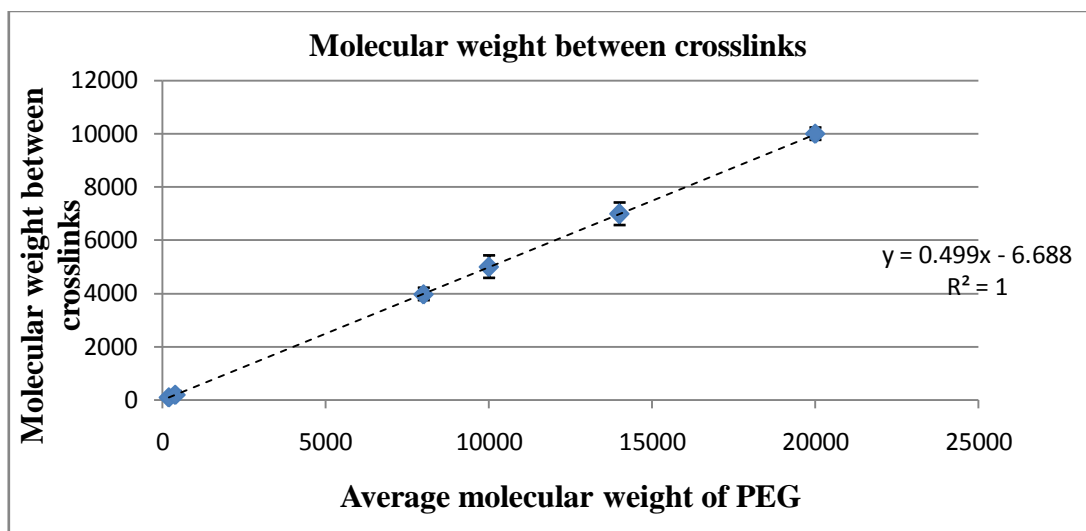


**Figure 4.3 Effect of average molecular weight on the molecular weight between crosslinks ( $M_c$ ). The dotted line represents the linear trendline fit**

The molecular weight between crosslinks, appears to increase linearly with increase in molecular weight of the gel. The mesh sizes also increases relatively linearly with

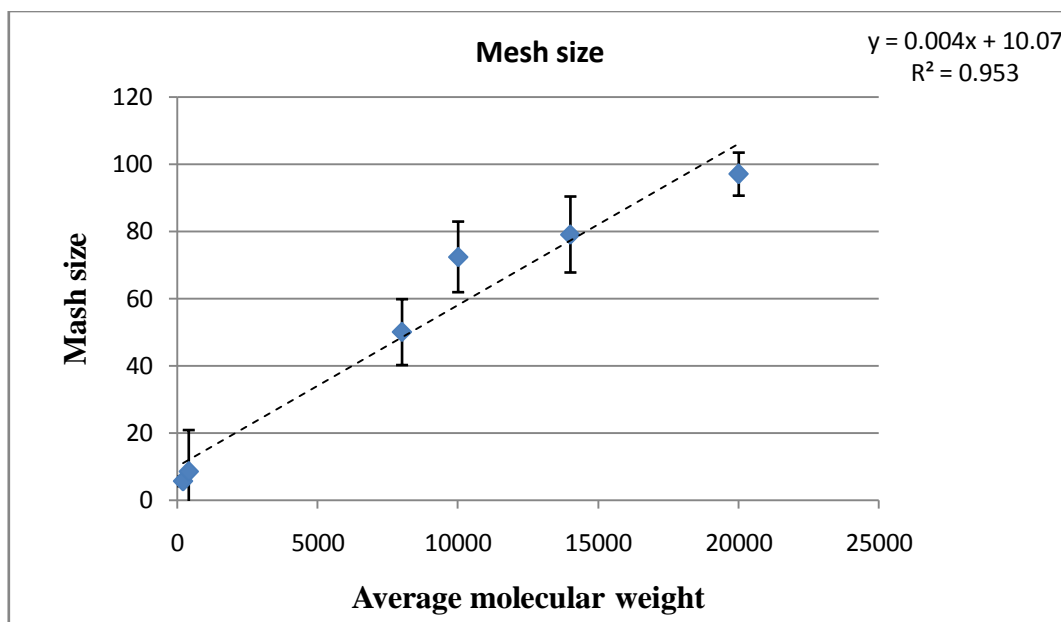


**Figure 4.4 Variation of mesh size with average molecular weight. The dotted line represents the linear trendline fit.**

increasing molecular weight. As the  $M_c$  increases due to increased swelling, the mesh widens, and increases the mesh size of the gel. PEG 200 and PEG 400 have very small mesh sizes, and show negligible swelling of the gel. These mesh sizes are small in comparison to the hydrodynamic diameter of most protein molecules, and thus may not be used for drug delivery. However the higher molecular weight PEGs show mesh size on the order of 90-100A which is closer to the diameter of several protein molecules. So diffusion of biomolecules into and from these large mesh size gels is possible. These higher molecular weight gels can be used as immobilization as well as drug delivery matrices.

#### 4.6.3 Swelling Studies and Analysis

Mesh size data gives us an idea about which PEGs would be ideal for drug delivery of small proteins and other drugs based on their hydrodynamic radii. However size is not the only consideration when selecting an ideal biomaterial. It is important to know the degree of gel swelling, as it is critical in understanding the diffusion mechanism. For this purpose swelling of

each PEG gel was recorded as a function of time and analyzed. Table (4.2) shows the values of n and k obtained by fitting this swelling data to power law Eq (4.9).

**Table 4.2 n and k values obtained from power law fit**

<b>PEG ( MW)</b>	<b>200</b>	<b>400</b>	<b>8000</b>	<b>10000</b>	<b>14000</b>	<b>20000</b>
<b>n</b>	0.47	0.439	0.547	0.4919	0.635	0.573
<b>95% Confidence</b>	1.72E-01	1.38E-05	8.80E-02	7.50E-02	2.08E-06	5.28E-02
<b>Variance</b>	8.32E-06	4.12E-06	4.43E-03	4.26E-02	3.95E-03	8.79E-03
<b>k</b>	2.09E-03	3.66E-03	1.09E-01	2.06E-01	9.16E-02	2.08E-01
<b>95% Confidence</b>	1.83E-03	1.79E-07	4.26E-02	1.19E-01	8.56E-07	3.44E-02
<b>Variance</b>	8.32E-06	4.12E-06	4.43E-03	4.26E-02	3.95E-03	8.79E-03

The values of k, the swelling constant gradually increases along with the molecular weight. The swelling constant represents the extent of swelling and, is dependent on the amount of solvent imbibed by the gel. As the mesh size increases, the swelling capacity of the gel also increases leading to higher and higher values of k. However PEG 14000 shows an anomalous k value of 0.091645 which is less than for PEG 10000. This is attributed to the fact that the nature of the gel after preparation was rubbery leading to erroneous results. The lower molecular weight PEGs, PEG 200 and 400 show n values close to 0.45, indicating that solvent diffusion can be described by Fick’s law. PEG 8000, PEG 10000, PEG14000, PEG20000 were all found to have values of n in the range  $0.45 < n < 0.85$ . According to Table (4.2), this implies anomalous diffusion takes place in these gels. Once the mechanism of swelling is determined, we were able to predict diffusion coefficients and thus examine the efficiency with which these gels can be utilized. Figure (4.5) shows the power law fit for PEG 200 and PEG 400, with n values close to 0.45.

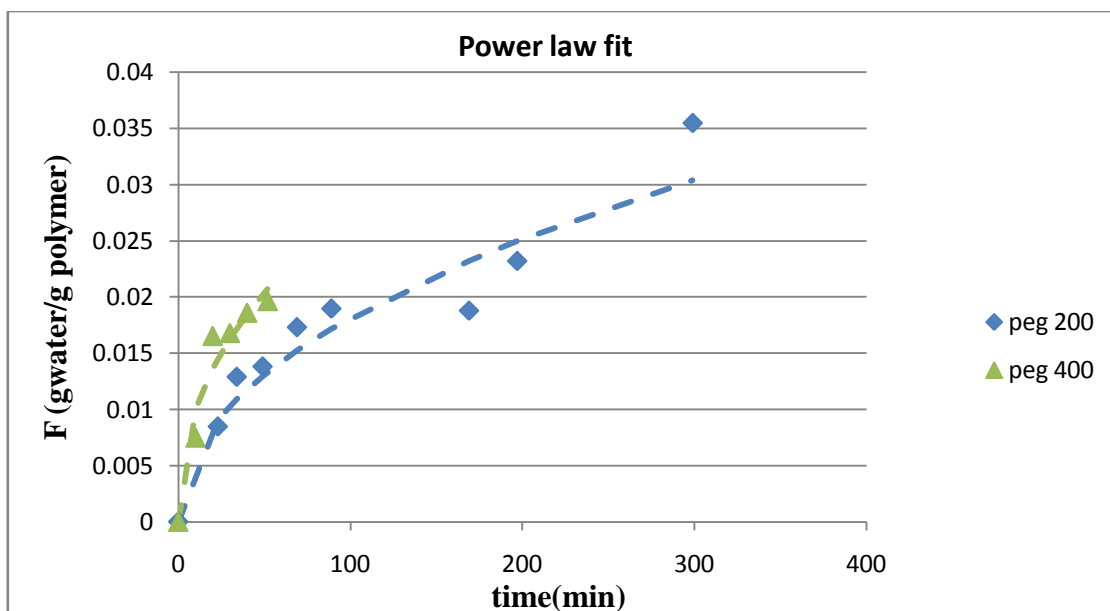


Figure 4.5 Power law fits for different PEG 200 and PEG 400. The dotted line represents equation fit

Fickian diffusion is approximated in all these gels, to allow calculation of diffusion coefficients. PEG 10000 and above have values of  $n$  much larger than 0.45, thus indicating a little Fickian contribution to the diffusion characteristics of the gels.

Table 4.3 Variation of diffusion coefficient with molecular weight

PEG(MW)	D(mm <sup>2</sup> /min)	Variance	95% Confidence
200	7.00E-06	7.00E-06	2.00E-06
400	1.70E-05	4.00E-06	5.00E-06
8000	3.56E-02	4.56E-03	2.68E-03
10000	7.74E-02	5.29E-02	8.92E-03
14000	5.53E-02	1.14E-02	5.49E-03
20000	6.89E-02	1.45E-02	4.06E-03

As expected, the diffusion coefficients increase with molecular weight, as the ease with which solvent molecules can diffuse increases. PEG 200 and PEG 400, owing to their low diffusion coefficient swell almost negligibly. While PEG 14000 and PEG 20000 should have D values

greater than that of PEG 10000, since PEG 14000 and PEG 20000 are not purely Fickian, their fit to the Fickian solution is unreliable. Thus the D values for these PEGs are inaccurate. The higher molecular weight PEGs are difficult to characterize, due to their non-Fickian character.

#### 4.6.4 Dye Diffusion Studies

Dye diffusion is studied as a mimic of small molecules such as drugs; and to understand the diffusion characteristics of the molecule from the gels. First the dye diffusion data was fit to the power law expression (4.9). The table below shows the values of parameters n and k obtained by fitting diffusion data to Eq(4.9). As expected, the values of the swelling constant increases with molecular weight, owing to increase in the degree of swelling. PEG 14000 and PEG 20000 however show anomalous values for k. These higher molecular weight PEGs have such high degree of swelling, that the diffusion of the dye becomes almost linearly dependent on time. This causes experimental error in predicting the mechanism of diffusion thus showing erroneous values of k.

**Table 4.4 n and k values obtained from power law fit**

<b>PEG(MW)</b>	<b>200</b>	<b>400</b>	<b>8000</b>	<b>10000</b>	<b>14000</b>	<b>20000</b>
<b>N</b>	0.543	0.421	0.43	0.5606	0.5315	0.739
<b>95% Confidence</b>	1.13E-04	3.72E-04	1.67E-03	3.62E-02	7.69E-02	4.35E-02
<b>Variance</b>	1.82E-04	3.70E-05	7.69E-04	2.92E-04	1.60E-05	5.00E-05
<b>K</b>	1.21E-02	2.88E-02	4.26E-02	3.43E-02	1.08E-02	1.55E-02
<b>95% Confidence</b>	6.00E-06	5.20E-05	3.24E-04	6.32E-03	3.67E-03	2.91E-03
<b>Variance</b>	1.82E-04	3.70E-05	7.69E-04	2.92E-04	1.60E-05	5.00E-05

PEG 400 and PEG8000 have values of n in the range of 0.45, and Fickian diffusion can be assumed to be dominant in these gels. PEG 200, PEG 10000, PEG 14000, PEG 20000 have values of n indicating that diffusion in these gels is anomalous. As for swelling data, dye data

was fit to Eq(4.10), and (4.11) estimated values of the diffusion coefficient D were calculated. Table (4.5) gives values of  $k_1$  and  $k_2$  and Ratios F/R for each PEG.

**Table 4.5 Peppas equation parametes.**

<b>PEG(MW)</b>	<b>200</b>	<b>400</b>	<b>8000</b>	<b>10000</b>	<b>14000</b>	<b>20000</b>
<b><math>k_1</math></b>	1.39E-02	2.30E-02	3.48E-02	3.97E-02	1.86E-02	2.70E-02
<b><math>k_2</math></b>	8.31E-05	-2.80E-04	-3.80E-04	5.29E-04	8.19E-05	2.60E-03
<b>F/R</b>	33.2	140	23.4	20.05	30.1	2.055

All the PEGs except for PEG 20000 have a F/R ratio greater than 20, implying that Fickian contribution is at least 20 times that of relaxation. We can thus approximate all these gels to follow Fick’s law of diffusion. PEG 20000 has an F/R ratio of 2, and its diffusion cannot be assumed to be predominantly Fickian. This is again caused by large degree of swelling, which makes the relaxation of the polymer the dominant mechanism of diffusion. Thus all PEGs except PEG 2000 can be assumed to follow Fick’s law, and their diffusion data can be fit to Eq(4.14) to obtain values of D (diffusion coefficient)

**Table 4.6 Variation of diffusion coefficients with molecular weight**

<b>PEG(MW)</b>	<b>D(mm2/min)</b>	<b>95% confidence</b>	<b>Variance</b>
200	4.69E-04	2.58E-05	2.58E-05
400	4.54E-04	3.48E-05	1.72E-04
8000	1.06E-03	1.67E-04	8.14E-04
10000	5.74E-03	6.99E-04	0.001806
14000	1.73E-04	1.15E-05	1.95E-05

Diffusion coefficient increases with molecular weight, indicating increasing ease of diffusion of dye. As swelling of the gel increases (opening the mesh), it becomes easier for solute molecules to diffuse out of the gel. PEG14000 has a lower value of D than expected, as high degree of swelling causes the gel to not conform to Fick’s law completely. The dye release

data for lower MW PEGs can be described by Fickian diffusion equations indicating that the diffusion of the dye is influenced only by concentration difference between the gel and its surrounding. In almost all cases, higher molecular weight PEGs (PEGs with MW >10000) are influenced by the relaxation of the gel, and Fick's law no longer applies.

#### **4.7 Conclusions**

Understanding the diffusion characteristics of polyethylene glycol involves not only understanding the structure of the gel and the mechanism of diffusion, but also being able to devise a simple method to predict the efficiency with which diffusion takes place. Mesh size calculation for these gels leads to the conclusion that the larger molecular weight gels would be good matrices for drug delivery due to their large mesh size. However, as the mesh size increases, it becomes difficult to find analytical solutions to help predict diffusion coefficients. Swelling experiments reinforce the dilemma surrounding these gels. PEG 14000 and greater show larger degree of swelling, and thus their diffusion coefficients are higher. However diffusion in these gels are highly anomalous, and influenced by the relaxation of the gel, so cannot be predicted using Fick's law. Using Peppas's equation, we can however develop a basis on which approximations can be made. In spite of the assumption of Fickian diffusion in these gels, in most cases, the results are unreliable.

Diffusion of dye was studied, as it would mimic closely small sized drugs in the same size range. Dye diffusion was very low for PEG 200 and PEG 400 as the small mesh size hindered the passage of the dye. As the mesh size increased, it became easier for solute molecules to diffuse out of the gel, and the diffusion coefficient increased. For PEG 14000 and PEG 20000, the mesh size is so large, that dye diffuses out quickly and it is the relaxation of the polymer which determines the characteristics of diffusion. Even though dye diffusion is taking place in large quantities, it becomes difficult to analyze, and cumbersome to develop equations

for prediction of D. Thus a balance must be maintained for PEG hydrogels to be useful as biomaterial carriers. The gel must allow diffusion of molecules easily and quickly, and also the diffusion mechanism should ideally be Fickian to enable easy interpretation and analysis. So, a hybrid gel with intermediate properties might be the ideal material for drug delivery.

## 4.8 References

- 4.1 Cruise, G.M., D.S. Scharp, and J.A. Hubbell, *Characterization of permeability and network structure of interfacially photopolymerized poly(ethylene glycol) diacrylate hydrogels*. *Biomaterials*, 1998. 19(14): p. 1287-1294.
- 4.2 Hennink, W.E. and C.F. van Nostrum, *Novel crosslinking methods to design hydrogels*. *Advanced Drug Delivery Reviews*, 2002. 54(1): p. 13-36.
- 4.3 Lin, C.-C. and A.T. Metters, *Hydrogels in controlled release formulations: Network design and mathematical modeling*. *Advanced Drug Delivery Reviews*, 2006. 58(12-13): p. 1379-1408.
- 4.4 Mellott, M.B., K. Searcy, and M.V. Pishko, *Release of protein from highly cross-linked hydrogels of poly(ethylene glycol) diacrylate fabricated by UV polymerization*. *Biomaterials*, 2001. 22(9): p. 929-941.
- 4.5 Merrill, E.W., K.A. Dennison, and C. Sung, *Partitioning and diffusion of solutes in hydrogels of poly(ethylene oxide)*. *Biomaterials*, 1993. 14(15): p. 1117-1126.
- 4.6 Pathak, C.P., A.S. Sawhney, and J.A. Hubbell, *Rapid photopolymerization of immunoprotective gels in contact with cells and tissue*. 1992. p. 8311-8312.
- 4.7 Peppas, N.A., et al., *Hydrogels in pharmaceutical formulations*. *European Journal of Pharmaceutics and Biopharmaceutics*, 2000. 50(1): p. 27-46.
- 4.8 Peppas, N.A. and J.J. Sahlin, *A simple equation for the description of solute release. III. Coupling of diffusion and relaxation*. *International Journal of Pharmaceutics*, 1989. 57(2): p. 169-172.
- 4.9 Perez, J.P.H., E. Lopez-Cabarcos, and B. Lopez-Ruiz, *The application of methacrylate-based polymers to enzyme biosensors*. *Biomolecular Engineering*, 2006. 23(5): p. 233-245.
- 4.10 Ritger, P.L. and N.A. Peppas, *A simple equation for description of solute release I. Fickian and non-fickian release from non-swellable devices in the form of slabs, spheres, cylinders or discs*. *Journal of Controlled Release*, 1987. 5(1): p. 23-36.
- 4.11 Russell, R.J., et al., *Mass transfer in rapidly photopolymerized poly(ethylene glycol) hydrogels used for chemical sensing*. *Polymer*, 2001. 42(11): p. 4893-4901.

- 4.12 Sawhney, A.S., C.P. Pathak, and J.A. Hubbell, *Interfacial photopolymerization of poly(ethylene glycol)-based hydrogels upon alginate-poly(l-lysine) microcapsules for enhanced biocompatibility*. *Biomaterials*, 1993. 14(13): p. 1008-1016.
- 4.13 Serra, L., J. Domenech, and N.A. Peppas, *Drug transport mechanisms and release kinetics from molecularly designed poly(acrylic acid-g-ethylene glycol) hydrogels*. *Biomaterials*, 2006. 27(31): p. 5440-5451.
- 4.14 Siepmann, J. and N.A. Peppas, *Modeling of drug release from delivery systems based on hydroxypropyl methylcellulose (HPMC)*. *Advanced Drug Delivery Reviews*, 2001. 48(2-3): p. 139-157.
- 4.15 Stringer, J.L. and N.A. Peppas, *Diffusion of small molecular weight drugs in radiation-crosslinked poly(ethylene oxide) hydrogels*. *Journal of Controlled Release*, 1996. 42(2): p. 195-202.
- 4.16 N.A. Peppas, "*Hydrogels and Drug Delivery*," *Curr. Opinion Coll. Interfac. Sci.*, 2, 531-537 (1997).
- 4.17 N.A. Peppas: *Hydrogels in Medicine and Pharmacy, Vol. 1. Fundamentals*, CRC Press, Boca Raton, FL, 1986, 180 pages.
- 4.18 Gregory M. Cruise, O.D.H.D.S.S.J.A.H., *A sensitivity study of the key parameters in the interfacial photopolymerization of poly(ethylene glycol) diacrylate upon porcine islets*. 1998. p. 655-665.
- 4.19 Sirkar, K. and M.V. Pishko, *Amperometric Biosensors Based on Oxidoreductases Immobilized in Photopolymerized Poly(ethylene glycol) Redox Polymer Hydrogels*. 1998. p. 2888-2894.
- 4.20 Russell, R.J., et al., *Poly(ethylene glycol) Hydrogel-Encapsulated Fluorophore-Enzyme Conjugates for Direct Detection of Organophosphorus Neurotoxins*. 1999. p. 4909-4912.
- 4.21 Pradyut Ghosh, M.L.A.W.M.L.M.V.P.R.M.C., *A Simple Lithographic Approach for Preparing Patterned, Micron-Scale Corrals for Controlling Cell Growth*. 1999. p. 1592-1595.
- 4.22 *The Mathematics of Diffusion (2nd Edition ed.)*, Oxford University Press, Oxford (1979), p. 35. 11
- 4.23 Takeru, H., *Rate of release of medicaments from ointment bases containing drugs in suspension*. 1961. p. 874-875.
- 4.24 Roseman, T.J., *Release of steroids from a silicone polymer*. 1972. p. 46-50.
- 4.25 Hasine, K., A. İsmail, and K. Ahmet, *The effect of PEG(400)DA crosslinking agent on swelling behaviour of acrylamide-maleic acid hydrogels*. *Polymer Bulletin*, 2005. 54(6): p. 387-397.

# Chapter 5 : Study of Mixtures of PEGDA Hydrogels

## 5.1 Introduction

PEGDA hydrogels of different molecular weights have been researched widely. PEGDA has vastly different characteristics, depending on molecular weight. The idea behind the study of mixture behavior was that a binary mixture of two different molecular weight PEGs could have combinatorial properties of its constituent PEGs. The properties of a particular gel matrix could thus be manipulated by using appropriate molecular weights in proportion to desired properties. So, combination mixtures of different molecular weight PEGs were studied, to determine their mesh sizes, polymer volume fractions, molecular weight between crosslinks, and swelling properties. Once various combinations had been studied, one particular combination was selected, in order to determine the dependence of mixture ratios on structural parameters, and thus swelling and diffusion properties. The mixture chosen was 200/14000 which would adequately represent an intermediate molecular weight, as well as intermediate properties of both lower molecular weight 200 as well as higher molecular weight PEG 14000. Ratios of the two different molecular weight PEGS were widely varied to address a wide range of mixture conditions. Swelling parameters obtained were then studied, to determine whether a direct correlation existed between the ratio of PEGs, and the structural parameters of mesh size, and  $M_c$ . This would enable us to synthesize a gel of required intermediate properties by using mixtures of PEGS, and varying their mass ratio to obtain the exact properties required for biomedical uses.

## 5.2 Materials and Methods

### 5.2.1 Materials

Poly (ethylene glycol) diacrylate with molecular weights 200, 400 were obtained from Polysciences (Warrington, PA). 0.1 molar phosphate buffered saline (PBS, pH 7.4) was prepared from potassium phosphate monobasic, sodium phosphate, potassium chloride, and 18 mega ohm deionized water via a standard preparation method. Poly (ethylene glycol) (molecular weights 8000, 10000, 14000, and 20000), acryloyl chloride, trimethylamine, and diphenyl (2, 4, 6 trimethylbenzoyl)-phosphine oxide/2-hydroxy-2-methyl propiophenone 50/50 were all obtained from Sigma Aldrich Co. (St. Louis, MO). 0.2 micron Teflon membrane filters as well as glass membrane filters were obtained from Molecular probes (Eugene, OR). All other reagents and chemicals, unless specifically mentioned, were supplied by Sigma-Aldrich (St. Louis, MO).

### 5.2.2 Preparation of Mixed PEGDA Hydrogels

Mixtures of PEGDA were prepared in a 50/50 mass ratio. Various combinations of different molecular weight pairs were chosen, such that a broad range of mixtures could be examined. The following PEGDA mixtures were prepared and investigated

**Table 5.1 Mixtures of PEGDA with its constituent molecular weights**

MOL WT(PEGDA)		
Sample	PEG1	PEG2
1	200	400
2	200	8000
3	400	10000
4	200	14000
5	400	20000
6	10000	20000

### 5.2.3 Sample Mixture Preparation

PEGDA 1 (0.5ml), PEGDA 2 (0.5ml), photoinitiator (1ml) and 0.1M phosphate buffer solution PBS (1ml) were combined and vortexed to obtain a well mixed solution. The solutions were heated, if necessary, in order to facilitate mixing. All combination mixtures were added in a 50/50 mass ratio, while the amount of photoinitiator, and PBS solution remained the same for all different molecular weight combinations. These solutions were then poured into acrylic tubes ( $D = 1/4$  in  $L = 2$ in), in order to shape the gels in the form of long cylinders. These tubes are then sealed with parafilm at one end, and exposed to UV radiation (INTELLI-RAY 600, 600 Watt, 115/230V) for a period of 40s. The dimensions of the cylindrical hydrogels formed were measured to ensure a maximum aspect ratio of 0.2. This aspect ratio ( $2a/L$ ) of 0.2 is the maximum aspect ratio for which the assumption of one dimensional diffusion in a cylinder is valid [5.1].

### 5.2.4 Calculation of Mesh Size

As with the individual molecular weight hydrogels, these combination hydrogels were subjected to swelling experiments. The cylindrical gels were weighed and placed in 10ml of 0.1 M phosphate buffer solution. The gel was kept in the solution for a period of one week in order to ensure maximum uptake of solution, and equilibrium swelling. The gel was again weighed, and left to dry for 48 hours. Once the gel was completely dry, the dry gel was again weighed. The following parameters were then calculated:

$W_{a,r}$  = sample weight after crosslinking

$W_{a,s}$  = sample weight after swelling

$W_{a,d}$  = sample weight after drying

These measurements were used to determine the volume of the hydrogel sample after crosslinking (but before swelling),  $V_{g,r}$ , and after equilibrium swelling,  $V_{g,s}$ . The following are the equations used to calculate these volumes.

$$V_{g,r} = \frac{W_{a,r}}{\rho_{a,r}} \quad (5.1)$$

$$V_{g,s} = \frac{W_{a,s}}{\rho_{a,s}} \quad (5.2)$$

$$V_p = \frac{W_{a,d}}{\rho_{a,d}} \quad (5.3)$$

Where,

$V_p$  = weight of dry polymer

$$\rho_{a,r} = \rho_{peg\ 1}x_{peg\ 1} + \rho_{photoinitiator\ (pi)}x_{pi} + \rho_{pbs}x_{pbs} + \rho_{peg\ 2}x_{peg\ 2}$$

$$\rho_{a,s} = \rho_{peg\ 1}x_{peg\ 1} + \rho_{photoinitiator\ (pi)}x_{pi} + \rho_{pbs}x_{pbs} + \rho_{peg\ 2}x_{peg\ 2}$$

$$\rho_{a,d} = \rho_{peg\ 1}x_{peg\ 1} + \rho_{photoinitiator\ (pi)}x_{pi} + \rho_{peg\ 2}x_{peg\ 2}$$

Here,

$\rho_{peg\ 1}$  = density of PEG mol wt 1

$\rho_{peg\ 2}$  = density of PEG mol wt 2

$\rho_{photoinitiator\ (pi)}$  = density of photoinitiator

$\rho_{pbs}$  = density of phosphate buffer solution

$x_{pi}$ ,  $x_{pbs}$ ,  $x_{peg\ 1}$ ,  $x_{peg\ 2}$ , are mole fractions of photoinitiator, PBS, PEG (mol wt 1), PEG (mol wt 2)

These above calculated values were then used to calculate the mesh size from the following equation:

$$\frac{1}{M_c} = \frac{2}{M_n} - \frac{\left(\frac{v}{v_1}\right) [\ln(1-v_{2,s}) + v_{2,s} + \chi_1 v_{2,s}^2]}{v_{2,r} \left[ \left(\frac{v_{2,s}}{v_{2,r}}\right)^{1/3} - \left(\frac{v_{2,s}}{2v_{2,r}}\right) \right]} \quad (4)$$

Here,  $\chi$  (polymer solvent interaction parameter) = 0.55 and  $M_n$  is the average molecular weight of PEG mixture. The average mesh size of the polymer network was calculated as described by Peppas and Merrill [5.2]. The root mean squared end-to end distance of a randomly coiled polymer bonds with a length  $l$  and characteristic ratio  $C_n$  was calculated as:

$$(r^2)^{1/2} = \chi C_n^{1/2} n^{1/2} l \quad (5.5)$$

where,  $C_n = 4.0$  and  $l = 1.54 \text{ \AA}$  (for vinyl bonds),  $n = \frac{2\bar{M}_c}{M_r}$

The average mesh size of the network was then,

$$\xi = v_{2,s}^{-1/3} (r^2)^{1/2} \quad (5.6)$$

### 5.2.5 Study of Swelling Characteristic of PEG 200/14000 Mixture

Once the mesh sizes for various mixtures of different molecular weight PEGs were calculated, one combination mixture was chosen and studied in detail. The mixture chosen was 200/14000 PEGs as it would provide the largest range of properties. Different concentration combinations of this mixture were prepared, and a wide concentration range was chosen. The following hydrogels with given mass fractions of 200/14000 peg were prepared as mentioned earlier (Section 4.3 Chapter 4). Each mixed gel was weighed and placed in 10ml of 0.1 M PBS solution. The weight of the gel was taken every 10 minutes for a period of three hours, taking care that no PBS remains on the surface of the gel during measurement. After the readings were taken, the gel was returned to the PBS solution for a week to ensure maximum absorption of solution into the gel.

**Table 5.2 Various concentration combination of PEGDA mixture 200/14000**

<b>PEG</b>	<b>Mass</b>	<b>Fraction</b>
<b>Sample #</b>	<b>200</b>	<b>14000</b>
1	0.1	0.9
2	0.2	0.8
3	0.3	0.7
4	0.4	0.6
5	0.5	0.5
6	0.6	0.4
7	0.7	0.3
8	0.8	0.2

Once this equilibrium swelling state was reached, the gel was taken out of solution, weighed and allowed to dry in air. After 48 hours, all the water had been desorbed and only the crosslinked polymer remained. At this point the gel was again weighed. This allowed for the calculation of both the transient swelling behavior and the mesh size for each combination gel sample. From the equilibrium swelling data, the mesh size was calculated as mentioned above (Eq (3.6)), accounting for the changes in mass fractions of the constituents in the gel. The following equation was used to determine the kinetics of the swelling process of these hydrogels [5.3]:

$$F = \left( \frac{W_s - W_p}{W_p} \right) = kt^n \quad (5.7)$$

Where,

F= g PBS/g polymer

$W_s$  = weight of swollen polymer at time t

$W_p$  = weight of the dry polymer at time t=0

Here k and n are the swelling constant and swelling exponent respectively. The above equation can only be applied to the first 60% of swelling. The swelling data obtained was fit to the above equation using POLYMATH (version 5.0) and values of n and k were calculated.

For Fickian diffusion of PBS from the gels, we can approximate the diffusion coefficient for swelling of these cylindrical gels. This allows for a better understanding and tailor ability of the transport properties of these gels. The diffusion coefficients were calculated by using the following equation:

$$F=4(Dt/\pi r^2)^{1/2} \quad (5.8)$$

Here,

D= coefficient of diffusion

r= radius of the cylindrical gel

In the above equation, radial diffusion is assumed as the sole form of diffusion, and all end effects are neglected. Also it is assumed that the diffusion mechanism is Fickian .Using POLYMATH (version 5.0), approximate values of D (coefficient of diffusion) were obtained and analyzed.

### **5.3 Results and Discussion**

Mixtures of different molecular weight PEGs were studied in an attempt to produce hybrid gels, with desired structural properties and swelling behavior. It was seen previously [Chapter 4, Section 4.6] that the properties of PEG vary drastically with molecular weight. The idea is to design a gel with adequate mesh size to facilitate the diffusion of penetrant to and from the gel, but simultaneously control the release behavior of a desired compound. Additionally the design should allow for simple and accurate prediction of diffusion coefficients. PEG mixtures of various molecular weights, were studied via swelling

experiments. A linear relation between mixture swelling properties, and individual PEG properties was established. It was apparent that changing quantities of constituent components had a significant effect on the properties of the gel. One combination mixture was selected, and its individual PEG ratios varied, to analyze the effect of changing PEG ratios. The diffusion regimes of these gels, and their approximate diffusion coefficients were also calculated as the first step in determining suitability of these gels as drug delivery devices.

### **5.3.1 Mesh Sizes for Different Mixture Combination**

Different mixture combinations of polyethylene glycol with differing molecular weights were studied for swelling behavior. A wide range of molecular weights was used to obtain a broad range of data. The constituting PEGs were in equal quantities in the gel. Mesh sizes of each combination gel was calculated from swelling studies using Flory-Rehner theory [5.4]. The mesh sizes were found to increase with the molecular weight between crosslinks ( $M_c$ ). There seemed to be a direct relation between the mixture  $M_c$ , and the  $M_c$  of the constituent molecular weight gels. Results from the swelling experiments are as shown in Table (5.3). The mesh sizes calculated for the mixtures from experimental data were compared with mesh sizes calculated from theoretical data. From the homogenous hydrogels (Table (5.1)), the theoretical mesh sizes for the mixtures were calculated as the weighted average of the individual mesh sizes of the two PEG gels. The theoretical molecular weight between crosslinks was also calculated similarly by averaging the individual  $M_c$ 's. The following figure (5.1) compares theoretical and calculated mesh sizes. In order to simplify comparison of mesh sizes, each mixture was represented by the weighted average of its constituent molecular weight PEGs. The above figure shows that for most of the combinations, the theoretical and calculated mesh sizes are almost equal. However as the average molecular weight of the mixture increases, so does the disparity in the values of the mesh sizes.

**Table 5.3 Mesh sizes and molecular weight between crosslinks for all mixture combinations**

PEG(MW)		mesh size(Å) (Experimental)	$M_c$ (experimental)	Mesh( Å) size(theoretical)	$M_c$ (theoretical)
PEG 1	PEG 2				
200	400	7.32E+00	1.48E+02	7.10E+00	1.47E+02
200	8000	2.96E+01	1.96E+03	2.79E+01	2.04E+03
200	14000	3.96E+01	2.56E+03	4.05E+01	2.60E+03
400	10000	4.32E+01	3.45E+03	4.24E+01	3.54E+03
400	20000	8.21E+01	5.10E+03	5.28E+01	5.10E+03
10000	20000	9.34E+01	7.50E+03	8.47E+01	7.50E+03

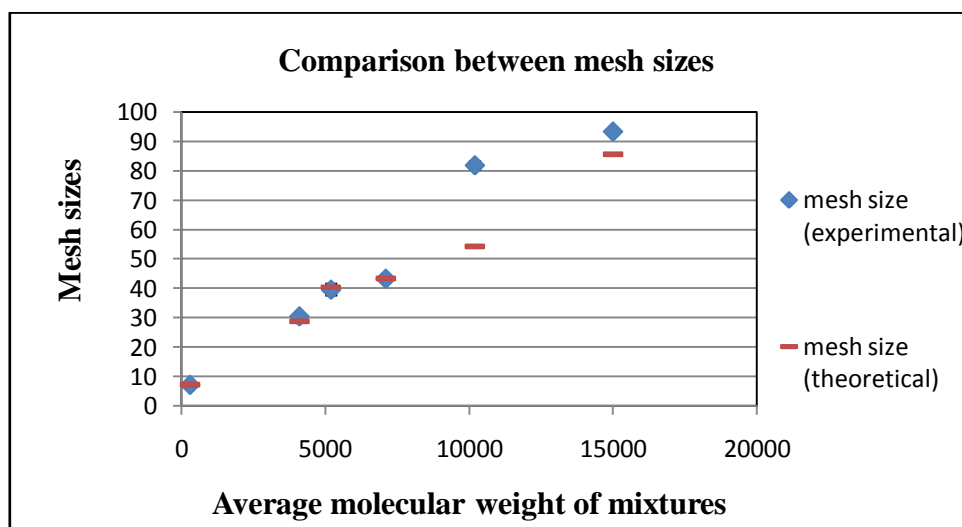


**Figure 5.1 Comparison of theoretical and calculated mesh sizes for all mixtures. The theoretical mesh size is the weighted average of individual PEG mesh sizes**

For combinations which involve PEG 20000, it is seen that there is a significant difference between calculated and experimental values. The experimental values are of a higher value than the expected theoretical values. That is when two PEGs of different molecular weight are combined; the mesh size of the combined gel in most cases is the same as the simple

combination of the mesh sizes of the two PEGs in question. However the relation is not so simple for higher molecular weight combinations. Gels involving PEG 20000 have a larger mesh size than expected. This is probably due to the fact that PEG 20000 swells to a large degree, overpowering the affects of any other PEG, leading to large mesh sizes. For the combination of PEG 20000 and PEG 200, the theoretical expected mesh size is 85.6Å, compared to an actual mesh size of 93.4 Å. This is a large variance, and is probably due to the fact that the contribution of PEG 200 was completely overshadowed by the swelling capacity of the PEG 20000 thus leading to an overall net higher mesh size. In the case of PEG 10000 and 20000 mixture, the discrepancy still exists, but to a lesser degree. Both PEG 10000 and 20000 swell, thus the PEG 20000 does not completely dominate the swelling process. However it does seem to have some semblance of control, as the mesh size is again larger than expected. These results show that mesh sizes of combination PEGs, can be influenced by one component more than the other.

In addition to mesh size, the molecular weight between crosslinks is another swelling property which provides insight into hydrogel characteristics. The figure below shows a comparison between theoretical and calculated mesh sizes for the given mixtures. Once again the mixtures are represented as average molecular weights of constituent PEGs. The theoretical  $M_c$ 's we obtained by the same method as the mesh sizes. The above figure (5.2) shows both the calculated and theoretical values of  $M_c$ . They are almost identical, indicating that there must be a linear relation individual  $M_c$  of PEGs, and the mixture  $M_c^{mix}$ . It appears that combining the two PEGs, gives the same  $M_c^{mix}$  as the simple average of the two individual PEGs. However it is difficult to draw conclusions as to the combined behavior of these gels, from the above data, as variations in quantities of the two PEGs was not investigated.

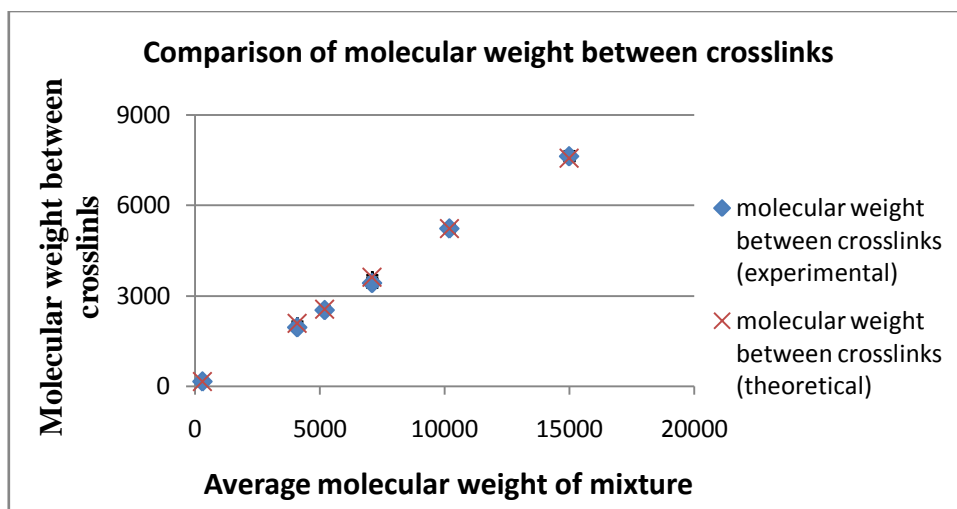


**Figure 5.2 Comparison of theoretical and experimental Molecular weight between crosslinks for mixtures. The theoretical values are weighted averages of the individual PEG  $M_c$  values**

. . From the above data, with equal amounts of both PEGs in the mixture, we are unable to determine if varying the amounts of PEG, still supports a linear relation between the weighted individual  $M_c$  and  $M_c^{mix}$ . For a complete analysis of the mixture behavior, a single mixture combination was chosen, and the amounts of the individual PEGs were varied.

### 5.3.2 Variation of Mass fractions in Mixture

One mixture combination was chosen, for further study of gel behavior. The mixture chosen was that of PEG 200 and PEG 14000. The above mixture provided the broadest range of gel behavior, ranging from low molecular weight 200 to high molecular weight PEG 14000. PEG 14000 was preferred over PEG20000 due to the excessive swelling presented by PEG 20000. The mass fractions of the mixtures were varied and the resulting gels were analyzed. The concentration of the gels is given in Table (5.2). The results of the above experiments are as shown in figures (5.3). The above curve demonstrates that there exists a linear relation between the theoretical  $M_c$  calculated from individual PEG data and mixture's net  $M_c$ . The theoretical  $M_c$  was calculated by adding the weighted averages of the  $M_c$ 's of the individual PEGs.

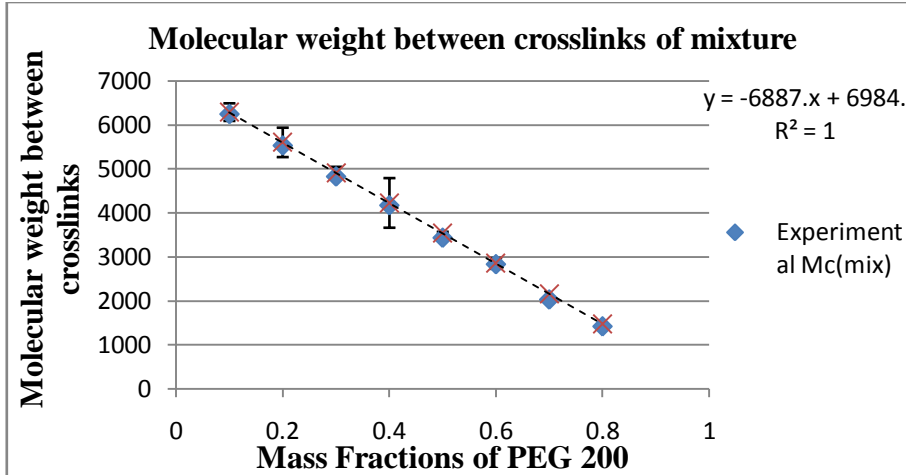


**Figure 5.3 Comparison of theoretical and experimental  $M_c$  (mixture) with variation of mass fractions of constituent PEGs. The increasing mass fractions represented are those of PEG 200.**

. We can see that both the calculated and theoretical values overlap, confirming the existence of a linear relationship between the mixture  $M_c$ , and the individual  $M_c$ 's. Table(5.4) shows both  $M_c$  values.

**Table 5.4 Table of calculated and experimental values of  $M_c$  for each mixture combination. The increasing mass fractions are those of PEG 200**

Mass Fraction	Experimental $M_c$	Theoretical $M_c$
0.1	6.25E+03	6.30E+03
0.2	5.53E+03	5.61E+03
0.3	4.83E+03	4.92E+03
0.4	4.17E+03	4.23E+03
0.5	3.44E+03	3.54E+03
0.6	2.84E+03	2.85E+03
0.7	2.03E+03	2.16E+03
0.8	1.42E+03	1.47E+03

Thus we can predict the following equation for mixture  $M_c$ .

$$M_c^{mix} = M_c^{PEG1} x_{PEG1} + M_c^{PEG2} x_{PEG2} \quad (5.9)$$

Where,  $M_c^{mix}$  is the molecular weight between crosslinks for the mixture.  $M_c^{PEG1}$  and  $M_c^{PEG2}$  are the individual molecular weight between crosslinks for the constituent PEGs in the mixture.  $x_{PEG1}$  and  $x_{PEG2}$  represent the mass fractions of the individual PEGs in the mixture. This equation is valid for the complete range of combination mixtures, and shows that one can predict the  $M_c^{mix}$  if the mass fractions of the constituent PEGs is known.

Another important parameter that was investigated with mass fraction variance was the mesh size. The figure (5.4) below shows the behavior of mixture mesh sizes with variance in mass fractions of its constituent PEGs. It is clear that as the fraction of PEG200 increases, the mesh size decreases. This is expected as more of the PEG 200 is incorporated, the properties of the mixture gel is dominated by the effects of the PEG 200 faction. From earlier analysis, it is known that PEG 200 has negligible swelling capacity due to its very small mesh size.

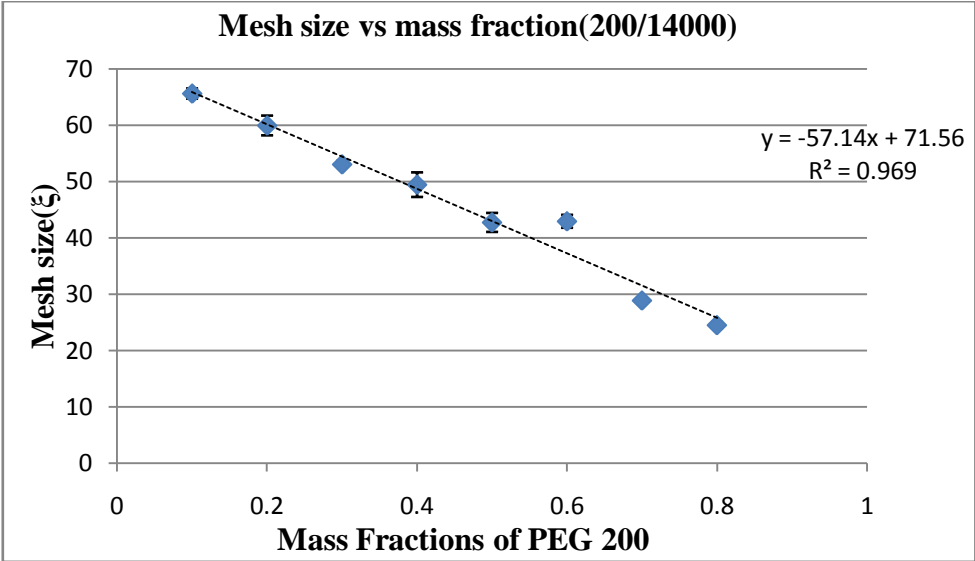


**Figure 5.4 Effect of changes in mass fraction ratios on the mesh size of the mixtures. The trend line shows a linear fit.**

Thus, the results prove that the mixture behavior is influenced by the ratio of the amounts of individual PEGs. So a gel can be tailor-made to exhibit certain properties and

behavior, by just simply altering the quantities of individual PEGs. This becomes a very useful tool when designing drug delivery matrices with pre-determined structural characteristics.

### 5.3.3 Swelling Properties of Mixture

The mixture combination of PEG 200 and PEG 14000 was studied, for swelling behavior. From the mesh size data obtained above, it was clear that as the mass fractions were varied, the properties of the gel mixture changed dramatically. Swelling of the gel, and study of the swelling parameters, gives us a detailed picture of how these properties of the gel change. Additionally, the swelling data also tells us how diffusion coefficients of these mixtures vary. The swelling behavior of these gels in the presence of PBS was investigated. The degree of swelling of the gel ( $F$ ) with time was recorded with time, and is shown below in figures [5.5] and [5.6]. Figure (5.5) represents swelling curves for the mixtures with lower mass fractions of PEG 200.

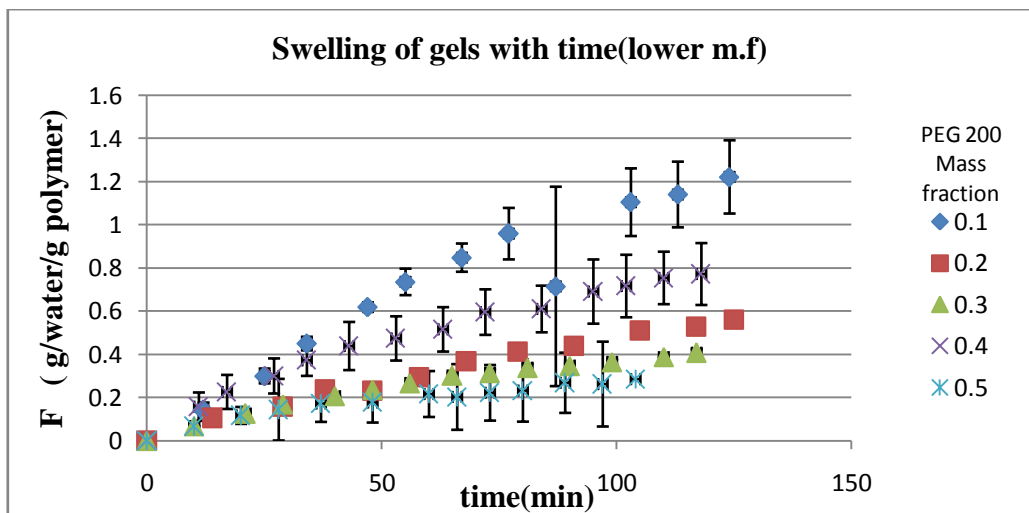


**Figure 5.5 Swelling of mixtures with time. The mixtures represented here are for PEG 200 mass fractions from 0.1 to 0.5**

Ranging from mass fractions 0.1 to 0.5, the curves show significant swelling of the gel with time. As the mass fraction of PEG 200 increases, the degree of swelling decreases. This is probably due to the fact that as fraction of PEG 200 increases, the mixture tends to behave more

as PEG 200, and thus swells to a much lesser degree. Figure (5.6) represents the swelling curves for mixtures with higher mass fractions of PEG200 ranging from 0.5 to 0.8. In figure (5.6), we expect that as mass fraction of PEG 200 increases, and that of PEG 14000 decreases, the degree of swelling should decrease. However there is no such distinct trend observed for the higher mass fractions of PEG 200. This may be due to the fact that the swelling degree substantially less. While a trend is difficult to quantify, it is noted that the degree of swelling is much less for lower mass fractions as expected. Further analysis of the above swelling data, was performed by fitting the above data to Eq(5.7), to determine the mechanism of transport for the mixtures. Table (5.5) shows values of n and k for each mixture. The values of n obtained from the data fitting gives a relatively good estimation of the transport behavior of the gel. For mixtures with lower mass fractions of PEG 200, the values of n are quite large ranging from 0.842 to 0.6285.

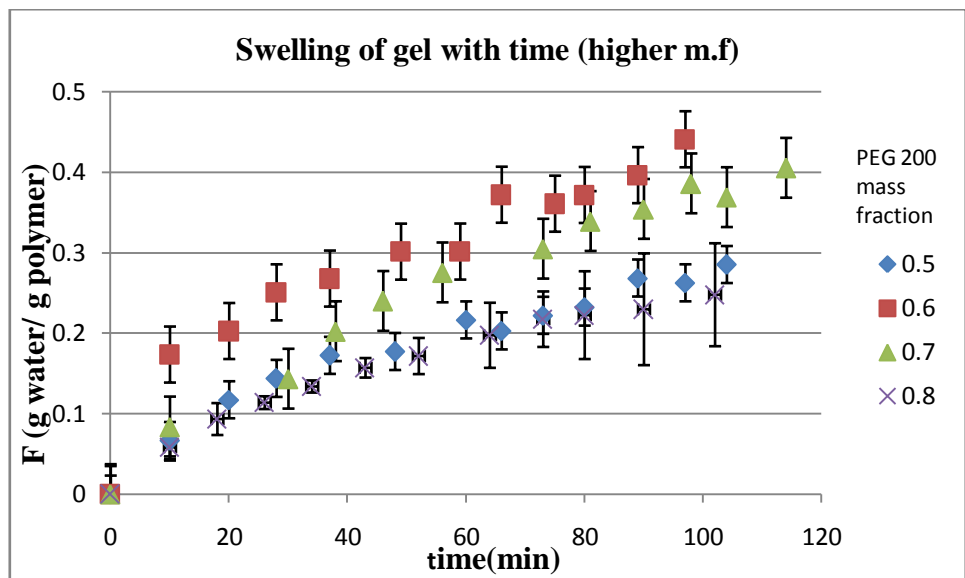


**Figure 5.6 Swelling of mixtures with time. The mixtures shown are gels with PEG 200 mass fractions ranging from 0.5 to 0.8**

The mixtures with PEG 200 mass fractions of 0.1 and 0.2 have values of n as, 0.76 and 0.842 respectively.

**Table 5.5 Values of n and k obtained from fitting swelling data to power law expression. The values are shown along with the variance and 95% confidence limits of the fit.**

<b>Mass fraction</b>	<b>0.1</b>	<b>0.2</b>	<b>0.3</b>	<b>0.4</b>	<b>0.5</b>	<b>0.6</b>	<b>0.7</b>	<b>0.8</b>
<b>(PEG 200)</b>								
<b>n</b>	0.76	0.84	0.64	0.63	0.54	0.43	0.65	0.58
<b>95% confidence</b>	3.35E-04	6.31E-05	5.19E-02	1.11E-03	2.28E-04	7.35E-02	8.11E-02	2.44E-02
<b>variance</b>	3.03E-03	2.72E-04	1.09E-04	2.11E-04	1.00E-04	2.96E-04	1.93E-04	2.35E-05
<b>k</b>	3.20E-02	1.00E-02	1.95E-02	3.90E-02	2.24E-02	5.73E-02	1.87E-02	1.73E-02
<b>95% confidence</b>	4.80E-05	2.86E-06	4.43E-03	1.90E-04	2.18E-05	1.75E-02	6.69E-03	1.78E-03
<b>variance</b>	3.03E-03	2.72E-04	1.09E-04	2.11E-04	1.00E-04	2.96E-04	1.93E-04	2.35E-05

. These values are close enough to the value 0.89, to assume Case-II type diffusion dominant in these gels. This is expected, as larger mass fractions of PEG 14000, leads to larger mesh sizes and large degrees of swelling. Consequently, polymer relaxation becomes dominant. The mass fractions of 0.3 and 0.4 have intermediate values of n. Thus these gels exhibit anomalous diffusional behavior, meaning that neither Fickian diffusion nor polymer relaxation is dominant. For higher mass fractions (greater than 0.5), we finally start seeing the effects of Fickian diffusion. The mesh size is small enough such that diffusion of penetrant follows Fick's law. In these mixtures, the swelling of the gel is relatively small, indicating polymer relaxation is negligible. As PEG 200 characteristics becomes dominant in the gel mixture, the gel diffusion characteristics becomes dominated by Fick's law. This is the reason for the dominance of polymer relaxation in the gel. However for the higher mass fraction (0.7, 0.8) one can see that the gel swells to a much lesser degree, thus Fickian diffusion is the dominant mode of transport. For intermediate mass fractions, it is seen that the curves overlap and exhibit intermediate swelling capacity, indicating that neither diffusion mechanism is dominant.

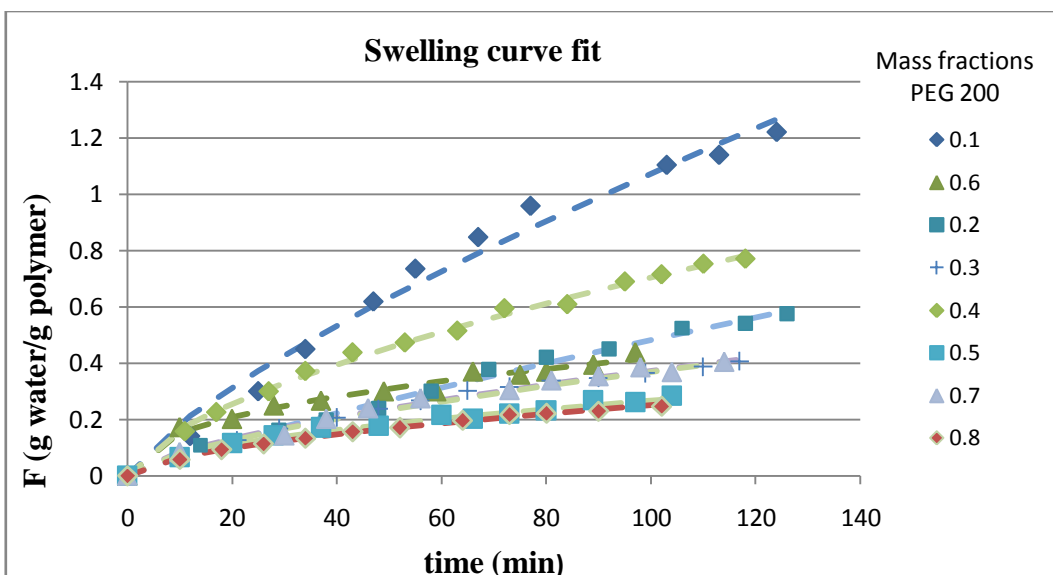


**Figure 5.7 Curve fitting of mixtures to power law expression. The mass fractions represented here are that of PEG 200. The dotted line represents the fitted data, while the markers represent experimental data**

It is evident then, that by controlling the ratios of mixture constituents, one can tune the gel to operate in any required diffusion regime.

For the gels in which diffusion is predominately Fickian, we can fit the swelling curves to known equations (5.8), to obtain approximate diffusion coefficients. Prediction of diffusion coefficients is essential for design of drug delivery systems. Thus the higher PEG 200 mass fraction gels were all fit to Eq (5.8), and parameter D (diffusion coefficient) was estimated. The following table (5.6) gives the values of D obtained after non linear regression was performed on the swelling data.

**Table 5.6 Diffusion coefficients for mixtures whose n value is close to 0.45**

Mass fraction (PEG 200)	0.5	0.6	0.7	0.8
D(mm <sup>2</sup> /min)	1.42E-03	3.70E-03	2.62E-03	1.16E-03
95% confidence	8.99E-05	2.94E-04	2.68E-04	7.17E-05
Variance	1.08E-04	3.71E-04	5.31E-04	6.88E-05

For mass fractions of 0.7 and 0.8, we see that the diffusion coefficient is small; this is due to its small mesh size. The mesh size in these cases becomes so small, that penetrant diffusion becomes difficult. Thus if we can operate in the Fickian regime, and control mesh size, so as to allow significant diffusion to take place, a system with the perfect combination of controlled release, and large diffusion coefficients becomes possible.

## **5.4 Conclusions**

It has been demonstrated that binary mixtures of PEGs, can be manipulated to exhibit certain characteristics by varying the PEG ratios. The swelling parameters mesh size and  $M_c$  vary greatly with constituent PEG molecular weight as well as concentration. The relationship being linear in nature becomes easy to interpret as well as predict. A gel can be prepared, by combining PEGs of two different molecular weights to obtain an intermediate gel that would possess accurate structural strength as well as diffusive properties. The gel can be further fine tuned for required characteristics by varying the ratios in which PEG is mixed. Combining the PEGs in this way enables researchers to incorporate favorable properties of large molecular weight PEGs (easy path for diffusion) as well as lower molecular weight PEGs (tight network, Fickian diffusion). This intermediate network structure in gel will be easy to analyze as Fickian diffusion is well documented in literature. It will also be of suitable mesh size, so that degree of swelling does not overcome the structural integrity of the gel, allowing easy handling of the matrix. One only needs to know the required mesh size and  $M_c$  ideal for drug delivery, the rest is just predicting from the linear relation which PEGs to use and in how much quantity. In most cases today, the required structural strength and penetrant mobility in the gel is obtained by adding crosslinking agents, or comonomers. These chemical are an additional cost, and in some cases can adversely affect the integrity of the gel. Thus a method to use PEG, and vary only the

molecular weight and PEG quantity is a simple and cost effective way to create gels for drug delivery.

## 5.5 References

- 5.1 Kaşgöz, H., İ. Aydın, and A. Kaşgöz, *The effect of PEG(400)DA crosslinking agent on swelling behaviour of acrylamide-maleic acid hydrogels*. Polymer Bulletin, 2005. 54(6): p. 387-397.
- 5.2 . Peppas, N.A., et al., *Hydrogels in pharmaceutical formulations*. European Journal of Pharmaceutics and Biopharmaceutics, 2000. 50(1): p. 27-46.
- 5.3 Ritger, P.L. and N.A. Peppas, *A simple equation for description of solute release I. Fickian and non-fickian release from non-swellable devices in the form of slabs, spheres, cylinders or discs*. Journal of Controlled Release, 1987. 5(1): p. 23-36

# Chapter 6 : Summary and Future Work

## 6.1 Summary

Hydrogels are three dimensional crosslinked matrices which have recently become one of the most widely used material for biomedical applications. The ability of the gel to imbibe biological fluids accounts for its biocompatibility and its use in varied clinical applications, ranging from drug delivery carriers, encapsulation matrices, and food additives. Drug delivery is one of the most prominent fields of research today, and the development of biocompatible, flexible and strong materials is one of the main concerns. Hydrogels are thus ideal materials for these applications. For development of efficient hydrogel based drug delivery devices, it is imperative that we understand the morphological structure, and the diffusional behavior of various solutes into and from the gels. Several monomers have been used as raw material for these hydrogels, ranging from PGLA to novel materials that exhibit specific predetermined properties. Hydrophilic polyethylene glycol is one of the most common hydrogel monomers, and researchers have utilized its 'stealth' properties to develop several PEG –based drug delivery devices. This begins to characterize the significant properties of PEG by varying its molecular weight and determining the variation in its diffusional properties. PEG hydrogels are greatly affected by their swelling ability in water, thus a thorough study of its swelling properties was conducted. It is the nanostructure of the gel which influences its swelling and diffusional ability, and, therefore, study of the gel mesh structure was also an important factor in determining the characteristics of the gel. To determine how efficiently certain biomolecules would diffuse from the gel, Fluorescein dye molecules were used to mimic this release process.

fluorescein molecules are small size molecules similar to several small drugs used for treatment of different ailments.

It was seen that PEG hydrogel properties vary significantly with molecular weight. The mesh size of the gels increases almost linearly with molecular weight. The mesh sizes range from 5 to 100 Angstrom units. Since most proteins have diameters ranging from 10 to 50 Å, they would be able to diffuse into and out of these gels. Swelling studies revealed that degree of swelling also increases with molecular weight. As the mesh size increased, more solvent was allowed to diffuse into the gel, thus increasing its swelling capacity. The lower molecular weight PEGs swelled in accordance with Fick's law. As swelling capacity increased, the relaxation of the gel became an important factor, and the diffusional transport mechanism became anomalous. PEG 20000 was almost completely dominated by the relaxation of the gel, and tended towards Case-II diffusion. Several analytical solutions have been formulated for predicting diffusion coefficients, however such solutions are not so simply available for anomalous and Case -II type diffusion problems. Diffusion studies with fluorescein dye confirmed similar diffusive characteristics for the PEG gels. So gels need to be developed which would have large mesh sizes, and yet have diffusion characteristics that can be easily formulated and predicted.

In search of these balanced gels, mixtures of PEG were studied. Combinations of different PEGs in equal quantities were subjected to swelling studies to determine their nanostructure as well as swelling behavior. The mixture  $M_c$  and the  $M_c$ 's of the individual PEGs were linearly related. It was shown that the mixture  $M_c$  was the same as the average of the individual  $M_c$ 's. The mesh size of the mixtures was linearly related to the individual PEG mesh sizes, showing deviation from linearity only in mixtures involving PEG 20000. This aberrant behavior is attributed to the large swelling degree of PEG 20K, whose effect

overpowers that of any other molecular weight PEG. All these mixtures contained PEGs in equal quantities, thus the effect of changes in concentration of constituent PEGs was not evaluated. To this end, PEG 200 and PEG 14000 were combined in different proportions to determine its effect on the mesh data, as well as swelling behavior. It was seen that there is indeed a linear relationship between mixture  $M_c$  and individual  $M_c$ . The mixture  $M_c$  is equivalent to the addition of the weighted averages of the constituent PEG  $M_c$ . Also the mesh size of the gel increased (or decreased) with the increase in mass fraction of PEG 14000(or PEG 200), indicating increasing effects of dominating PEG in the properties of the mixture. These simple linear relationships make it easy to fine tune gels in accordance with required properties of gels for use in drug delivery.

Mechanism of swelling is another important factor in determining suitability of gel as a drug delivery matrix. It was determined that for intermediate mass fractions, 0.5,0.6,0.7 of PEG 200, the effect of PEG 14000 is such that it allows easy penetration of solvent, however the effect of PEG 200 makes the diffusion mechanism predominantly diffusion, dominating the relaxation of the gel. Thus it has been shown that combining different molecular weight PEGs in correct proportion forms a gel with exact mesh size, structural properties as well as diffusion characteristics which are easy to analyze and interpret. These hybrid gels can thus be custom made, according to requirements of particular drug to be delivered, site of delivery, and mode of delivery. This approach of mixed PEG gels may be part of an avenue of research helping to create novel biomaterials with specific properties, specially designed for simple and effective drug delivery.

## **6.2 Future Work**

This paper attempts to characterize the diffusion characteristics of PEG hydrogels for different biomedical applications. We have considered that diffusion from a cylinder is one

dimensional only, neglecting the effects of axial diffusion. The next step in this study would be to use models, such as Siemann and Peppas model (sequential layer) which accounts for analyte transport in both radial and axial directions. These empirical models are, however, unable to fully explain how swelling affects drug release, thus mechanistic models that have been elucidated in review articles could be used. These models would be able to predict accurately the diffusion of penetrant from a cylinder without the difficulty of analyzing anomalous diffusion results. Even though these mechanistic models are difficult to solve numerically, they are superior in their accurate estimation of parameters.

Diffusion of dye gives us an estimate of the diffusion of small drugs and proteins from the gel. If we are to fully understand the potential of these materials for drug delivery, diffusion of small and, larger molecules (immunoglobins), must also be studied. Peppas and other researchers have studied the diffusion of such molecules from PEG hydrogels, but have done so for only selected homogenous molecular weight PEGs. Similar studies on the combination mixtures [Chapter 5] could provide insight into the usefulness of these mixtures for real time drug delivery applications. If the mixtures prove useful as diffusion carriers, then custom made PEG hydrogels could be manufactured according to exact specifications and requirements. Furthermore, ternary PEG mixtures could be used to further tune properties of the PEG gel, and investigated for further simulated drug delivery.

Once the analysis of these gels are complete, the final goal would be to formulate a mathematical model for PEG mixtures taking into account axial diffusion, as well as anomalous diffusion characteristics, and unifying all data obtained to a single model that can predict the diffusion characteristics of any penetrant of given hydrodynamic radius. This all encompassing model would be an ideal reference for creating a gel with predetermined properties and characteristics to be used as a drug delivery carrier.

# Vita

Anushree Datta is a native of Calcutta, India. Anushree completed her Bachelor of Engineering degree from the University of Pune in 2005. She started her graduate studies in chemical engineering at Louisiana State University in Fall 2005. She is going to be working at Siemens Energy and Automation following the completion of her graduate course, and will be working in the engineering design field.